Doctor Thesis

Kinetochore assembly requires non-kinetochore component proteins, ASURA and RBMX

(動原体形成には非動原体構成タンパク、ASURA および RBMX を必要とする)

Lee Mei Hann

Department of Biotechnology, Graduate School of Engineering,

Osaka University, Japan

2011

Doctor Thesis

Kinetochore assembly requires non-kinetochore component proteins, ASURA and RBMX

(動原体形成には非動原体構成タンパク、ASURA および RBMX を必要とする)

Lee Mei Hann

Department of Biotechnology, Graduate School of Engineering,

Osaka University, Japan

2011

Contents

List of abbreviations i

Nomenclature iv

Chapter 1: General introduction **1-10**

1.1 Outline of mitotic cell cycle 1

1.2 Overview of ASURA (identical to PHB2 or prohibitone, BAP37, and REA) 4

1.3 The RBMX (RNA binding motif protein, X-linked) 7

1.4 Objective of this study 9

Chapter 2: Functional analysis of ASURA and RBMX **11-38**

2.1 Introduction: Molecular architecture of the kinetochore 11

2.2 Materials and methods 15

2.3 Results

2.3.1 ASURA and RBMX do not specifically localize to the kinetochore throughout the cell cycle 19

2.3.2 Mitotic progression was impaired by depletion of ASURA and RBMX 22

2.3.3 Kinetochore proteins mislocalization correlates with chromosome misalignment in the absence of ASURA and RBMX 25

2.3.4 Hec1 is required for retention of sister chromatid cohesion 28

2.4 Discussion 31

2.5 Summary 37

Chapter 3: Kinetochore maturation **39-59**

3.1 Introduction: Kinetochore structure 39

3.2 Materials and methods 40

3.3 Results: Kinetochore in each mitotic phase 42
3.3.1 Prophase 44
3.3.2 Prometaphase 46
3.3.3 Metaphase 51
3.3.4 Anaphase 52
3.3.5 Telophase 56
3.4 Discussion 57
3.5 Summary 58
Chapter 4: ASURA and RBMX are required for kinetochore assembly 60-77
4.1 Introduction: Kinetochore assembly pathways 60
4.2 Materials and methods 63
4.3 Results
4.3.1 Immature kinetochore development in ASURA and RBMX depletion 65
4.3.2 Microtubule attachment was decreased in ASURA and RBMX RNAi 73
4.3.3 Defects in kinetochore formation after ASURA or RBMX depletion were similar to that of Hec1 disruption 75
4.4 Discussion 76
4.5 Summary 77
Chapter 5: General conclusion 78-83
References 84
List of Publications 95
Acknowledgements 96

List of abbreviations

AP	**A**lkaline **P**hosphatase
APC/C	**A**naphase-**P**romoting **C**omplex/**C**yclosome
BAP	**B**-cell receptor **A**ssociated **P**rotein
BCIP	5-**B**romo-4-**C**hloro-3-**I**ndolyl **P**hosphate
BUB1	**B**udding **U**ninhibited by **B**enzimidazoles **1**
BUBR1	**B**udding **U**ninhibited by **B**enzimidazoles **R**elated **1**
CCAN	**C**onstitutive **C**entromere-**A**ssociated **N**etwork
CCD	**C**harge-**C**oupled **D**evice
CDC20	**C**ell-**D**ivision **C**ycle protein **20**
CENP	**CEN**tromere **P**rotein
CH	**C**alponin **H**omology
CREST	**C**alcinosis, **R**aynaud's phenomenon, **E**sophageal dysmotility, **S**clerodactyly, and **T**elangiectasia
DIC	**D**ifferential **I**nterference **C**ontrast
DMEM	**D**ulbecco's **M**odified **E**agle's **M**edium
Dsn1	**D**osage **s**uppressor of **NNF1**
E2	**E**stradiol
EM	**E**lectron **M**icroscopy
ER	**E**strogen **R**eceptor
Esco	**Es**tablishment of **co**hesion
FBS	**F**etal-**B**ovine **S**erum
FPLC	**F**ast **P**rotein **L**iquid **C**hromatography
Hec1	**H**ighly **e**xpressed in **c**ancer **1**
HJURP	**H**olliday **JU**nction **R**epair **P**rotein
hnRNP	**H**eterogeneous **n**uclear **R**ibo**N**ucleo**P**rotein
KMN	**K**NL1-**M**is12 complex-**N**dc80 complex
KNL1	**K**inetochore **Nu**cl**L**i **1**

LIS1	Type I human LISsencephaly
MAD	Mitotic Arrest Deficient protein
MCAK	Mitotic Centromere-Associated Kinesin
Mis	Minichromosome stability
MPS1	MultiPolar Spindle 1
NBT	Nitro Blue Tetrazolium
Ndc80	Nuclear division cycle 80
NEB	Nuclear Envelope Breakdown
Nnf1	Necessary for nuclear function 1
Nsl1	NNF1 synthetic lethal 1
NTD	Nascent Transcripts-targeting Domain
Nuf2	Nuclear filament-containing protein 2
PBS	Phosphate Buffered Saline
PFA	*Para*-FormAldehyde
PHB	ProHiBitin
Plk1	Polo-like kinase 1
PP2A	Protein Phosphatase 2A
PtK	Rat kangaroo cell lines
PVDF	Poly Vinylidene DiFluoride
RBD	RNA-Binding Domain
RBMX	RNA Binding Motif protein, X-linked
REA	Repressor of Estrogen receptor Activity
RNAi	RNA interference
RNP	RiboNucleoProtein domain
ROD	ROugh Deal
RRM	RNA Recognition Motif
SA1/2	Stromalin Antigens 1/2
SAC	Spindle Assembly Checkpoint
Scc	Sister chromatid cohesion protein
Sgo	Shugoshin

Sir2	**S**ilent **i**nformation **r**egulator protein-**2**
siRNA	**S**mall **i**nterfering **RNA**
SIRT2	**SIRT**uin **2**
SMC	**S**tructural **M**aintenance of **C**hromosomes
Spc	**S**pindle **p**ole body **c**omponent
TBST	**T**ris-**B**uffered **S**aline **T**ween-20
Txnip	**T**hioredo**xin** **i**nteracting **p**rotein
Wapl	**W**ings **ap**art-like
ZW10	**Z**este **W**hite **10**
Zwint	**ZW**10 **int**eractor

Nomenclature

Centromere

Centromere (from the Greek 'centro-', meaning 'central', and '-mere', meaning 'part') is the site of the primary constriction, a specialized condensed region of each chromosome that appears during mitosis where the chromatids are held together to form an "X" shape (Cheeseman and Desai 2008). In this dissertation, the centromere is refers to the region of chromosomal DNA that directs kinetochore assembly.

Kinetochore

The term kinetochore (from the Greek 'kineto-', meaning 'move', and '-chore', meaning 'means for distirbution') is the proteinaceous structure that associates with the centromeric DNA. The terms "centromere" (Darlington 1937) and "kinetochore" (Sharp 1934) have been used as synonyms until 1981. In 1981 Ris and Witt defined the term "kinetochore" as the precise region on the chromosome that becomes attached to spindle and it is visible only in ultra-thin electron microscope sections. Centromere is the chromosomal region with which the kinetochore is associated (Rieder 1982). Generally, nowadays, the former is refers to the molecular viewpoint, while the latter is used in a structural viewpoint. In this dissertation, kinetochore is refers as the proteinaceous structure that forms on the centromere.

Kinetochore (component) protein(s)

Kinetochore (component) protein is any protein that is transported to, or maintained at, the kinetochore. Kinetochore (component) proteins are generally divided into two groups:

1. Constitutive kinetochore proteins (inner kinetochore proteins)

Constitutive kinetochore proteins, such as CENP-A, CENP-B, and the CCAN (constitutive centromere-associated network), are associated with the centromere throughout the cell cycle. CCAN is a group of 15 proteins, comprising CENP-C, H, I, K-U and W. CCAN proteins are grouped on the basis of their co-localization with the CENP-A throughout the cell cycle. They are known as the inner kinetochore proteins. From a structural viewpoint, during interphase or early mitotic phase, even when the inner kinetochore plate is not visible, inner kinetochore proteins are associated with the centromere.

2. Transient kinetochore proteins (outer kinetochore and fibrous corona proteins)

Transient kinetochore proteins localize at the kinetochore only at a certain time point during the cell cycle, mostly from late interphase (G2) until telophase (See Fig. 2-1A for details). The KMN network, spindle assembly checkpoint (SAC) proteins, kinetochore nucleoporins, motor proteins and other fibrous corona components are the transient kinetochore proteins that assemble and disassemble from the kinetochore.

The KMN network consists of KNL1, Mis12 complex (comprising 4 subunits: Mis12, Mis13 or Dsn1, Mis14 or Nsl1, and Nnf1) and Ndc80 complex (comprising 4 subunits: Hec1 or Ndc80 in yeast, Nuf2, Spc24 and Spc25). The KMN network forms a hairpin-like structure (Cheeseman et al. 2006), acting as the core kinetochore-microtubule attachment site (See Fig. 2-1B for details). From a structural viewpoint, they are the main components of the outer kinetochore plate. In the absent of microtubules, a fibrous corona is seen to radiate outward from the outer plate (Rieder 1982). The

fibrous corona is formed by a dynamic network of resident and temporary proteins implicated in the spindle checkpoint, in microtubules anchoring and in the regulation of chromosome behavior (Maiato et al. 2004). The fibrous corona components, such as CENP-E and CENP-F are facilitating the stability of microtubule binding. CENP-E, a kinesin-7 family member of the motor proteins, plays a key role in the movement of chromosomes toward the metaphase plate during mitosis (Kapoor et al. 2006; Cai et al. 2009) (See Fig 2-1C for details).

In the current studies, I found two proteins, ASURA and RBMX, which are required for the kinetochore functions but yet have no specific localization at the kinetochore. These proteins are acting differently from the rest of the kinetochore (component) proteins to date, and therefore are referred to as non-kinetochore component proteins.

Chromosome orientation

Chromosome orientation is a process whereby kinetochores attach end-on to microtubules emanating from the pole(s) (Compton 2007). Microtubules bundle interacts end-on to the kinetochore are known as kinetochore fiber (k-fiber). Bi-orientation is the phenomenon whereby sister kinetochores of a chromosome attach to the microtubules emanating from opposite poles, resulting in the sister chromatids moving to opposite poles of the cell during cell division. Mono-orientation arises when one kinetochore forms microtubule attachments before its sister, resulting in single unattached kinetochore. Lateral/side-on attachment is form when the kinetochore interacts with the lateral surface of microtubule(s). Mono-orientation and lateral attachment are common during initial microtubule capturing (Rieder and Alexander 1990). See Fig. 2-1C and 3.3.2 in Chapter 3 for details.

Chapter 1

General introduction

1.1 Outline of mitotic cell cycle

Chromosomal instability has been recognized as a hallmark of human cancer (Schvartzman et al. 2010) and is caused by continuous chromosome mis-segregation during cell division (Kingsbury et al. 2006). Equal partition of the duplicated genetic information (one set each on sister chromatids) is prerequisite to avoid chromosomal instability (Kops et al. 2005). Eukaryotic cells replicate their entire nuclear DNA during S phase, and sister chromatids are physically connected with each other from the time of their synthesis (Hauf and Watanabe 2004). Upon entry into mitosis, compaction of replicated interphase chromatin occurred concomitantly with the formation of a special structure on the surface of the primary constriction, termed kinetochore (Maddox et al. 2006). After nuclear envelope breakdown (NEB), with the aid of bipolar spindle apparatus linking centromeric DNA with opposite poles (i.e., bi-orientation), sister chromatids carrying identical genetic information are apportioned to a pair of daughter cells (Kops et al. 2010). Error-free sister chromatid separation is orchestrated by: (1) pairing of sister chromatids via cohesin until anaphase onset (Peters et al. 2008); and (2) a faithful physical link between spindle microtubules and centromeric DNA via kinetochore (Cleveland et al. 2003), so that sister chromatids are attached to the opposite poles and are moved in opposite directions to finally form two genetically identical daughter cells in cytokinesis (Fig. 1-1A).

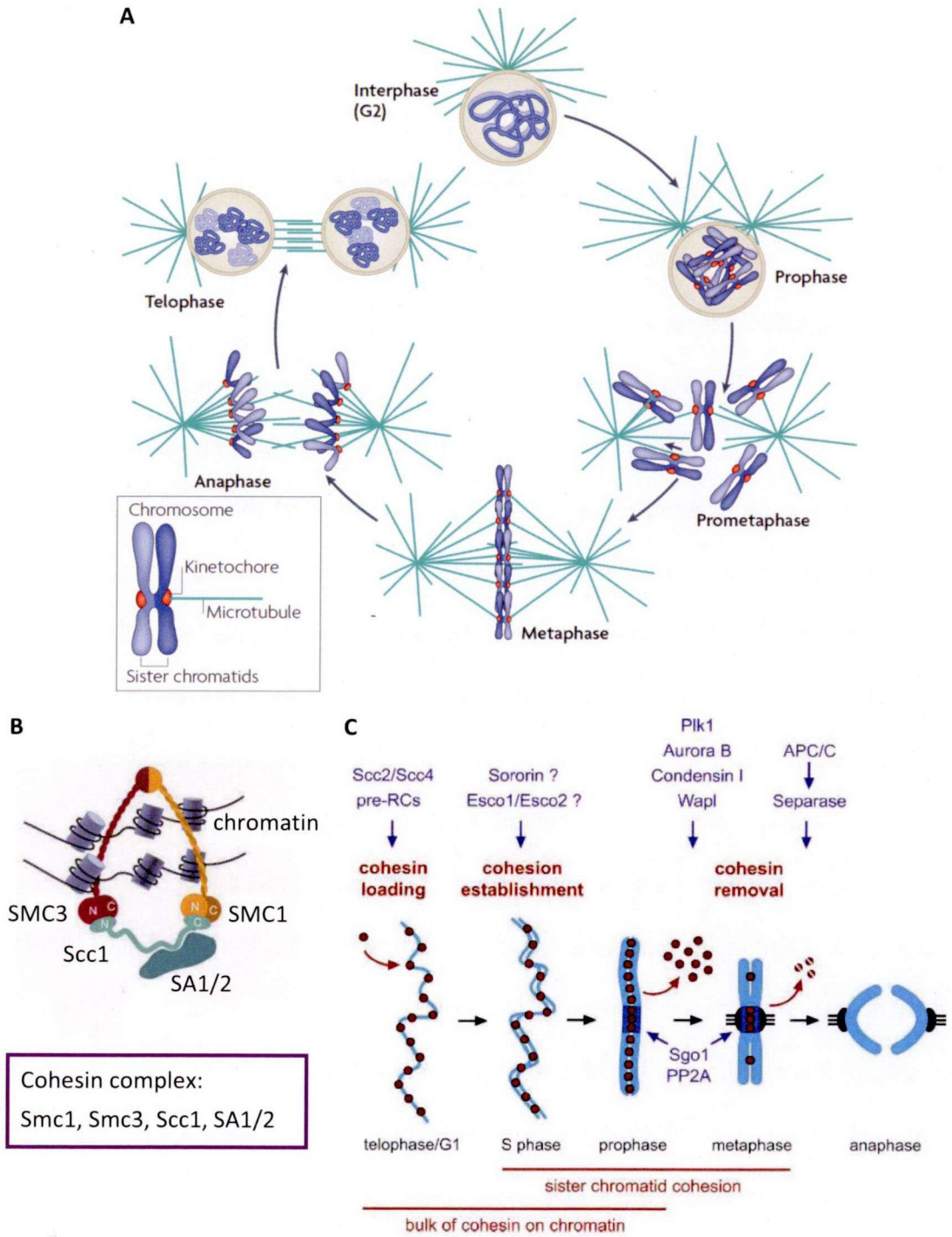

Fig. 1-1 Chromosome segregation and the regulation of sister chromatid cohesion in vertebrate cells. (**A**) Mitotic chromosome segregation (Cheeseman and Desai 2008). (**B**) Model for the architecture of the cohesin complex in somatic vertebrate cells. The cohesin core complex forms a ring-like structure with an outer diameter of ~50nm to bind chromatin (Peters et al. 2008). (**C**) Regulation of sister chromatid cohesion during the vertebrate cell cycle (Peters et al. 2008)

The cohesin complex in somatic vertebrate cells consists of SMC1 (structural maintenance of chromosomes 1), SMC3, Scc1 and either SA1 (stromalin antigens 1) or SA2, but never both (Losada et al. 2000; Sumara et al. 2000) (Fig. 1-1B). In somatic cells, cohesin with SA2 is about threefold more abundant than cohesin with SA1, whereas *Xenopus* eggs contain 10 times more cohesin with SA1 than cohesin with SA2. The functional differences between cohesin consist of either SA1 or SA2 is yet to be clarified. In mitosis, cohesin is removed from the chromosomes by two pathways (Peters et al. 2008) (Fig. 1-1C). During prophase, the bulk of cohesin dissociates from chromatin (Losada et al. 1998; Sumara et al. 2000), and this removal is regulated by Plk1 (polo-like kinase 1), Aurora B kinase, condensin I, Wapl (wings apart-like) and phosphorylation of SA2 (Losada et al. 2002; Gimenez-Abian et al. 2004; Hirota et al. 2004; Hauf et al. 2005; Gandhi et al. 2006; Kueng et al. 2006). Cohesin at centromeres is protected by Sgo1 (shugoshin 1) (Salic et al. 2004) and PP2A (protein phosphatase 2) (Kitajima et al. 2006). At the metaphase-to-anaphase transition, separase is activated by the APC/C (anaphase-promoting complex/cyclosome) and cleaves centromeric cohesin as well as residual cohesin on chromosome arms, enabling sister chromatid separation.

Kinetochore is a protein supercomplex which achieves full assembly on the surface of the centromere during mitotic phase (Cheeseman and Desai 2008). Accumulating strands of evidence reveal that the kinetochore performs at least four functions: 1) a chromosomal attachment site for spindle microtubules during cell division (Schrader 1953; Rieder 1982; Brinkley et al. 1989); 2) a complex machine that exerts the force for poleward chromosome motion (Gorbsky et al. 1987; Nicklas 1989; Rieder and Alexander 1990); 3) simultaneously controlling the dynamics of its associated microtubules (Mitchison et al. 1986; Mitchison 1988; Wise et al. 1991); 4)

generating the cell-cycle checkpoint that delays anaphase onset until all chromosomes are bi-oriented and aligned at the spindle equator (Rieder and Salmon 1998; Maiato et al. 2004; Tanaka 2005). Since kinetochore is only established during mitotic phase, proper kinetochore assembly is essential for all its functions to finally achieve stable kinetochore-microtubule attachment.

Our previous efforts in elucidating chromosome morphogenesis based on their constituent proteins enabled us to identify over 200 proteins by proteome analysis of human metaphase chromosomes (Uchiyama et al. 2005; Takata et al. 2007a). Further purification procedures identified 107 compositions, comprising a majority of proteins essential for chromosome structure and functions. In addition, a group of proteins with unknown mitotic functions were among the list, and we therefore were particularly interested in these proteins in terms of their roles, if any, in chromosome structure and/or function. Two proteins which are relatively abundant, are ASURA (PHB2) and RBMX (hnRNP G), and of our particular interest. Both are known as multifunctional proteins but yet have no mitotic functions reported.

1.2 Overview of ASURA (identical to PHB2 or prohibitone, BAP37, and REA)

ASURA has a molecular weight of 34 kDa and consists of three domains, an N-terminal hydrophobic transmembrane helix, a middle (PHB) domain and a C-terminal coiled coil region (Winter et al. 2007) (Fig. 1-2A). ASURA is one of the prohibitins (PHBs), which are reported to implicate cell cycle progression, transcriptional regulation, cellular signaling, apoptosis and mitochondrial biogenesis, and mitochondrial cristae morphogenesis (Merkwirth and Langer 2009). While prohibitin 1 is usually referred to as PHB1, its human orthologue is known as B-cell receptor associated protein 32 (BAP32) (Terashima et al. 1994). The related protein prohibitin 2 (PHB2) is also known

as prohibitone (Lamers and Bacher 1997), and the human orthologue is known as BAP37. Prohibitin orthologues have also been identified in other mammals, *Drosophila*, plants and yeast. In yeast, PHB1 (prohibitin) and PHB2 (prohibitone) assemble into a ring-like macromolecular complex mainly localized to the mitochondrial inner membrane (McClung et al. 1989; Artal-Sanz and Tavernarakis 2009). Although subcellular localization of PHBs has been confined to mitochondria, a nuclear localization of PHBs has also been reported (Fusaro et al. 2003; Tatsuta et al. 2005). Human PHB2 is involved as a repressor of nuclear estrogen receptor activity, and is identical to a protein earlier identified as REA (repressor of estrogen receptor activity) (Montano et al. 1999). REA is identified as a histone deacetylase interacting partner that modulates the activity of a defined subset of nuclear hormone receptors in rat, mouse and human cell lines (Kurtev et al. 2004).

In HeLa cells, PHB2 is translocated into the nucleus in the presence of ERα (estrogen receptor alpha) and E2 (estradiol) where it interacts with and inhibits the transcriptional activity of the ER (estrogen receptor) (Kasashima et al. 2006). Besides these early reports, we previously revealed that ASURA is required for chromosome congression by protecting sister chromatid cohesion in early mitotic phases (Fig. 2-1B-E; Takata et al. 2007b). Because of its multiple functional roles, we therefore term this protein as 'ASURA' after the fierce Buddhist demigod that has three faces and six arms demonstrating multiple functions.

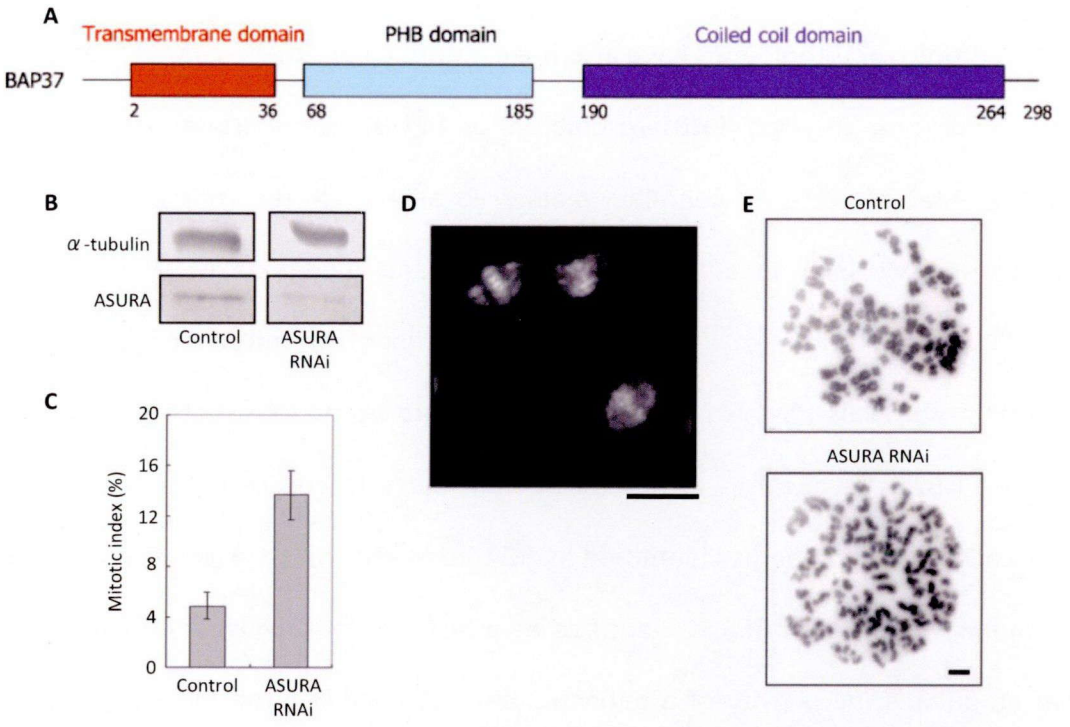

Fig. 1-2 Schematic representation of full-length human BAP37 (ASURA) and mitotic defects in ASURA RNAi. (**A**) Domain structure of ASURA. Numbers in corresponding colors refer to the respective amino acid residues (Winter et al. 2007). (**B**) Immunoblots showing effective depletion of ASURA. α-tubulin was used as loading control. (**C**) Mitotic indexes of control and ASURA RNAi cells. The mitotic index of ASURA depleted cells was increased to nearly three-fold of the control. (**D**) Major phenotype of mitotic cells in ASURA RNAi cultures. Most cells showed nonalignment. Scale bar represents 10 μm. (**E**) Chromosome morphologies in control and ASURA RNAi cells. More than 50% of ASURA RNAi cells showed untimely lost of sister chromatid cohesion. Scale bar is 5 μm (**B-E**) Cited from Takata et al. (2007b)

1.3 The RBMX (RNA binding motif protein, X-linked)

RBMX is a 43-kDa heterogeneous nuclear ribonucleoprotein (hnRNP), identical to hnRNP G. hnRNP G is implicated in the spicing control of several pre-mRNAs, either positively or negatively depending on the mRNA substrates (Hofmann and Wirth 2002; Nasim et al. 2003; Martinez-Contreras et al. 2007; Glisovic et al. 2008), and hnRNP G promotes the expression of tumor-suppressor Txnip and protects the fidelity of DNA end-joining activity (Shin et al. 2007; 2008). While conserving the N-terminal RNA recognition motif (RRM, also known as RNA-binding domain, RBD or ribonucleoprotein domain, RNP) (Soulard et al. 1993), hnRNP G possesses a centrally-positioned short domain (NTD, nascent transcripts-targeting domain) required for nuclear targeting in amphibian oocytes, and recognizes RNA motifs predicted to adopt an hairpin structure via the C-terminal RBD (Kanhoush et al. 2010) (Fig. 1-3A). In addition, the relatively low-abundant hnRNP G protein is unique among hnRNPs (Kanhoush et al. 2010) for being glycosylated (Soulard et al. 1993).

In human cells, the gene coding for hnRNP G is located in the X chromosome, and therefore it is also known as RBMX (RNA-binding motif protein, X chromosome). RBMX is subjected to X chromosome inactivation (Soulard et al. 1993), and is critical for proper neural development of zebrafish and frog embryos (Tsend-Ayush et al. 2005; Dichmann et al. 2008). Multiple processed copies of RBMX are present in the human genome, suggesting that RBMX has multiple roles (Lingenfelter et al. 2001). In addition to the early reports, we previously revealed that RBMX is required for chromosome alignment and cohesion defects were significant in RBMX depleted cells (Fig. 1-3B, C; Matsunaga et al. unpublished data).

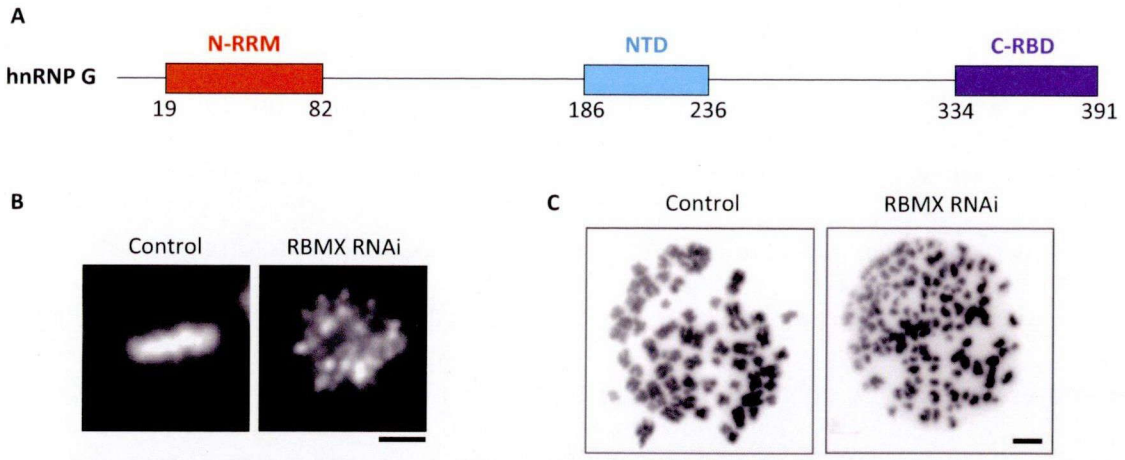

Fig. 1-3 Domain topology of human hnRNP G (RBMX) and mitotic phenotypes in cells lacking RBMX. (**A**) Schematic representation of the full-length RBMX protein referred to Kanhoush et al. (2010). (**B**) Major phenotype of control and RBMX RNAi cells. For the control, metaphase cell is indicated. The majority of mitotic cells with RBMX disruption showed nonalignment. (**C**) Chromosome morphologies in control and RBMX RNAi cells. Over 90% of mitotic cells in RBMX RNAi cultures showed precocious sister chromatid separation. (**B**, **C**) Cited from Matsunaga et al. (unpublished data). Scale bars represent 5 μm

1.4 Objective of this study

ASURA and RBMX are relatively abundant in isolated human chromosomes, suggesting that they play important roles in chromosome formation or mitotic events (Uchiyama et al. 2005; Fukui and Uchiyama 2007; Takata et al. 2007a). However, their mitotic functions have not yet been elucidated well. Besides the early reports, our screening for chromosomal proteins implicated in cell cycle progression revealed that both ASURA and RBMX RNAi led to an accumulation of mitotic cells, as a result of spindle assembly checkpoint activation (Takata et al. 2007b; Matsunaga et al. unpublished data). Further investigation showed that the majority of mitotic cells were arrested at the prometaphase, because of the failure of chromosomes to align at the metaphase plate. Both ASURA and RBMX RNAi cells showed premature lost of sister chromatid cohesion and were arrested at the prometaphase.

Given that chromosome congression require both sister chromatid cohesion and stable kinetochore-microtubule attachment, in this study, I focus on whether stable kinetochore-microtubule attachment is formed after ASURA and RBMX RNAi by investigating the kinetochore assembly because full kinetochore assembly is a prerequisite for stable microtubule interactions. To test this hypothesis, I examined if ASURA and RBMX are the kinetochore components, and whether they are required for kinetochore proteins localization. Furthermore, to investigate the effects of ASURA and RBMX RNAi on kinetochore formation, I studied the kinetochore assembly in HeLa cells using electron microscope (EM), and accordingly proposed a practical classification scheme for kinetochore maturation (i.e., how pre-kinetochores assemble into the mature three-layer structure). This classification scheme was used for the analysis of kinetochore assembly in RNAi treated cells.

To obtain a better insight into the structural significance of the kinetochore in the

RNAi transfected cultures, in addition to the mock control, I analyzed Hec1 RNAi samples with the above EM system as a control. Hec1 is a subunit of the Ndc80 complex, a rod shape heterotetramer (Ciferri et al. 2008), comprising Hec1 (Ndc80 in yeast), Nuf2, Spc24 and Spc25 (Wigge and Kilmartin 2001; Janke et al. 2001). The C-termini of Spc24-Spc25 dimer interacts with the inner kinetochore via Mis12 complex (Petrovic et al. 2010). N-terminal domains of Hec1-Nuf2 interact directly with the plus ends of spindle microtubules (DeLuca et al. 2006; Wan et al. 2009) by forming an oligomeric ring structure (Alushin et al. 2010). The calponin homology (CH) domain and tail domains of Hec1 generate essential contacts between kinetochores and microtubules in HeLa cells (Sundin et al. 2011). Hec1 and Nuf2 show co-localization throughout the cell cycle in DT40 (Hori et al. 2003). DeLuca et al. (2005) showed by using EM that Hec1 and Nuf2 localized at the kinetochore outer layer (also refer to Fig. 2-1B), and when they depleted Nuf2 (Hec1 is depleted at the same time) from the cells, normal formation and/or maintenance of the kinetochore were disrupted, which was later confirmed by Liu et al. (2006). Hec1 and Nuf2 interact directly with microtubules and stabilize kinetochore fiber (microtubules bundle that connects kinetochores to spindle poles) formation (DeLuca et al. 2005). The advantage of employing Hec1 RNAi is that, among the kinetochore proteins that we have tested, Hec1 is well studied both molecularly and structurally. Therefore, Hec1 was used as a model protein throughout this study.

Chapter 2

Functional analysis of ASURA and RBMX

2.1 Introduction: Molecular architecture of the kinetochore

The mammalian kinetochore is a small and yet an elaborate structure, providing physical attachment to the microtubules, force generation and SAC signaling that delays anaphase onset until all chromosomes are attached to the spindle (Maiato et al. 2004; Tanaka et al. 2005; Cheeseman and Desai 2008). This intricate cellular machinery comprises of more than 120 components (Ohta et al. 2010), and an ever-increasing number of proteins are being implicated in, and changing our understanding of the kinetochore functions.

The kinetochore is first described by Brinkley and Stubblefield (1966) as a trilaminar structure based on the observation using electron microscopy (EM). Only about two decades later, the discovery of anti-centromere antibody, CREST (Earnshaw and Rothfield 1985) enabled other researchers to investigate the role of each centromeric protein. Biochemical and structural analyses have provided crucial information about kinetochore assembly.

The trilaminar structure of the kinetochore is reflected in its molecular composition, where pools of proteins assemble to the kinetochore in different ways (Fig. 2-1A; Cheeseman and Desai 2008; McEwen and Dong 2010). Inner kinetochore proteins localize to the centromere throughout the cell cycle. Loading of centromere-specific histone H3 variant CENP-A requires a deposition factor, HJURP (Holliday junction recognition protein) (Foltz et al. 2009; Dunleavy et al. 2009) and was

thought to be essential for all other kinetochore proteins assembly (Liu et al. 2006). The association of CENP-A with heterochromatin specifies the site of the kinetochore on the chromosome (Marshall and Choo 2008; Foltz et al. 2009; Okada et al. 2009). CENP-C and CENP-T/W interact with CENP-A by forming two distinct pathways for the localization of other constitutive centromere-associated network (CCAN) components (Goshima et al. 2003; Hori et al. 2008; Marshall and Choo 2008; Foltz et al. 2009; Okada et al. 2009; Amano et al. 2009). In the interphase, immuno-EM using CREST antisera revealed that, mammalian centromere/inner kinetochore undergoes a regular unfolding-refolding cycle, displaying small beadlike subunits tandemly arranged along a linear thread of centromeric DNA, and apparently lacking kinetochore plates (He and Brinkley 1996).

The localization of outer kinetochore and the corona components are cell cycle-dependent, mostly from G2 phase until after nuclear envelope breakdown (NEB) (Maiato et al. 2004; Chan et al. 2005; Liu et al. 2006). More recent reports revealed that CENP-C (Przewloka et al. 2011) and CENP-T/W complex (Gascoigne et al. 2011) function as core kinetochore assembly factors in vertebrate cells, independent of CENP-A, although CENP-A recruits both CENP-C (Goshima et al. 2003; Gascoigne et al. 2011) and CENP-T/W (Hori et al. 2008) to the centromere. All other kinetochore component proteins are known to be recruited by other kinetochore proteins upstream (i.e., localized to the kinetochore in a self-assembly manner) (Maiato et al. 2004; Chan et al. 2005; Liu et al. 2006; Cheeseman and Desai 2008). Mis12 complex interacts with CENP-C (Screpanti et al. 2011; Przewloka et al. 2011; Gascoigne et al. 2011), while Ndc80 complex interacts with the CENP-T/W complex (Gascoigne et al. 2011), linking the inner and outer kinetochores. The KMN network (KNL-1/Mis12/Ndc80 complex) functions at kinetochores to form a core attachment site between kinetochore and

microtubules (Cheeseman et al. 2006). From a structural viewpoint, kinetochores are visible on the surface of the primary constrictions as roughly circular patches of finely fibrillar materials as cells enter mid prophase and gradually differentiate into the trilaminar morphology that is visible until the end of mitosis (Roos 1973; Rieder 1982).

The stepwise manner of protein assembly (Liu et al. 2006) and the molecular architecture of this layered structure (Wan et al. 2009; Santaguida and Musacchio 2009; Ribeiro et al. 2010) provided crucial insights into kinetochore assembly pathways. Although structural models have enabled many missing molecular networks to be linked (Maresca 2011), understanding the very fundamental question of how the trilaminar kinetochore is developed remains challenging.

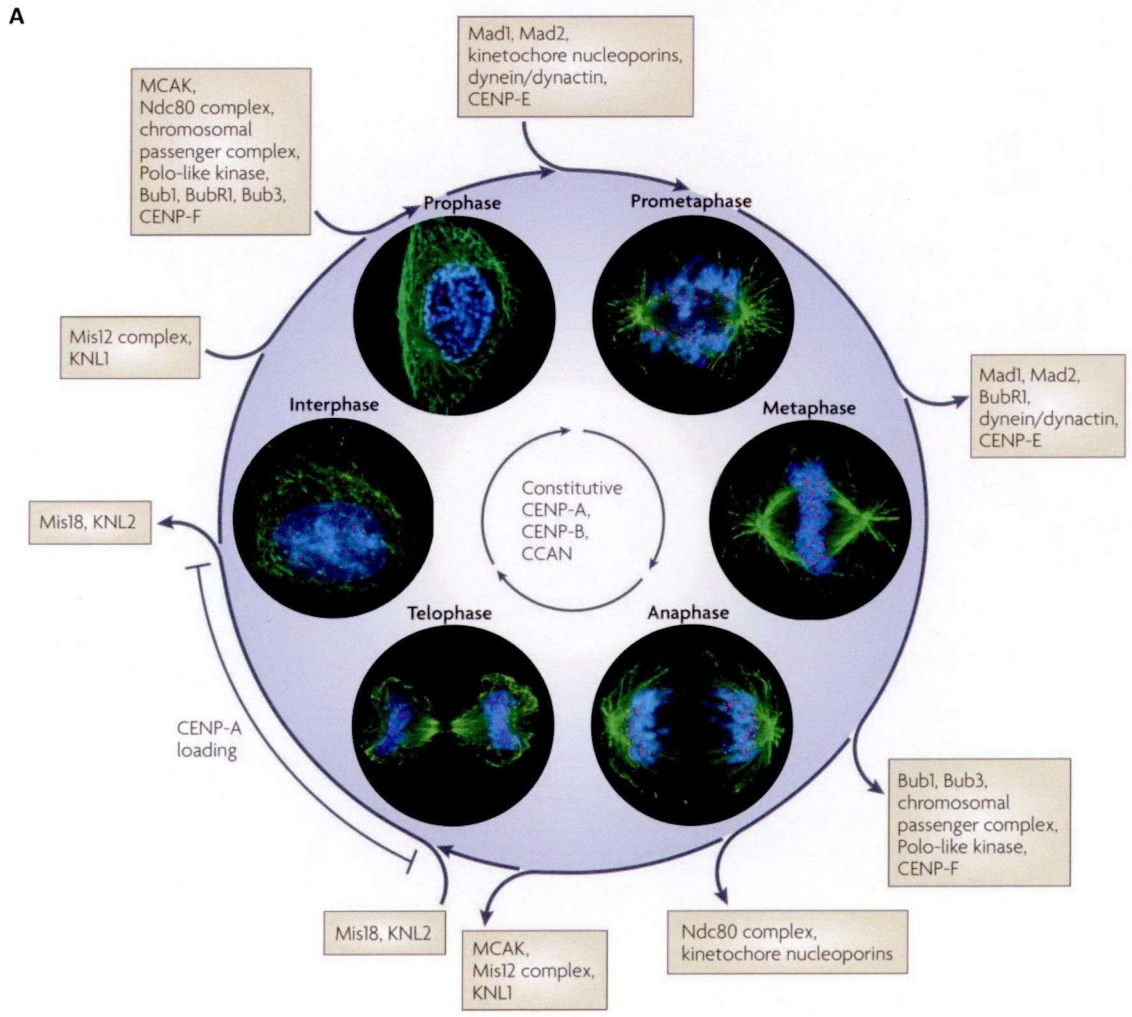

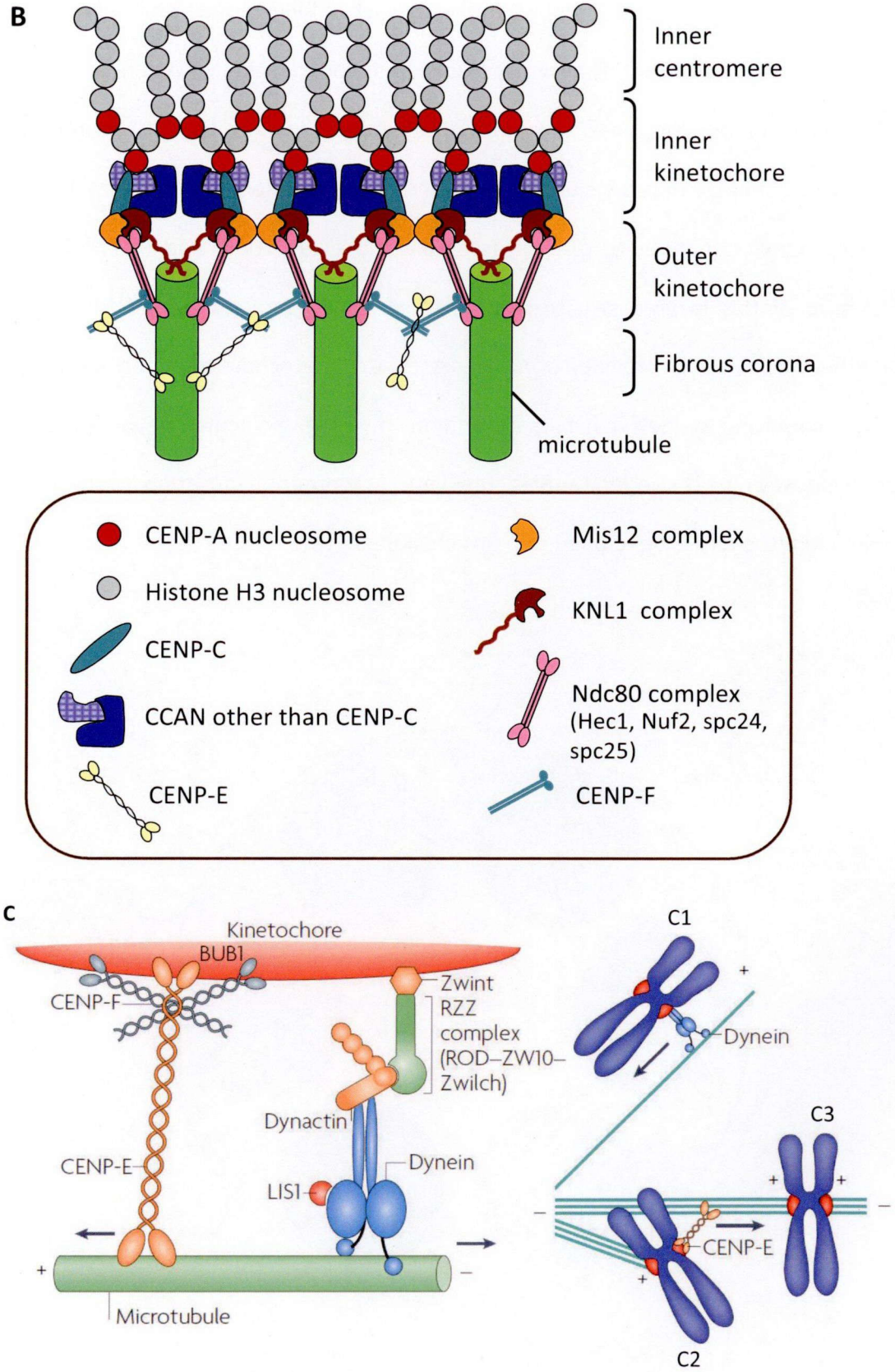

Fig. 2-1 Molecular composition of the kinetochore. (**A**) Kinetochore composition is

dynamically regulated during cell cycle (Cheeseman and Desai 2008). Immunofluorescence images showing DNA (blue), microtubules (green) and kinetochore localization (red) throughout the cell cycle in human cells. Arrows on the periphery of the circle outline when the corresponding protein(s) begin to associate with, or delocalize from, the kinetochore during the cell cycle. Arrows representing dissociation indicate the initial reduction of protein levels, but not necessarily the absolute loss of the components listed. (**B**) Protein architecture of the human metaphase kinetochore. Inner centromere refers to the heterochromatic domain where cohesins are targeted to and is located between the two sister kinetochores. The inner kinetochore is a region of distinct chromatin composition containing centromere specific histone H3 variant (CENP-A), at the interface with the inner centromere. The outer kinetochore is the site of microtubule binding. Fibrous corona is the outermost domain of the kinetochore, which can be visualized by conventional EM only in the absence of microtubules, containing mostly SAC and motor proteins. (**C**) Kinetochore translocation along microtubules (Cheeseman and Desai 2008). The two motor proteins that are localized to kinetochores (mainly to the outer kinetochore and fibrous corona) are CENP-E and dynein. Dynein translocates laterally associated kinetochores (C1) to the vicinity of spindle poles. CENP-E translocates along the kinetochore fiber of an already bi-oriented chromosome (C3) to move a mono-oriented chromosome (C2) towards the metaphase plate. LIS1 (type I human lissencephaly) and the ROD–ZW10–Zwilch (RZZ) complex associate with dynein and contribute a poleward force at end-on attached kinetochores (left kinetochore of C2 and kinetochores in C3) that contributes to the chromosome alignment and segregation

2.2 Materials and methods

Cell culture

HeLa cells were maintained in Dulbecco's modified Eagle's medium (DMEM; GIBCO BRL) supplemented with 10% fetal-bovine serum (FBS; Equitech-Bio) at 37°C and 5% CO_2.

Antibodies

The following antibodies were used in immunofluorescence microscopy and

immunoblotting. A rabbit ASURA polyclonal antibody and a rabbit polyclonal anti-RBMX antibody (for immunofluorescence use) were generated as described previously (Takata et al. 2007b) and were used at a dilution of 1:1000. In brief, full-length ASURA or RBMX cDNA was inserted into the vector pDEST17 (Invitrogen). His-tagged ASURA or RBMX was expressed in *Escherichia coli*, purified with an FPLC system (GE Healthcare), and was used to immunize a rabbit. The antibody produced was affinity-purified using antigen. The other primary antibodies were anti-CENP-F rabbit polyclonal (1:2000, Novus Biologicals), anti-Hec1 mouse monoclonal (1:1000, Affinity Bioreagents), anti-CREST (1:1000, Cortex Biochem), anti-RBMX goat polyclonal (for immunoblot analysis use) (1:1000, Santa Cruz Biotechnology) and anti-β-actin mouse monoclonal (1:10000, Sigma). Secondary antibodies for immunoblot analyses were anti-mouse IgG (H+L) AP (alkaline phosphatase) (1:2000, Vector Laboratories), anti-rabbit IgG (H+L) AP (1:2000, Vector Laboratories) and anti-goat IgG (H+L) AP (1:2000, Vector Laboratories). For immunofluorescence analyses, secondary antibodies were Alexa Fluor 488 anti-mouse monoclonal (1:500, Molecular Probes), Alexa Fluor 488 anti-rabbit monoclonal (1:500, Molecular Probes), and anti-human IgG (1:200, Sigma).

siRNA methods

HeLa cells were transfected using Lipofectamine 2000 according to the manufacturer's instructions at a final concentration of 100 nM with ASURA-siRNA (5'-GAAUCGUAUCUAUCUCACATT-3', PHB2 siRNA-1 in Takata et al. 2007b), RBMX-siRNA (5'-UCAAGAGGAUAUAGCGAUATT-3') or Hec1 siRNA (5'-AAGTTCAAAAGCTGGATGATC-3', Martin-Lluesma et al. 2002). Cells transfected with Lipofectamine alone were used as the mock control. Cells were collected 48h post-transfection for use in analysis.

Immunoblotting and gel electrophoresis

Cells (siRNA or mock transfected) grown in 24-well plate (4.3 x 10^5 cells/well) were collected (2 wells for each treatment) and lysed in 2x Laemmli Sample Buffer (Santa Cruz Biotechnology) with an equal amount of PBS (phosphate buffered saline, pH 7.4) buffer to obtain a final volume of 120 µl. 3µl of protein extracts (approximately 2.2 x 10^4 cells) were applied to each lane and were fractionated on 12% polyacrilamide gels and then transferred onto PVDF (poly vinylidene difluoride) membrane. The immunoblots were blocked with 1% BSA-TBST (0.1% Tween 20, 25 mM Tris-HCl pH 7.4, 137 mM NaCl, 25 mM KCl) and labeled with the primary and secondary antibodies. The immunoreactive protein bands were detected by NBT/BCIP solution (Roche) diluted in AP buffer (100 mM Tris-HCl, pH 9.5, 100 mM NaCl, 1 mM $MgCl_2$). The band intensities were analyzed with the Image J program (http://rsb.info.nih.gov/ij/download.html).

Immunofluorescence microscopy

Localization analysis of ASURA and RBMX was performed as follows. HeLa cells grown on poly-L-lysine coated coverslips (unless otherwise stated, all coverslips used were the same) were fixed with 4% PFA (*para*-formaldehyde) either containing 0.01% (for ASURA staining) or 0.5% (for RBMX staining) Triton X-100 in PBS for 15 minutes at room temperature. Cells were then blocked in 1% BSA in PBS and proceeded for immunostaining as described later. For mitotic index calculation, cells grown on coverslips were transfected with target siRNA, fixed with 4% PFA in PBS for 15 minutes at 37°C, and stained with Hoechst 33342 (Sigma). Mitotic index is a measure for the proliferation status of a cell population. It is defined as the ratio between the number of cells in mitosis and the total number of cells (Fig. 2-3B). HeLa cell cycle is 24 hours and a mitotic cycle is approximately 1 hour. Therefore, mitotic index is normally 4-5%.

For proteins localization analyses, cells grown on coverslips were fixed either with 4% PFA containing 0.5% Triton X-100 in PBS for 15 minutes at room temperature (for Hec1 and CREST staining) or 100% ice-cold methanol for 10 minutes at -20°C (for CENP-F and CREST staining). Alternatively, cells were arrested at metaphase by adding colcemid (final concentration 0.1 μg/ml) into the culture medium for 3 hours at 37°C and were collected for metaphase-chromosome spreads as described earlier (Ma et al. 2007) with some modifications. Briefly, cells were treated with hypotonic solution (75 mM KCl) for 15 minutes at 37°C and were cytospun onto coverslips. Then, cells were fixed with 4% PFA in PBS and permeabilized by 0.2% Triton X-100 in PBS for 15 minutes, respectively. Cells were then blocked with 1% BSA in PBS for 30 minutes prior to primary and secondary antibody interactions. Unless otherwise stated, all primary and secondary antibody interactions were performed at the same condition, 1 hour at room temperature, respectively. Samples were then mounted in Vectorshield mounting medium (Vector Laboratories) and examined under an Axioplan II imaging fluorescence microscope (Carl Zeiss) equipped with a CCD camera (MicroMax, Roper Scientific) driven by the IP Lab software (Takata et al. 2007b).

The fluorescence intensities of the kinetochore signals were analyzed using Image J software. Small circles were drawn around kinetochores and the total pixel intensity above background within each circle was measured. The mean values of all kinetochore signals from at least 10 cells were quantified. Kinetochore intensity measurements for each protein were normalized relative to prometaphase and metaphase of control siRNA-treated cells.

2.3 Results

2.3.1 ASURA and RBMX do not specifically localize to the kinetochore throughout the cell cycle

ASURA and RBMX were identified as chromosomal proteins by our proteome analysis using isolated human metaphase chromosomes (Uchiyama et al. 2005; Takata et al. 2007a), suggesting their association with chromosomes during mitotic phase. To ascertain this possibility, I first examined the dynamics of ASURA throughout the cell cycle. Immunofluorescence microscopic study showed that ASURA localizes to the nucleus and cytoplasm during interphase (Fig. 2-2A; Kasashima et al. 2006). As the cells enter prophase, ASURA distributed evenly throughout the cells, slightly enriched at the chromosomes until prometaphase. This observation showed that active trans-membrane transport of ASURA occurs before NEB. From metaphase to cytokinesis, ASURA diffused to the cytoplasm and slightly enriched at the spindle. These data showed that ASURA may interact actively with the chromatin/chromosome during interphase, prophase and prometaphase.

During interphase, RBMX is distributed throughout the nucleoplasm with a speckled pattern (Soulard et al. 1991), as in Fig. 2-2B. When the cells enter prophase, RBMX increasingly localizes at the chromosomes. After NEB, RBMX disperses throughout the cytoplasm while associating with the chromosomes, and gradually enriches at chromosome peripheral region as the cells proceed to the metaphase. RBMX predominantly localized at the cytoplasm after anaphase onset.

We previously showed that both ASURA and RBMX RNAi resulted in premature sister chromatid separation, and may have some role in kinetochore formation (Takata et al. 2007b; Matsunaga et al. unpublished data). To test if ASURA and RBMX localized to the centromere region, the cells were co-immunostained with Hec1 from the outer

kinetochore. Unlike Hec1, which localized to the kinetochore during mitotic phase, there were no obvious signals of ASURA and RBMX specifically to the kinetochore or centromeric region throughout the cell cycle, indicating that ASURA and RBMX are not the kinetochore components (Fig. 2-2A, C).

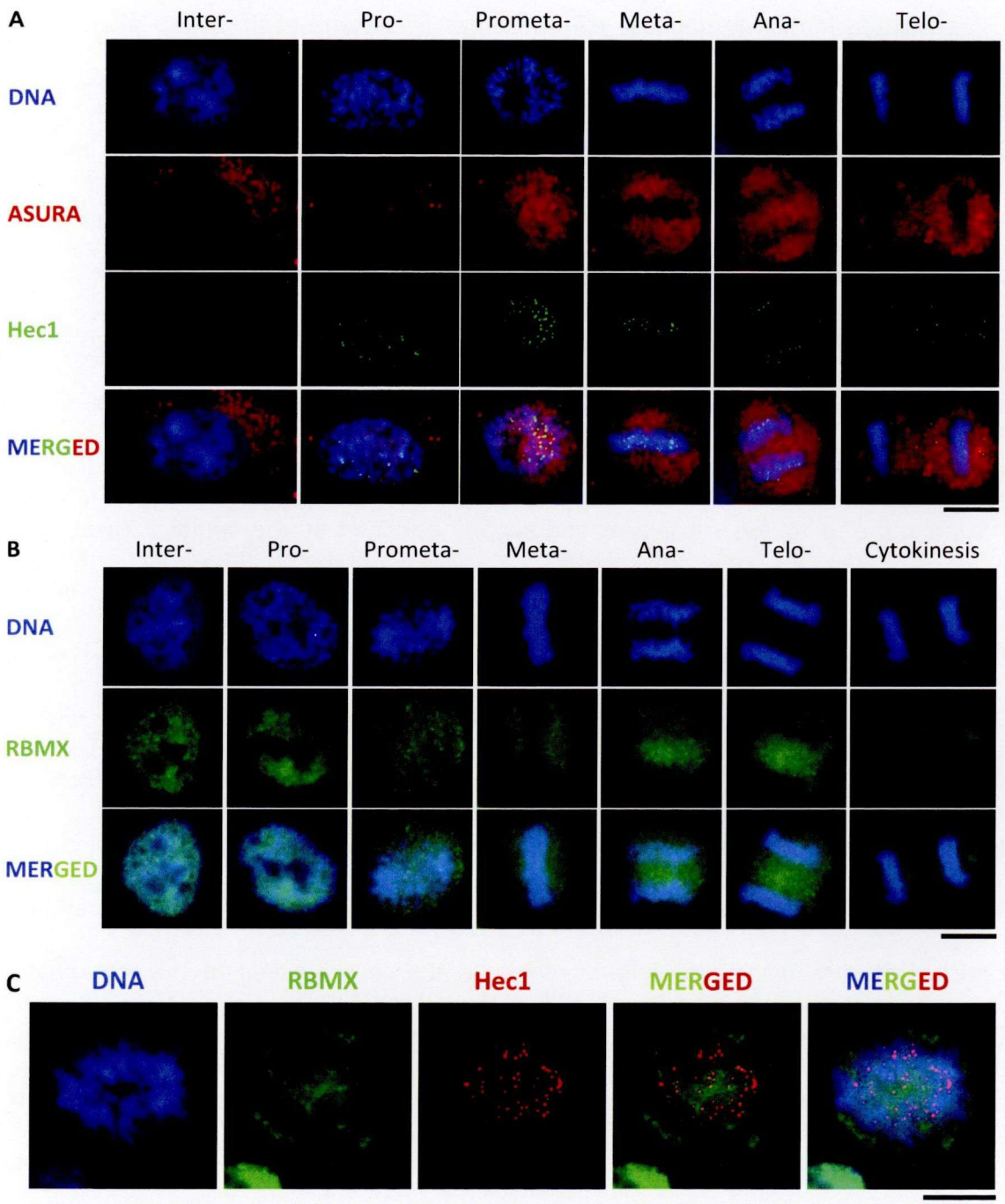

Fig. 2-2 Localization patterns of ASURA and RBMX throughout the cell cycle. Interphase (Inter-), prophase (Pro-), prometaphase (Prometa-), metaphase (Meta-),

anaphase (Ana-), telophase (Telo-) and cytokinesis cells were examined. (**A**) No specific co-localization of ASURA and Hec1 throughout the cell cycle. ASURA localized to both cytoplasm and nucleus during interphase. In prophase and prometaphase, ASURA localized to chromosomes and cytoplasm, but was mainly cytoplasmic from metaphase until the end of the mitotic phase, although some signals were detected at the chromosomes. (**B**) Localization profile of RBMX. RBMX is mainly localized to the cytoplasm during mitosis, although some signals were detected at the chromosomes. (**C**) RBMX signal is not overlapping with or adjacent to the Hec1 signal. A prometaphase cell is indicated. (**A-C**) Scale bars are 10 μm

2.3.2 Mitotic progression was impaired by depletion of ASURA and RBMX

ASURA has been well studied for its roles in mitochondria and estrogen receptor especially during interphase. Similarly, RBMX is well studied for its functions in interphase, particularly in the splicing control of several pre-mRNAs. However, the mitotic functions of ASURA and RBMX remain to be elucidated. To assess the functional roles of ASURA and RBMX in mitosis, an RNAi-mediated gene-silencing approach was employed to knockdown either ASURA or RBMX from the cells. Hec1 RNAi was used as a control in addition to the mock control. As a result, ASURA expression levels were strongly reduced 48 hours after transfection (26% of control) as shown in Fig. 2-3A. Immunoblot analysis of HeLa cultures subjected to RBMX siRNA treatment for 48 hours revealed a decline in the expression level of RBMX of less than 20% when compared with mock transfected cells.

Cytological analyses immediately indicated a high degree of aberration as the cells lacking either ASURA or RBMX were assayed for the mitotic profiles. Mitotic arrest was significant, as indicated by a 3-fold increase in mitotic index comparing to that of the control (4.7±0.3%) (Fig. 2-3C). The mitotic index was 13.4±1.9% in ASURA RNAi cultures and 13.1±3.3% in RBMX RNAi cultures. The mitotic index of Hec1 RNAi (12.9±2.3%) was similar to that of ASURA and RBMX RNAi. Apparently, most of the mitotic cells lost their ability to congress chromosomes at the metaphase plate, characterized by a high percentage of prometaphase cells, 82.0±2.5% in ASURA RNAi, 87.3±4.8% in RBMX RNAi, and 88.2±1.0% in Hec1 RNAi, more than double the control (36.9±3.1%) (Fig. 2-3D). Typically, chromosomes disperse throughout the cells at varying degrees (nonalignment), or apparently align at the spindle equator along with some scattered chromosomes (misalignment) (Fig. 2-3E-I).

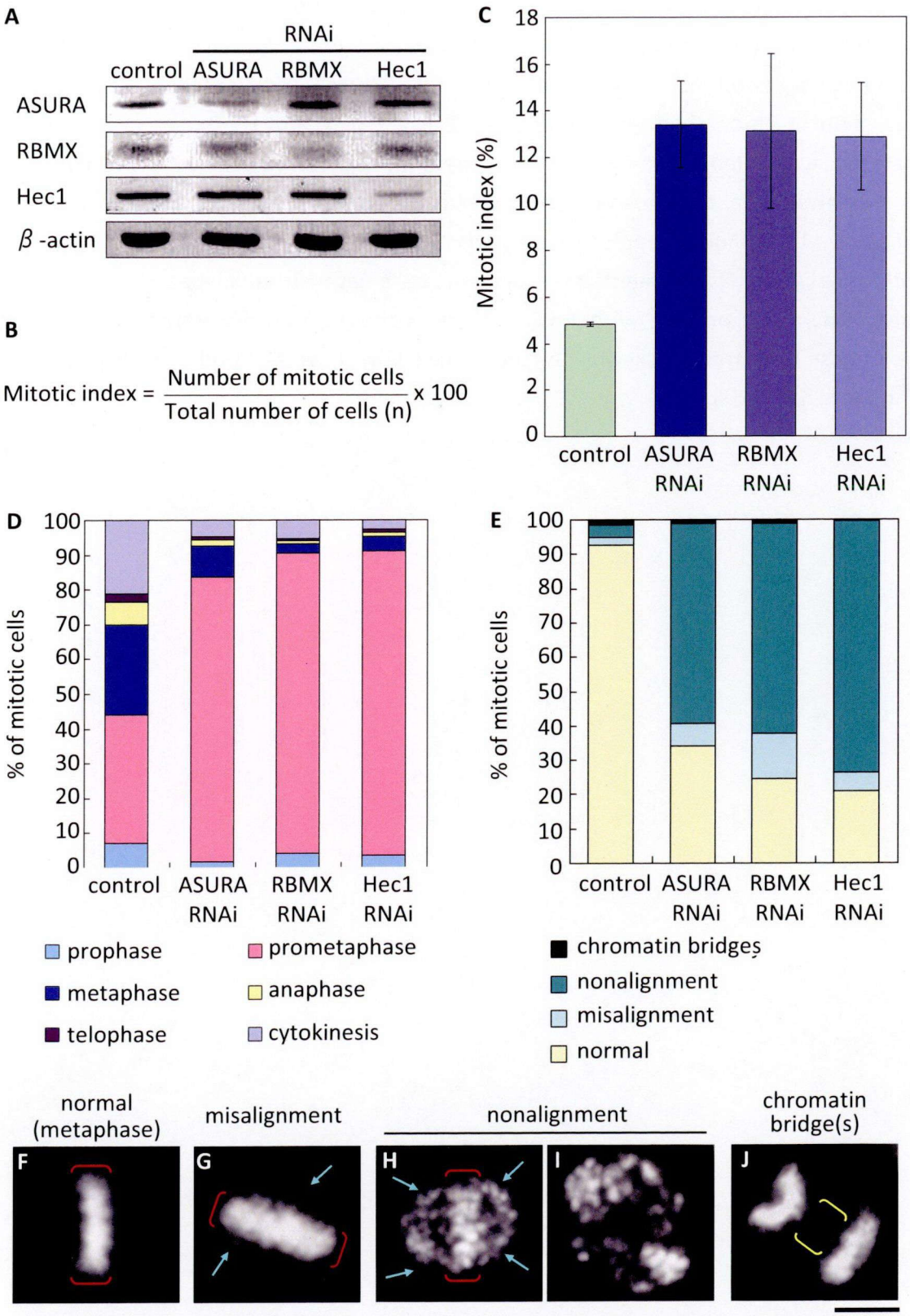

Fig. 2-3 Abnormal chromosome congression and mitotic defects associated with ASURA and RBMX depletion. (**A**) Depletion of ASURA, RBMX and Hec1 by RNAi treatments were analyzed by Western blot. β-actin was used as loading control. (**B**) The

definition of mitotic index. (**C**) Mitotic indexes of ASURA, RBMX and Hec1 depleted cells (n >1000). Three independent experiments were performed for each set of treatment. (**D**) Percentages of each mitotic phase of ASURA, RBMX and Hec1 depleted cells. (**E**) Distortion of chromosome alignment in ASURA, RBMX and Hec1 depleted cells. (**F**) Metaphase cell. Red bracket indicates the metaphase plate. (**G**) Cell with misalignment. Blue arrows reveal chromosome/chromatid clusters outside the metaphase plate (red bracket). Misalignment represents cells with ≤10 unaligned chromosomes. (**H, I**) Cells with nonalignment. Nonalignment represents cells with >10 unaligned chromosomes/ chromatids (blue arrows), either with (H) or without (I) an apparently recognizable metaphase plate (red bracket). (**J**) Anaphase cell with chromatin bridge (yellow bracket). (**F-J**) Scale bar is 10 μm

2.3.3 Kinetochore proteins mislocalization correlates with chromosome misalignment in the absence of ASURA and RBMX

Increased mitotic index as a result of failure in chromosome alignment implicates that ASURA and RBMX are essential for chromosome congression. In addition to precocious sister chromatid separation, aberrant microtubule association are a common feature of chromosome congression defects. I therefore questioned if stable microtubule attachments were formed. Often, irregular kinetochore formation couples with chromosome-to-spindle attachment defects. Since ASURA and RBMX do not show stable interaction with the kinetochore or centromere, at least that was not apparent from its localization pattern (Fig. 2-2), I evaluated whether kinetochores assemble properly with ASURA and RBMX depletion by investigating the localization of Hec1 and CENP-F, which normally associate transiently with mitotic kinetochores. CENP-F is a component of the outer kinetochore and the fibrous corona (Rattner et al. 1993), and is required for proper kinetochore formation (Liu et al. 2006) and stable microtubule attachment (Feng et al. 2006).

Both Hec1 and CENP-F exhibit aberrant kinetochore targeting in ASURA- and RBMX-depleted cells (Fig. 2-4). With depletion of ASURA, Hec1 intensity decreased to 50% of the control (Fig. 2-4A, C), and kinetochore localization of CENP-F (Fig. 2-4B, C) was abolished. As for RBMX RNAi, kinetochores showed a mean reduction in both Hec1 and CENP-F fluorescence intensities of ~30% (Fig. 2-4). CREST intensity, an indicator of the centromere, remained relatively unaltered in all RNAi treatments. In mock transfected cultures, Hec1 (Fig. 2-4A) and CENP-F (Fig. 2-4B) localized normally at the outer kinetochore. CENP-F localizes to the kinetochore since late G2 phase (Liao et al. 1995), although the intensities were slightly decreased as the cells proceeded from prometaphase to metaphase, CENP-F enrichment is observed throughout mitosis.

CENP-F enrichment at the kinetochore was hardly detected after ASURA, RBMX and Hec1 RNAi. Hec1 and CENP-F are the major components of the fibrous network of the outer kinetochore (Dong et al. 2007), essential for proper kinetochore formation (Deluca et al. 2005; Liu et al. 2006) where stable kinetochore-microtubule attachment to achieve bi-orientaion is attained (Liu et al. 2007; Feng et al. 2006). Therefore, mislocalization of Hec1 and CENP-F in ASURA and RBMX RNAi suggests that kinetochore formation is impaired at least to some degree.

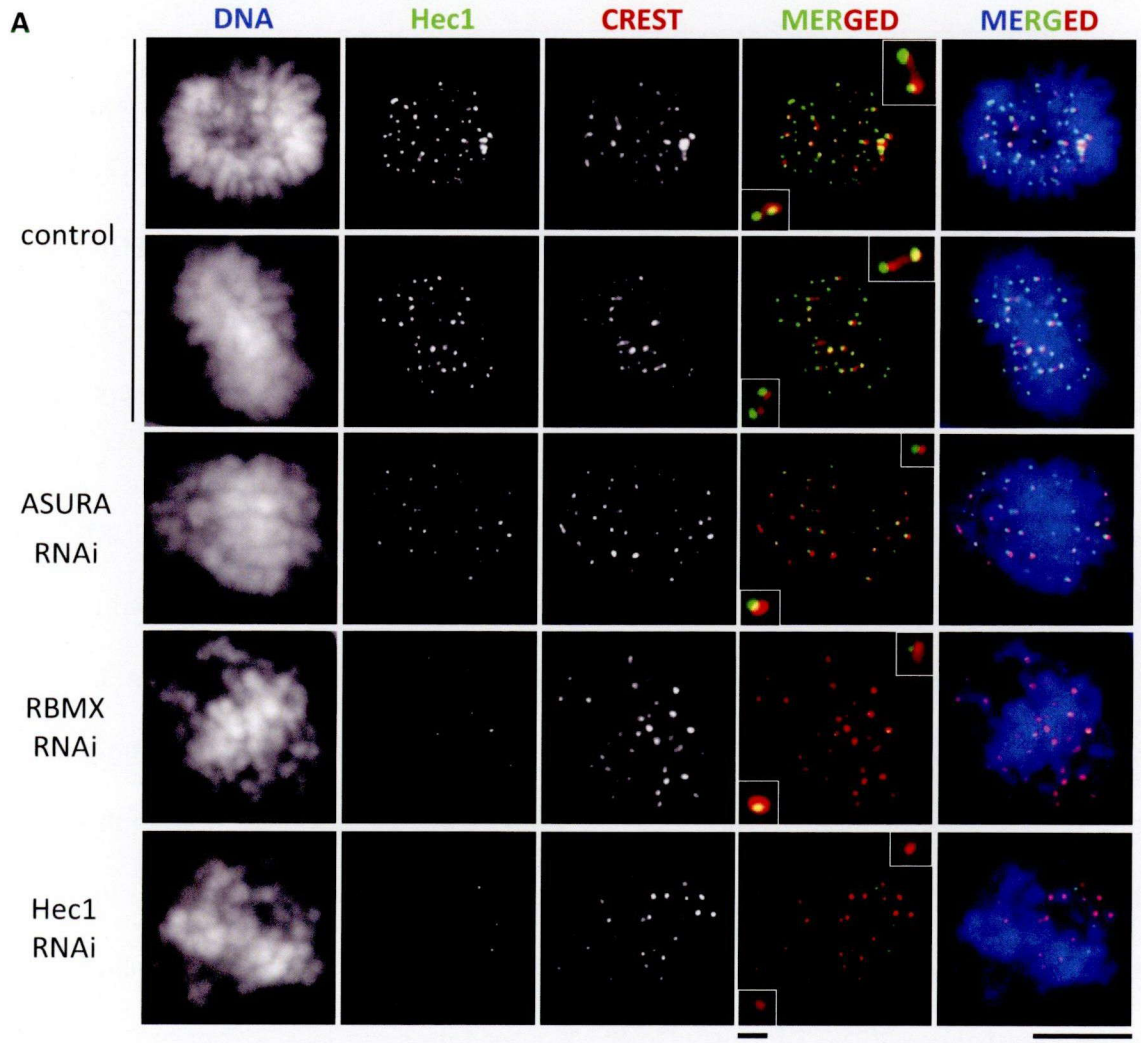

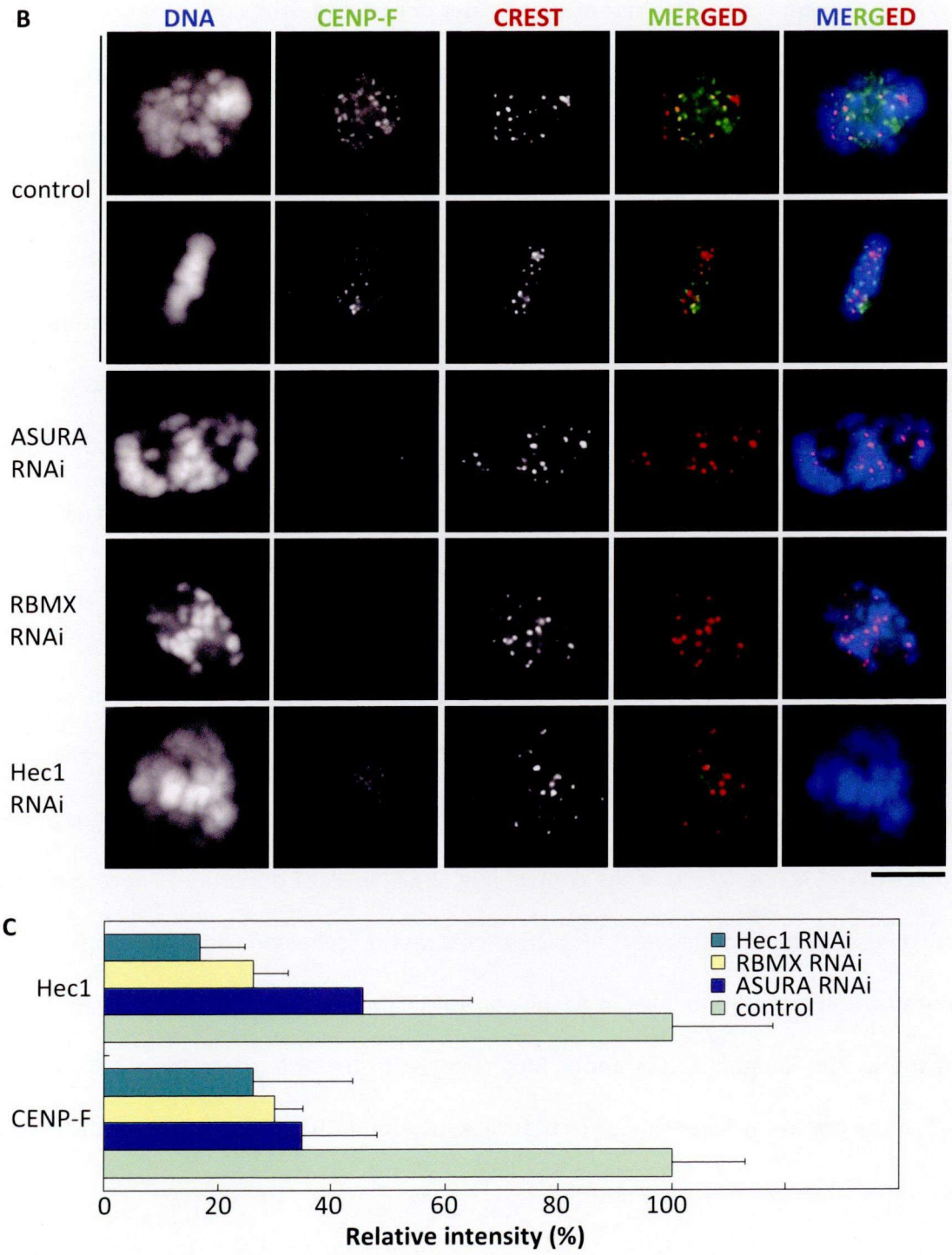

Fig. 2-4 ASURA and RBMX depleted cells showed reduction of CENP-F and Hec1 at kinetochore. (**A**) Signal intensity of Hec1 was decreased after ASURA, RBMX and Hec1 RNAi. Cells with unpaired kinetochore signals (compare insets with those of the control) were significant. (**B**) Enrichment of CENP-F at the kinetochore was diminished after ASURA, RBMX and Hec1 RNAi. (**A**, **B**) Scale bars are 10 μm, and 1 μm for the insets. (**C**) Quantitative measurement of signal intensities of Hec1 and CENP-F

2.3.4 Hec1 is required for the retention of sister chromatid cohesion

As I examined the signal intensity of kinetochore proteins in ASURA, RBMX and Hec1 RNAi cells (Fig. 2-4), I found that in many cells the signals were not paired, even in Hec1 depletion (compare the CREST signals with control cells in Fig. 2-4A, B). Therefore, I performed chromosome spread of Hec1 RNAi cells to ascertain these observations. ASURA RNAi cells were used to facilitate the analysis. Loss of ASURA resulted in premature sister chromatid separation (Fig. 2-5A) in about 50% of the mitotic cells (Fig. 2-5B), as reported earlier (Takata et al. 2007b). Interestingly, even in Hec1-depleted cultures, some 30% of cells (Fig. 2-5B) showed premature sister chromatid separation (Fig. 2-5A), which has not been reported elsewhere.

Although the defects in cohesion were less severe in Hec1 depletion, it is feasible that lowered Hec1 intensity contributed partially to the premature chromatid separation phenotype associated with ASURA and RBMX RNAi. Further analyses showed that sister chromatids were separated only when Hec1 intensities were equal or lower than 5% (Fig. 2-6D) of the control (Fig. 2-6A) in Hec1 depletion. Therefore, this data revealed that deficiency in sister chromatid cohesion derived from Hec1 mislocalization was not obvious in ASURA or RBMX depletion. In particular, when Hec1 intensity at the kinetochore is about 50% (Fig. 2-6B) or 30% (more than 10% in Fig. 2-6C) of the control, a level similar to that of ASURA and RBMX disruption, respectively, sister chromatids were rarely separated.

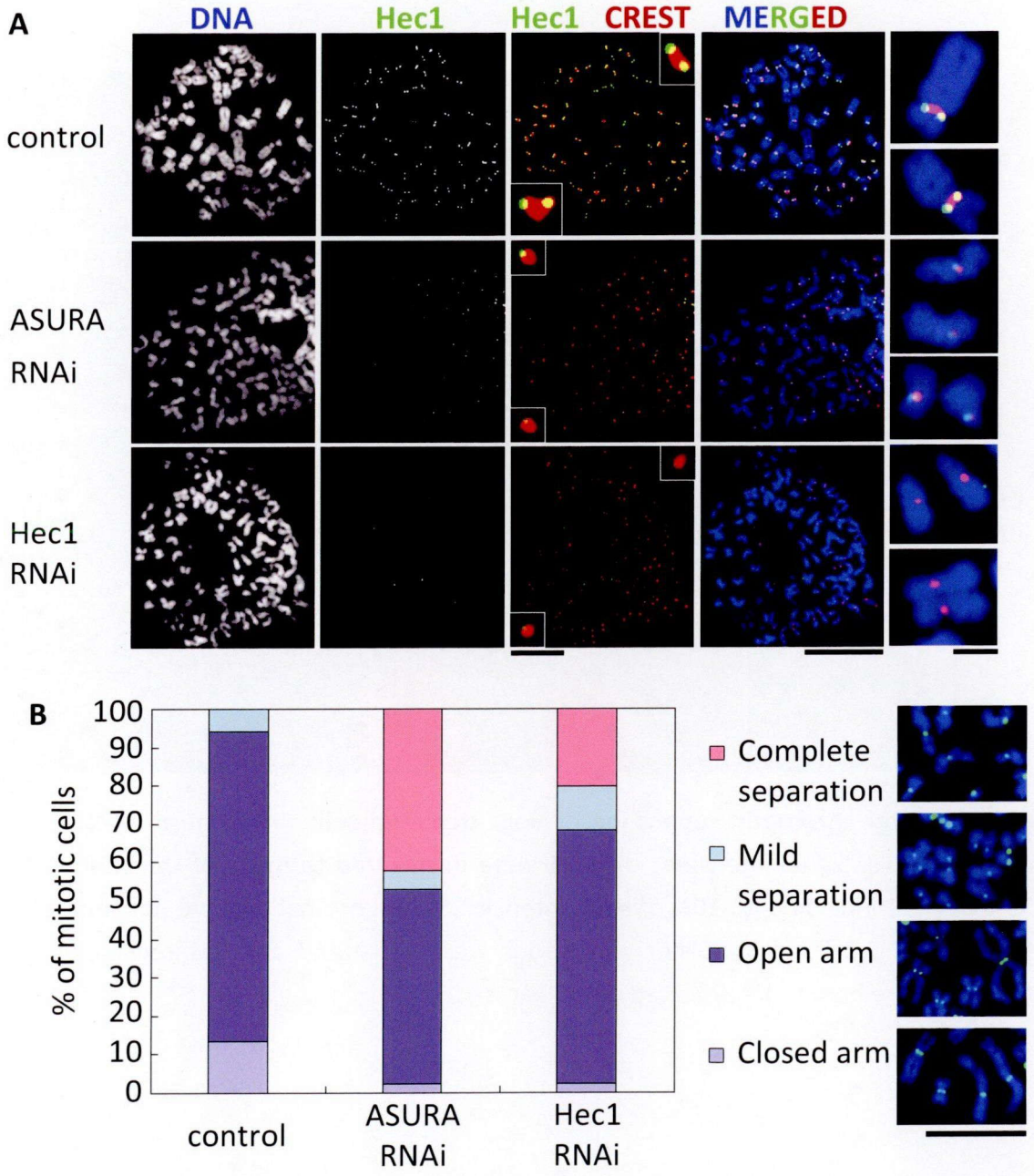

Fig. 2-5 ASURA and Hec1 depleted cells showed defects in sister chromatid cohesion. (**A**) Sister chromatids were separated both in ASURA and Hec1 RNAi. CREST signal appeared as a single dot. Scale bars are 10 μm, and 1 μm for the insets. (**B**) Quantitative measurement of sister chromatid cohesion after ASURA and Hec1 RNAi. Scale bar is 10 μm

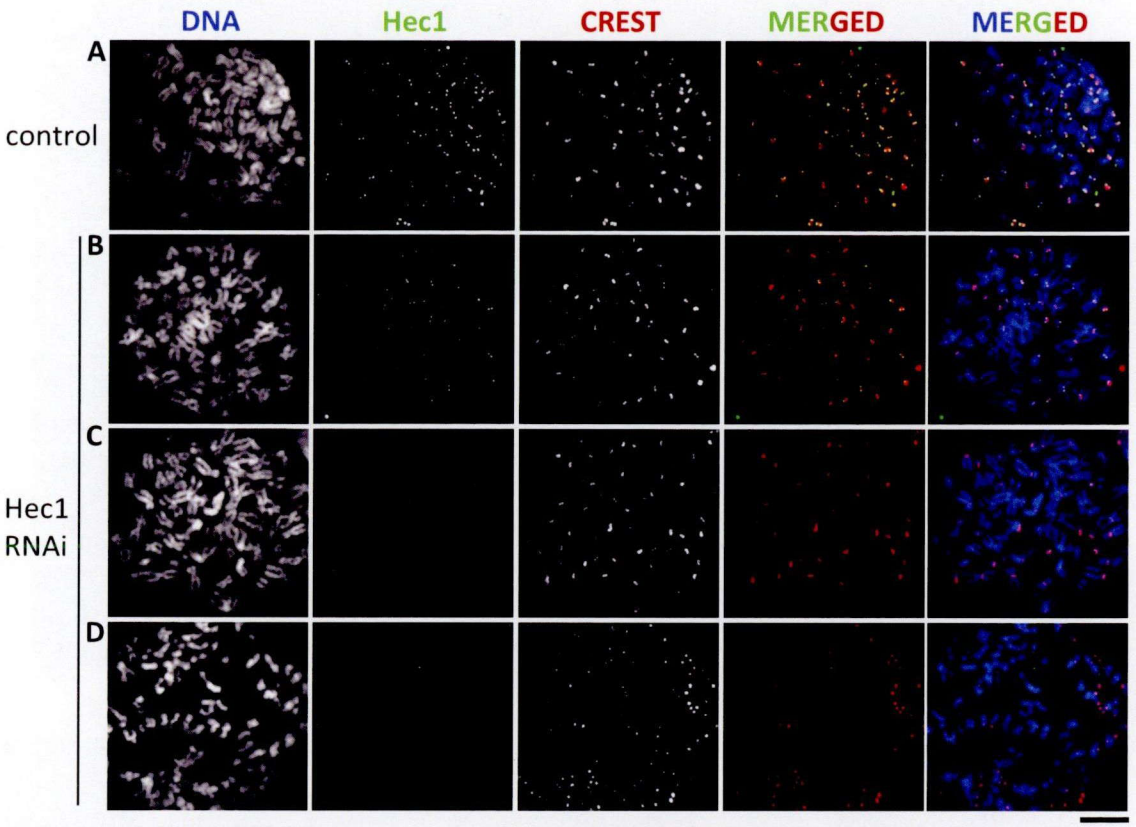

Fig. 2-6 Sister chromatid separation in Hec1 depleted cells. (**A**) Control. (**B-D**) Hec1-depleted cells. Signal intensities of Hec1 were normalized to those of the control. (**B**) 50% of Hec1 intensity. (**C**) 10% of Hec1 intensity. Sister chromatids were not separated. (**D**) 5% of Hec1 intensity. Sister chromatids were separated. Signal intensities lower than 5% were hard to be detected. Scale bar is 10 μm

2.4 Discussion

Since both ASURA and RBMX do not specifically localize to the centromere/kinetochore, their contributions to the kinetochore formation as well as cohesion are unique. To test if the phenotypes are specific to ASURA and RBMX depletion, we confirmed that mitotic defects were rescued by expressing RNAi-refractory ASURA or RBMX plasmid in the same RNAi condition (Takata et al. 2007b; Matsunaga et al. unpublished data). In addition, to exclude the possibility that cells with sister chromatid separation were indeed bypassed SAC and entering anaphase, we confirmed that ASURA or RBMX RNAi cells were arrested in prometaphase or metaphase by several experiments. First, expression levels of cyclin B and securin, proteins that are degraded at anaphase onset, were unaltered in ASURA or RBMX RNAi cells comparing to control metaphase cells. Second, the percentage of mitotic defects was unchanged by the proteasome inhibitor MG132 treatment to inhibit anaphase onset.

How Hec1 might contribute to cohesion protection is unclear. In this study, I found that CENP-F enrichment at the kinetochore required Hec1 (Fig. 2-4B, C), which is consistent with the results obtained by Miller et al. (2008), although previous reports suggested the different results (Martin-Lluesma et al. 2002; Liu et al. 2006). Repression of CENP-F weakens centromeric cohesion in about 28% of metaphase spread chromosomes (Holt et al. 2005). The present study indicate that premature separation was found in about 30% of the metaphase spread chromosomes after Hec1 knockdown (Fig. 2-5B), while CENP-F intensities at the kinetochores were less than 25% of the control (Fig. 2-4B, C). These results suggest the possibility that loss of sister chromatid cohesion with Hec1 RNAi recapitulate partially, if not all, the phenotypes in decreased levels of CENP-F. Alternatively, a recent report showed that Aurora B and Hec1 recruited Mps1 to the kinetochore to ensure that mitotic checkpoint is efficient at the

onset of mitosis (Saurin et al. 2011). This study, in agreement with those demonstrated by Meraldi et al. (2004) indicating that Hec1 localization at the kinetochore is crucial for SAC activation, and mitotic arrest is abrogate when Hec1 is totally depleted from the kinetochore. Therefore, it is also feasible that the cells with premature loss of sister chromatid cohesion were indeed cells that had overridden the mitotic checkpoint and entered anaphase as the Hec1 levels were very low (Fig. 2-6D). Nevertheless, the possibility that the loss of sister chromatid cohesion in ASURA or RBMX depletion was due to the lower levels of Hec1 was not apparent from the data. Hec1 expression remains unperturbed in the absence of ASURA and RBMX (Fig. 2-3A). Hec1 RNAi alone does not impair sister chromatid cohesion as much as ASURA or RBMX depletion. In particular, when Hec1 intensity at the kinetochore is above 10% of the control, a level similar to that of ASURA and RBMX disruption, sister chromatids were rarely separated.

A recent study indicated another possibility for the untimely sister chromatid separation, referred to as cohesion fatigue, which is due to prolonged mitotic arrest (Daum et al. 2011). Whether this is the case in Hec1, ASURA and RBMX RNAi is unknown, because stable microtubule interactions were very few (Takata et al. 2007b; Matsunaga et al. unpublished data), whereas cohesion fatigue requires microtubule pulling forces.

To understand the underlying mechanism, interaction partner(s) of ASURA or RBMX localized to the kinetochore should be determined. However, initial mass spectrometry screening did not detect any kinetochore protein from ASURA or RBMX immunoprecipitates. In addition, previous yeast-two-hybrid system screening for protein interactions provided by the MitoCheck consortium (Neumann et al. 2010; www.mitocheck.org) did not identify any kinetochore component interacting with either ASURA or RBMX. How can ASURA and RBMX be involved in kinetochore

assembly without being integrated in the kinetochore or stably interacting with the kinetochore proteins? There are three major possibilities:

1. Functions of ASURA and RBMX other than mitotic functions

ASURA, also known as PHB2, is required for histone deacetylase recruitment (Kurtev et al. 2004). Human SIRT2 (sirtuin 2), homologs to the yeast Sir2 protein, preferentially deacetylases tubulin and histone H4 (Inoue et al. 2007), and show interaction with PHB2 by yeast-two-hybrid screening (Ewing et al. 2007). In budding yeast, Sir2 is an essential silent chromatin (a repressive chromatin structure that functionally resembles heterochromatin of higher eukaryotes) component. Recent study showed that binding of cohesin to silent chromatin to a small carboxyl terminal fragment of Sir2 targeted sister chromatid cohesion, which does not required Sir2 deacetylase activity (Wu et al. 2011). Another report indicated that hypoacetylated H4K16 is important for maintaining the integrity of the kinetochore and accurate chromosome segregation, whereas Sir2 is the H4K16 deacetylase (Choy et al. 2011). However, the functions of human SIRT2 have not yet been determined, moreover the correlation with ASURA is largely unknown. Similarly, whether the role of ASURA as transcription repressor contributes to kinetochore assembly or cohesion is largely unknown. No significance difference in protein expression levels of Hec1 (Fig. 2-3A) and Scc1 (the cohesin subunit) (Takata et al. 2007b) was detected after ASURA RNAi.

As for RBMX, whether its role in pre-mRNA spicing regulation is involved in kinetochore assembly and/or cohesion protection is not known, however the expression levels of several kinetochore proteins and Scc1 was unaltered in RBMX depletion (Fig. 2-3A; Matsunaga et al. unpublished data). Whether RNA binding is essential for the localization of RBMX on the chromosomes is under investigation. A study of maize CENP-C revealed that centromeric RNA helps to recruit CENP-C to the

inner kinetochore by stabilizing its DNA binding (Du et al. 2010). However, the direct correlation of centromeric RNA and RBMX mitotic functions are not clear.

2. Sister chromatid cohesion is required for kinetochore assembly

We found that both ASURA (Ilma Master Thesis 2010) and RBMX (Akatsuchi Master Thesis 2011) interact with cohesin. In addition, since Hec1 RNAi also resulted in premature sister chromatid separation, I considered whether cohesion itself is required for kinetochore development. Shugoshin (Sgo) localized to the inner centromere and is protecting centromeric cohesion until anaphase. Loss of Sgo in human cells reduced the kinetochore localization of CENP-E and CENP-F by 2.9- and 2.3-fold, respectively, whereas Hec1 localization is highly unperturbed (Salic et al. 2004). However, Vagnarelli et al. (2004) showed that specific inhibition of topoisomerase II, which is required for decatenation of replicated chromosomes, can bypass the cohesin requirement for metaphase chromosome alignment and spindle checkpoint silencing. Since the kinetochore effects of Scc1 deficiency can be compensated for by topoisomerase II inhibition, Scc1 is not absolutely required for kinetochore assembly or function, and that its principal role in allowing the onset of anaphase is the establishment of sufficient inter-kinetochore tension to allow bi-orientation. Therefore, the effect of cohesion to kinetochore formation may not be significant.

3. ASURA and RBMX may be the targeting factors for kinetochore protein(s)

ASURA localizes at the nucleus/chromosome and cytoplasm during G2 phase, prophase and prometaphase. RBMX localizes at the nucleus during interphase, while associates with chromosomes during prophase and prometaphase (Fig. 2-2). Hec1 (Liu et al. 2006) and CENP-F (Liao et al. 1995) assemble at the kinetochore since late G2. Although ASURA and RBMX do not localize specifically to the centromere region or kinetochore, they are required for the localization of Hec1 and CENP-F. Therefore, ASURA and RBMX

may act as targeting factor for kinetochore protein(s) during late G2 or early mitosis.

Combining the present data with our previous studies (Takata et al. 2007b; Matsunaga et al. unpublished data), kinetochore proteins mislocalized after ASURA (green boxes) or RBMX (indicated in blue font) depletion are as follows (Fig. 2-7). Both ASURA and RBMX are required for the localization of Hec1, CENP-E and CENP-F, while RBMX RNAi also reduced the localization of Mis13 (a subunit of the Mis12 complex). Kinetochore localization of all subunits of the human Mis12 complex is interdependent (Kline et al. 2006). The possible pathways involved in according to early reports (Liu et al. 2006; Cheeseman and Desai 2008; Hori et al. 2008) are indicated (Fig. 2-7). Hec1 RNAi abolished CENP-F enrichment at the kinetochore, and therefore is acting upstream of CENP-F (red arrow). CENP-E required CENP-C and CENP-F for its localization. It is feasible that RBMX is required for Mis12 complex localization, whereas ASURA is required for Hec1 targeting. Liu et al. (2006) showed by EM that Mis12 and Hec1 RNAi exhibited very distinct phenotypes, although Hec1 required Mis12 complex for its localization. Accordingly, they are proposed to be involved in two different pathways, where Hec1 is the hub of the two pathways. Because Hec1 (in ASURA RNAi) and Mis13 (in RBMX RNAi) acting upstream among all kinetochore proteins have been tested, the immunofluorescence results suggest that ASURA is involved either in the CENP-I or CENP-C pathway by targeting Hec1, whereas RBMX is most probably involved in the CENP-C pathway by targeting Mis13 (See Chapter 4 for details). By EM study, it is possible to determine which pathways ASURA and RBMX are involved in.

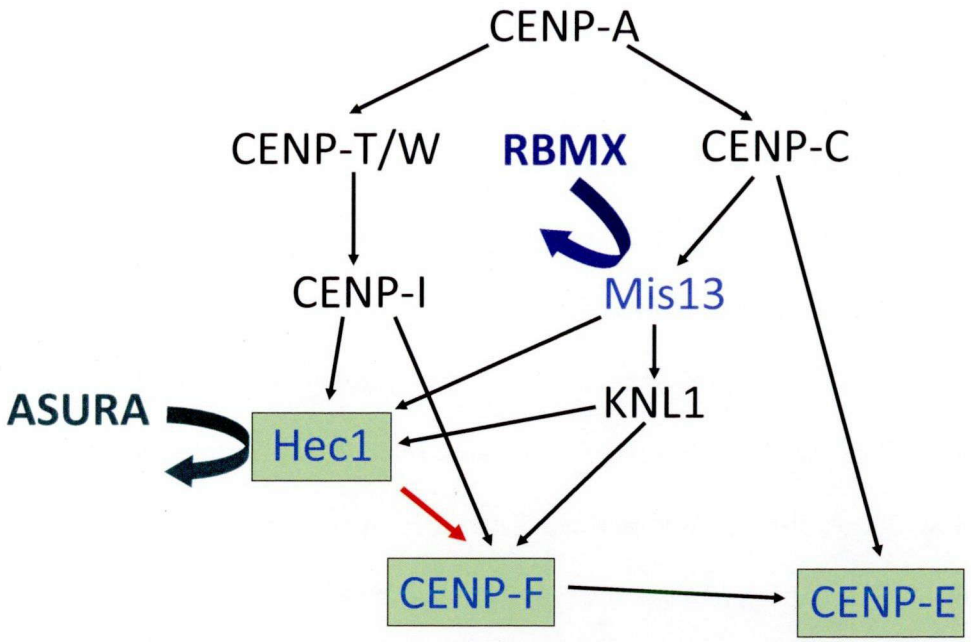

Fig. 2-7 Possible pathways ASURA and RBMX may be involved in targeting kinetochore protein(s). Proteins mislocalized after ASURA and RBMX depletion were indicated as green boxes and in blue font, respectively. Arrows show the dependencies of the kinetochore proteins targeting. Black arrows indicating the dependencies reveal by previous studies. CENP-F requires Hec1 for its kinetochore localization (red arrow). Round arrows (green and blue) indicate that both ASURA and RBMX are not the kinetochore component proteins

2.5 Summary

ASURA and RBMX make important contributions to chromosome segregation due to its importance in regulating sister chromatid cohesion and proper kinetochore assembly. Interestingly, both ASURA and RBMX do not show specific localization at the kinetochore or centromeric region. Kinetochore proteins, except for CENP-A where HJURP serves as its deposition factor (Dunleavy et al. 2009; Foltz et al. 2009), are known to be recruited by other kinetochore proteins upstream (Maiato et al. 2004; Chan et al. 2005; Liu et al. 2006; Cheeseman and Desai 2008). Therefore, the involvement of ASURA and RBMX are unique as they are not integrated in the kinetochore.

ASURA and RBMX associate with the chromosome during late G2 and early mitotic phases. In agreement with their localization patterns, outer kinetochore proteins accumulated at the kinetochore from late G2 phase, and some of them achieve full complement during prometaphase, including Hec1 and CENP-F (Cheeseman and Desai 2008). Therefore, it is feasible that ASURA and RBMX act as targeting factors for kinetochore protein(s), which is the third possibility described above. ASURA and RBMX are required for Hec1, CENP-F and CENP-E localization (Fig. 2-4; Takata et al. 2007b; Matsunaga et al. unpublished data). RBMX RNAi also disrupted Mis13 of the Mis12 complex (Matsunaga et al. unpublished data), which is required for Hec1 localization. These suggested that ASURA is targeting Hec1 (or Ndc80 complex), whereas RBMX is required for Mis13 (or Mis12 complex) loading.

Based on the pattern of chromosome distribution, the nonalignment phenotype associated with ASURA and RBMX RNAi was similar to that observed after depletion of Mis12 complex (Goshima et al. 2003; Kline et al. 2006) and Hec1 (Ndc80 complex). To further investigate how ASURA and RBMX might contribute to kinetochore formation,

particularly to determine their involving pathway(s), I turned to EM analysis to study kinetochore structures after the RNAi treatments in order to obtain some clue of how both proteins contribute to kinetochore development.

Chapter 3

Kinetochore maturation

3.1 Introduction: Kinetochore structure

Almost a century after the discovery of centromere by Walter Flemming in 1879, electron microscopic (EM) studies provided the first insight into the layered structure forming at the primary constriction of the chromosome (Brinkley and Stubblefield 1966). This structural body was termed kinetochore, and the trilaminar morphology was later established by several studies using conventional chemical fixation procedures and thin-section transmission EM of chromosomes in vertebrate cells (Jokelainen 1967; Comings and Okada 1971).

Kinetochore morphogenesis has been well documented in for mammalian cells (Rieder 1982), especially in PtK (Roos 1973). Correlative light microscopy and EM revealed that, during mitosis, the kinetochore is visible on the surface of the primary constrictions as roughly circular patches of fine fibrillar materials (fibrillar ball), which gradually differentiated into two layers within the ball and developed finally into the trilaminar morphology. This layered structure of kinetochore becomes visible on the surface of the chromosome from late prophase, about the time of nuclear envelope breakdown, but before the acquisition of microtubules (Roos 1973). Innermost is an inner plate, which forms the interface with chromatin. The central kinetochore layer (15-30 nm thick) appears as a less electron dense interzone. Outer kinetochore plate (35-40 nm thick) is a dense but loosely organized flexible network of 10-20 nm fibers (Rieder and Salmon 1998), which interacts with multiple microtubules by either

extending out from the plate to bind microtubule walls or embedded the microtubule plus-end tips in a radial mesh (Dong et al. 2007). The outermost is a moderately dense filamentous material extended ~100-300 nm away from the outer layer, termed fibrous corona, which can only be visualized in the absence of microtubules. Most mammalian kinetochores ranged from 100-500 nm in diameter (Rieder 1982), whereas human kinetochores are 200-500 nm in size (Wendell et al. 1993). The diminutive size of the kinetochore makes the electron microscope the only tool available for visualizing kinetochore structure.

As kinetochores undergo a cycle of assembly and disassembly during each mitotic division, defects observed in kinetochore after ASURA and RBMX RNAi may be derived from disruption of the maturation process. I first ascertained the kinetochore assembly in HeLa cells. Based on the stepwise ultrastructural alteration of the kinetochore in each mitotic phase, I developed a classification scheme represent kinetochore assembly and disassembly (refer to Fig. 3-11 for details).

3.2 Materials and methods

Cell culture

HeLa cells were maintained in DMEM (GIBCO BRL) supplemented with 10% FBS (Equitech-Bio) at 37°C and 5% CO_2.

Live cell imaging

HeLa cells cultured in 35 mm poly-L-lysine-coated glass-bottom dishes (Matsunami) were transfected with or without Lipofectamine 2000 (Invitrogen). The medium was changed to a CO_2-independent medium, phenol-red free DMEM (GIBCO BRL) containing 10% FBS, 0.1 mg/ml penicillin/streptomycin, 20 mM glutamine, and 100

mM HEPES at 1 hour before imaging. The dishes were placed on the inverted platform of a fluorescence microscope (IX-81; Olympus) equipped with a CO_2 chamber set at 37°C. DIC images were acquired every 15 minutes with a 403 objective controlled with the MetaMorph software (Universal Imaging Corporation). Stacks of images were assembled and processed with the MetaMorph software.

Electron microscopy

HeLa cells grown on plastic coverslips (mono-layer) were transfected with Lipofectamine 2000 alone and were fixed for 1 hour in 3% glutaraldehyde and 0.2% tannic acid in PBS buffer at room temperature. Post-fixation was in 2% OsO_4 for 20 minutes. The cells were dehydrated through an increasing ethanol series and infiltrated with epoxy resin (Quetol 812). The resin was polymerized at 37°C for 12 hours, 45°C for 12 hours and 60°C for 48 hours. Cells of interest embedded in the resin were chosen under an optical microscope and trimmed to ~1.0 mm^2. Samples were cut into 70-80 nm thick serial sections with an ultramicrotome equipped with a diamond knife (ULTRACUT E; Reichart-Jung). The sections were stained with uranyl acetate and lead citrate for examination with a transmission electron microscope (JEM-1200EX; JOEL).

3.3 Results: Kinetochore in each mitotic phase

In human, descriptions of the mature trilaminar kinetochores are abundant, but yet, ultrastructural studies of the kinetochore assembly process are lacking. Therefore, before further analyses of the RNAi defects could be performed, kinetochore maturation, particularly in human should be elucidated in detail. For this purpose, I analyzed 1 prophase, 23 prometaphase, 8 metaphase, 5 anaphase and 3 telophase cells from the mock control (transfected with Lipofectamine 2000 alone).

During observation, I found that the appearance of individual kinetochores varied even in successive thin serial sections (Fig. 3-1A), which has also been reported for Indian muntjac chromosomes (Zinkowski et al. 1991). Hence, several adjacent serial sections were observed for individual kinetochores to determine their structures. Adjacent serial sections were indicated by serial numbers of i-v. In addition, cells transfected with Lipofectamine 2000 often resulted in 'full of holes' appearance as depicted in Fig. 3-1B and many other electron micrographs (describe below). Cells were monitored for the effects of Lipofectamine 2000 treatment. Cells either transfected with (+) or without (-) Lipofectamine 2000 were examined (Fig. 3-1B). 20 cells without treatment and 40 transfected cells were recorded. There was no significant difference in mitotic duration (i.e., prophase until cytokinesis) between both conditions. Moreover, despite the 'full of holes' appearance, Lipofectamine 2000 treatment did not apparently affect the viability of those cells.

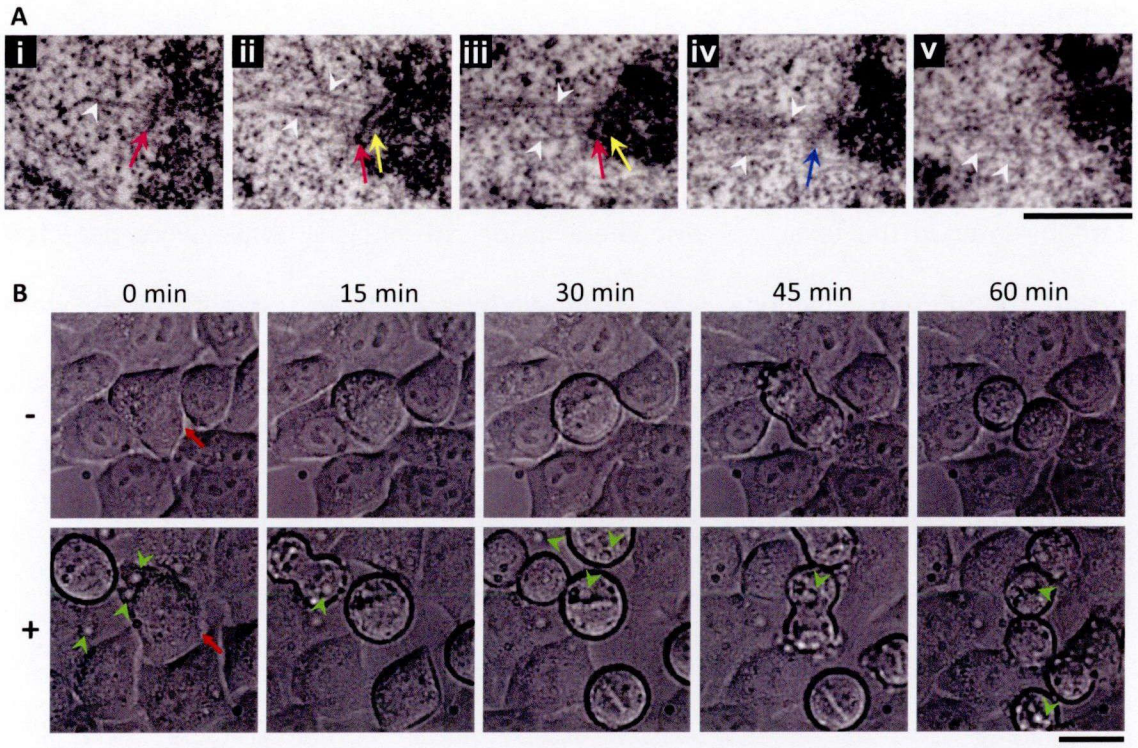

Fig. 3-1 Serial sections of a trilaminar kinetochore with robust microtubule attachment and the effects of Lipofectamine 2000 transfection to the cells. (**A**) **i-v** Continuous adjacent serial sections of a trilaminar kinetochore. Outer plate (red arrows) and inner plate (yellow arrows) are apparent. Microtubules are indicated by white arrowheads. **iv** The kinetochore was rather fuzzy (blue arrow). Scale bar is 500 nm. (**B**) Time-lapse of cells treated with or without Lipofectamine 2000, indicated as + and -, respectively. Red arrows denoted cells at the time point of 0 minute (min). Bubbles or 'holes' that were generated by Lipofectamine 2000 treatment are indicated by green arrowheads. Scale bar is 10 μm

3.3.1 Prophase

Fig. 3-2A showed a prophase HeLa cell. The nuclear envelope (green arrows) and nucleoli (red arrowheads) are visible. Microtubules were not found on kinetochore (describe later in the text), nor elsewhere inside the nucleus, while were detected outside the nuclear envelope (Fig. 3-2B, white arrowheads). Kinetochores were observed as: 1. fibrous mass (Fig. 3-2D, E, blue arrows); 2. Fuzzy ball with a partially constructed kinetochore plate (Fig. 3-2C, E, red arrows). Both structures attached to opposite lateral faces of the primary constriction of chromosomes.

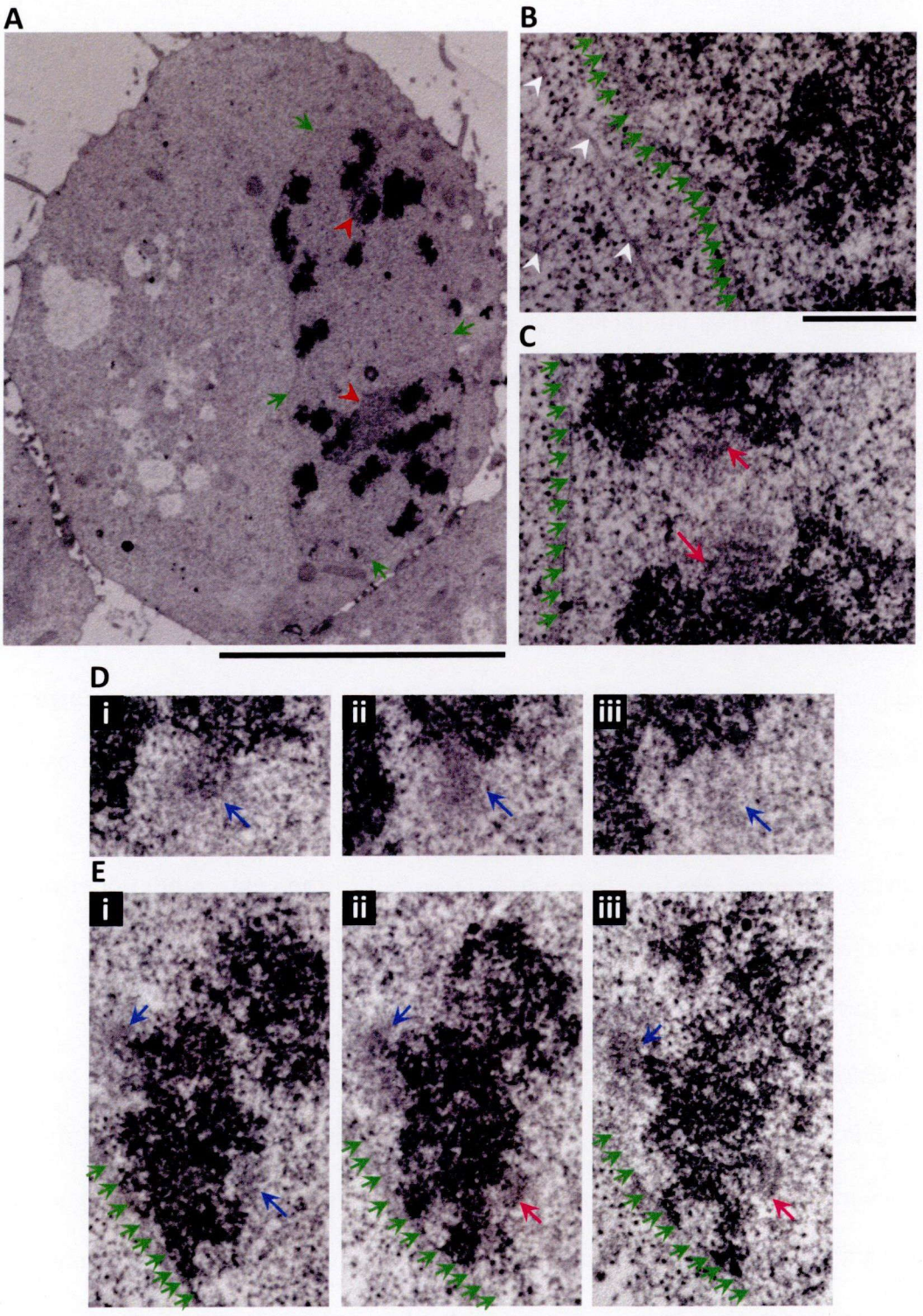

Fig. 3-2 Prophase. Green arrows showed the nuclear envelope and red arrowheads indicated nucleoli. Red arrows showed the outer kinetochore plate and blue arrows revealed the fuzzy ball appearance. (**A**) Low magnification of a prophase cell. Scale bar is 10 μm. (**B-E**) High magnification electron micrographs. (**B**) Microtubules (white arrowheads) were observed outside the nucleus. (**C-E**) Kinetochores in the prophase.

(**C**) Fibrillar balls with faint outer plates. (**D**) Fuzzy ball. (**E**) Fibrillar ball with (right, red arrows) or without (left, blue arrows) partially constructed outer plate. (**B-E**) All micrographs are shown in the same magnification. Scale bar is 500 nm

3.3.2 Prometaphase

After nuclear envelope breakdown, kinetochores gradually differentiated into the layered structure while interacting with spindle microtubules. In prometaphase, kinetochores showed a vast variety of appearances according to its maturation and microtubule association. Three types of kinetochores can be distinguished. 1. Fuzzy balls with finely fibrillar materials without internal structure, similar to those in prophase, although they apparently associated with the microtubules (Fig. 3-3D, 3-4G). 2. Fibrillar mass with a somewhat distinguishable outer plate. They are usually stretched upon microtubules pulling (Fig. 3-3C, E, 3-4B-D, 3-5B, D). 3. The unambiguous triple layered structure. An electron dense band (outer plate) and the chromosome body were separated by an electron-lucent middle layer (Fig. 3-3F-H, 3-5B, C). Occasionally, the other electron dense band attached to the centromere (inner plate) was visible (Fig. 3-4E, F).

3.3.2-1 Early prometaphase

An overview of the cell showed chromosomes interaction with the spindle microtubules (Fig. 3-3A). Kinetochores facing the pole (Fig. 3-3B) interacted with robust microtubules (Fig. 3-3C). Kinetochores were usually fuzzy (Fig. 3-3D), however, faint outer layer (red arrows in C and E) were somewhat visible. Nevertheless, the kinetochores are often stretched. In some kinetochores, the outer plate were more electron dense, as shown in Fig. 3-3F-H. Without microtubule attachment, the fibrous corona (blue arrowheads) was visible in 3-3H.

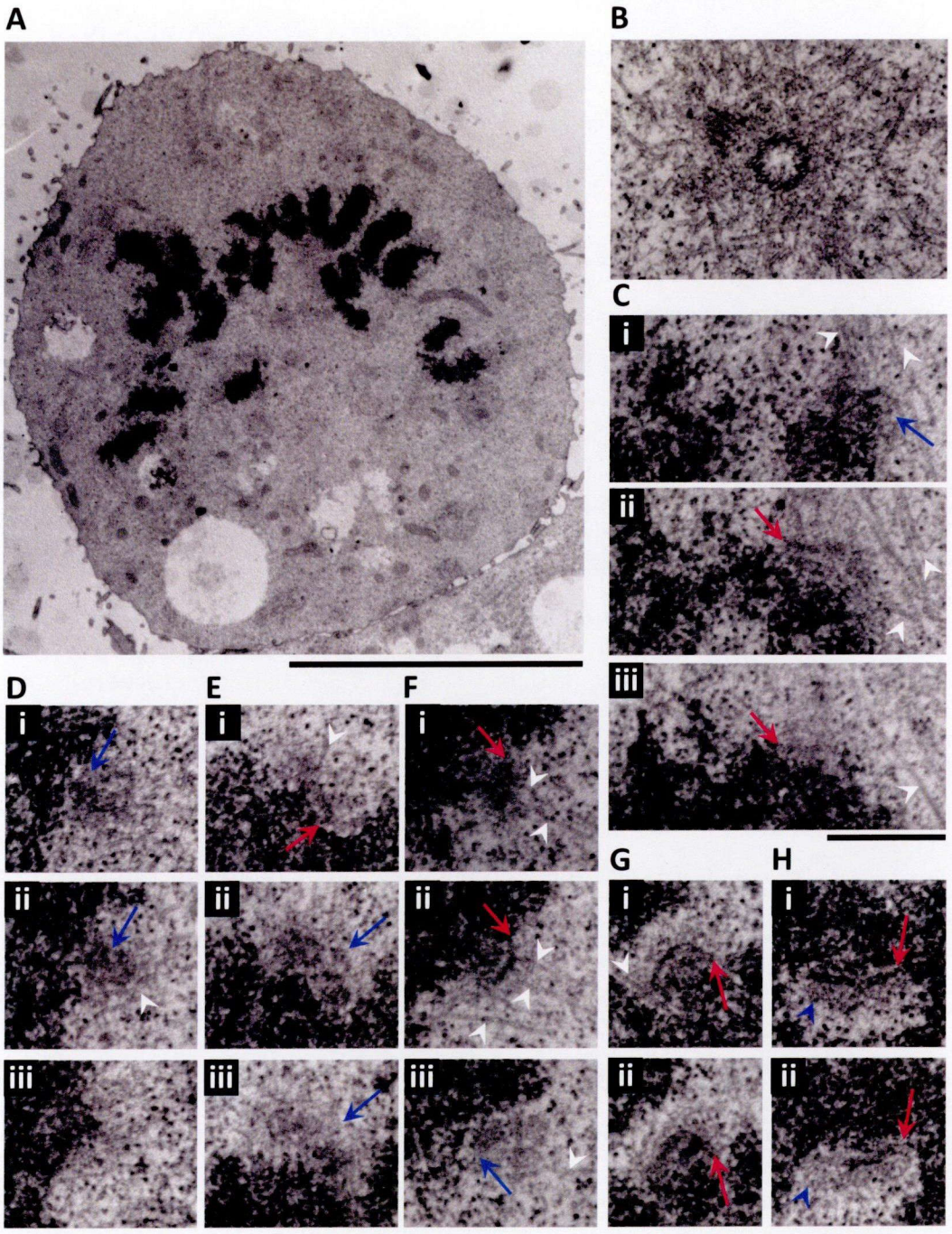

Fig. 3-3 Early prometaphase. Red arrows showed the outer kinetochore plate and blue arrows revealed the fuzzy ball appearance. Microtubules are indicated by white arrowheads. (**A**) Low magnification. Scale bar is 10 μm. (**B**) Centriole as the center of the aster. (**C**-**H**) Higher magnification of kinetochores. (**B**-**H**) All micrographs are shown in the same magnification. Scale bar is 500 nm

3.3.2-2 Mid prometaphase

Chromosomes begin to align at the metaphase plate (Fig. 3-4A). Almost all kinetochores were oriented to face (centrosomes or) each pole, and the faint outer plates were visible (Fig. 3-4B-D), although many of them were stretched while interacting with the microtubules (Fig. 3-4C, left kinetochore in D). Some kinetochores showed the distinct triple layered structure (red and yellow arrows in Fig. 3-4D-F), although some were remained as fuzzy ball without internal structural differentiation (blue arrows in Fig. 3-4G).

3.3.2-3 Late prometaphase

Outer plates were developed in almost all kinetochores (Fig. 3-5B-D) although they were less distinct in Fig. 3-5B (left kinetochore) and D. Most chromosomes were bi-oriented (Fig. 3-5C) and congressed to the metaphase plate (Fig. 3-5A), although a laterally associated kinetochore (left kinetochore in Fig. 3-5B) was found, probably by gliding on the microtubules of bi-oriented kinetochores (Kapoor et al. 2006). During prometaphase, kinetochores facing the poles are favorable in capturing microtubules (Rieder and Alexander 1990). Once this association is established, kinetochores were transported poleward via the corona (Rieder and Alexander 1990), forming lateral interactions with any stabilized microtubule bundles (Cai et al. 2009). Even if chromosomes fail to achieve bi-orientation at the poles, the chromosomes glide along the kinetochore fibers with the aid of CENP-E from the corona to obtain bi-orientation at the metaphase plate (Kapoor et al. 2006), which is known as the mono-oriented pathway (Cai et al. 2009).

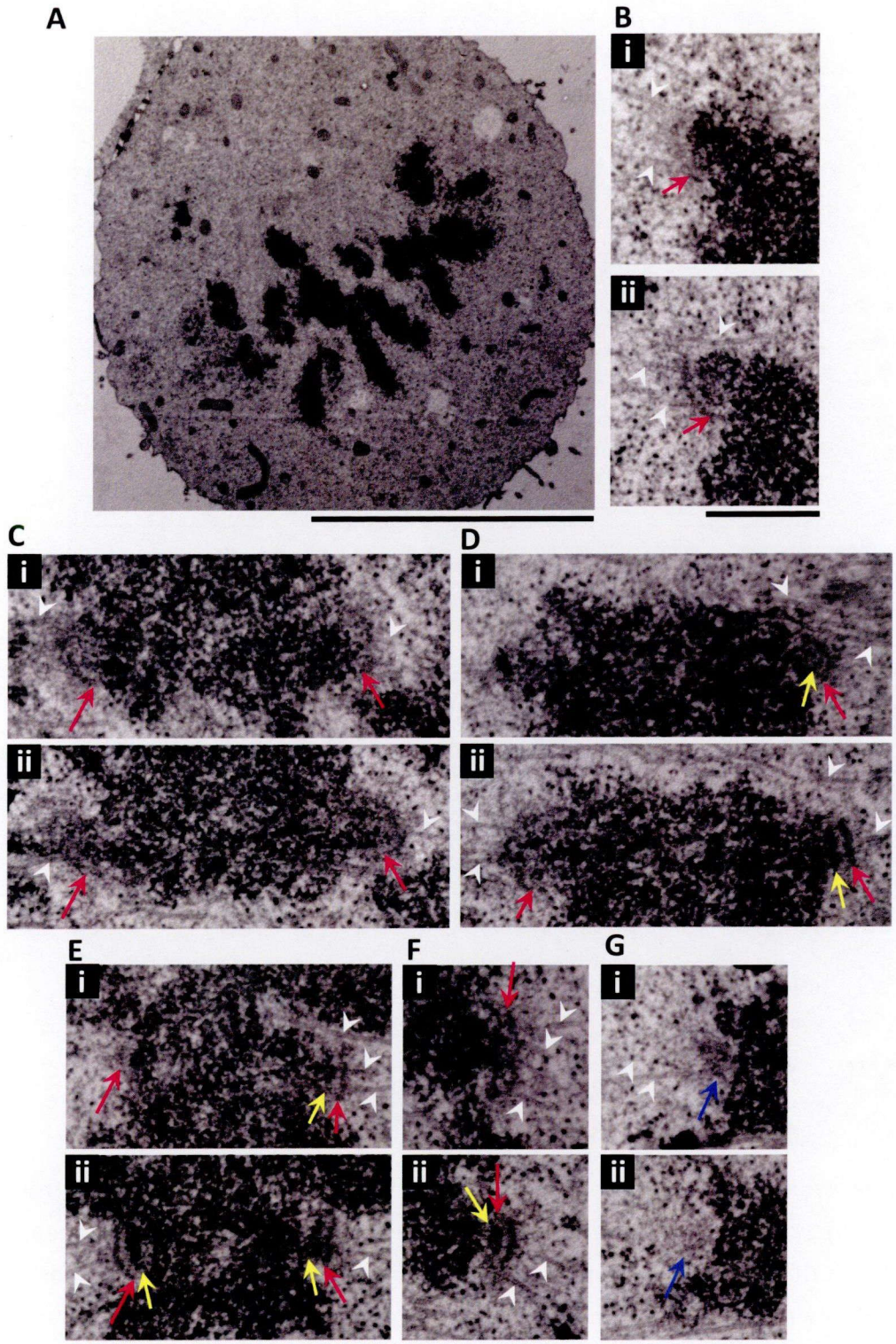

Fig. 3-4 Mid prometaphase. Red and yellow arrows showed the outer and inner plate, respectively. Blue arrows revealed the fuzzy ball appearance. Microtubules are indicated by white arrowheads. (**A**) Low magnification. Scale bar is 10 µm. (**B**-**F**) Outer kinetochore plates are visible. (**G**) Fuzzy ball. (**B**-**G**) All micrographs are shown in the same magnification. Scale bar is 500 nm

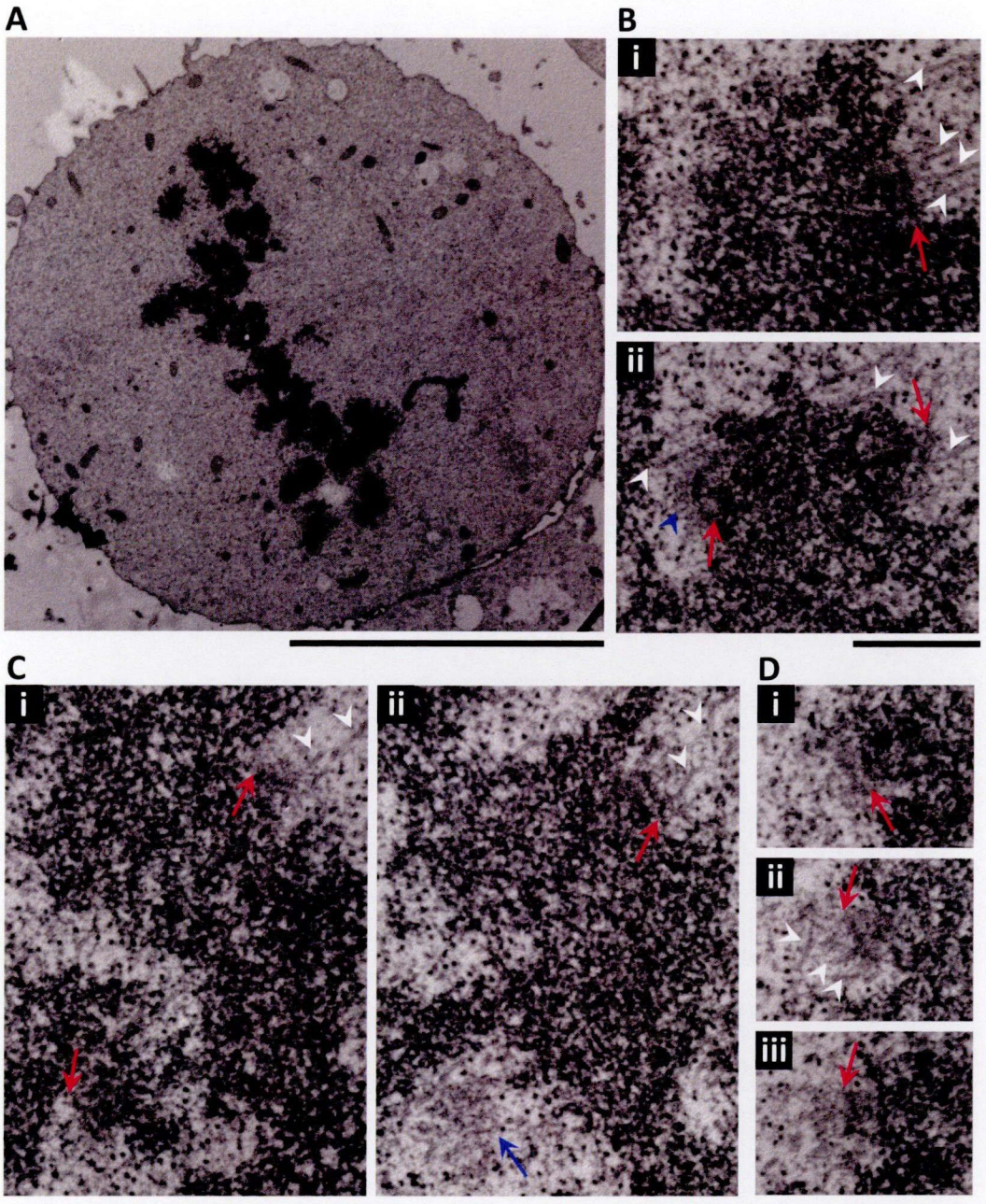

Fig. 3-5 Late prometaphase. Red arrows showed the outer plate and blue arrows revealed the fuzzy ball appearance. Microtubules are indicated by white arrowheads. (**A**) Overview of the cell in low magnification. Scale bar is 10 µm. (**B**) The kinetochore at the left is interacting side-on with a microtubule running close-by, and the fibrous corona (blue arrowhead) is visible. The right kinetochore is interacting end-on with robust microtubules. (**C**) Bi-oriented kinetochores. (**D**) Kinetochore with a less distinct outer plate. (**B-D**) All micrographs are shown in the same magnification. Scale bar is 500 nm

3.3.3 Metaphase

Almost all kinetochores showed the distinct trilaminar structure, with robust microtubules interaction (Fig. 3-6B-D). Chromosomes were bi-oriented (Fig. 3-6B, C and E) and aligned at the metaphase plate (Fig. 3-6A).

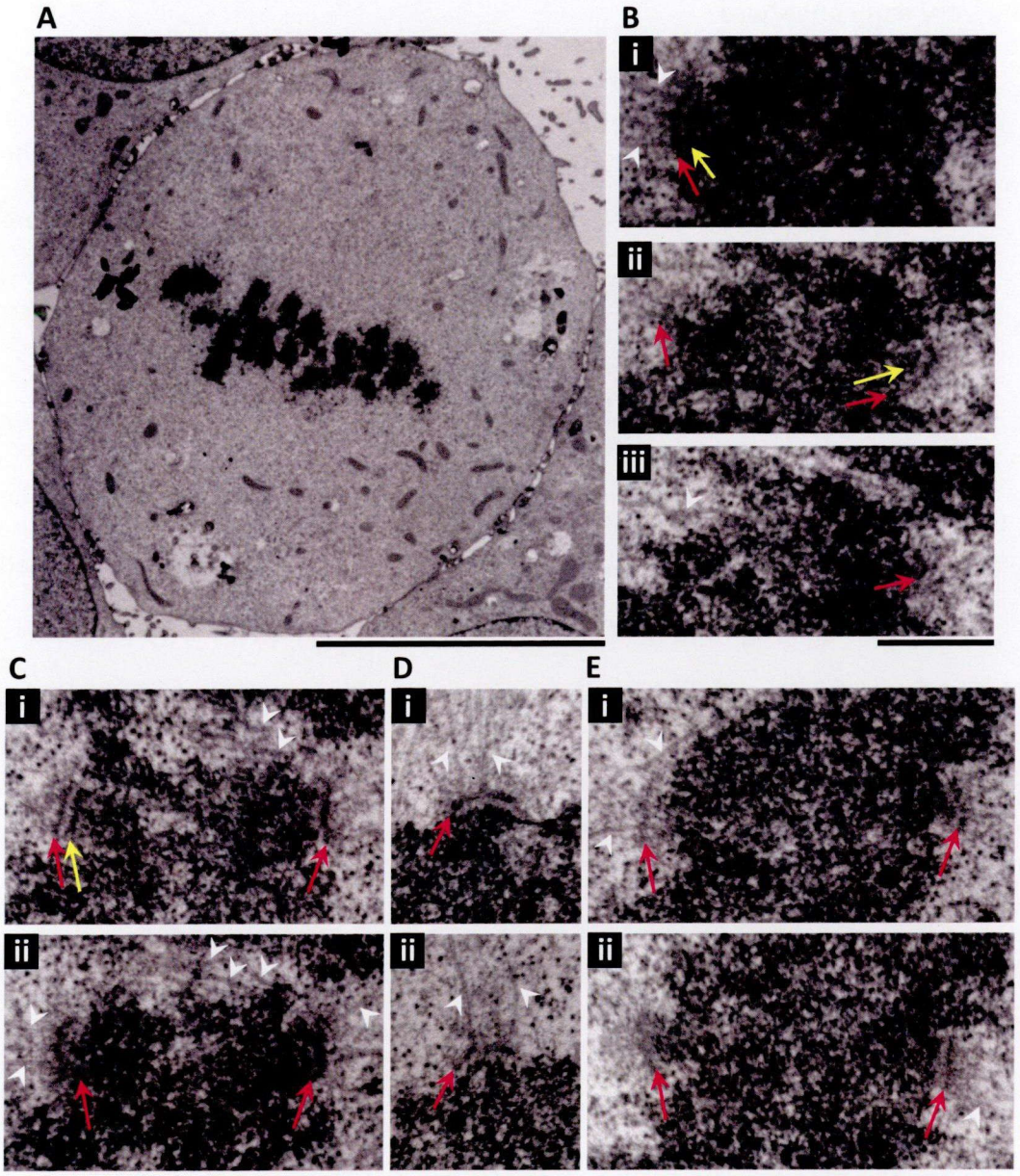

Fig. 3-6 Metaphase. Red and yellow arrows showed the outer and inner plates, respectively. Microtubules are indicated by white arrowheads. (**A**) Chromosomes aligned at the metaphase plate. Scale bar is 10 µm. (**B-D**) Unambiguous trilaminar kinetochores with robust microtubule interactions. (**E**) Less distinct layered structure. (**B-E**) All micrographs are shown in the same magnification. Scale bar is 500 nm

3.3.4 Anaphase

In anaphase, sister chromatids separated and moved to the opposite poles. Two types of kinetochores were observed. 1. Distinct trilaminar kinetochore as in metaphase. 2. Fibrous mass with less distinct layered structure.

3.3.4-1 Very early anaphase

Chromosomes remained aligned at the metaphase plate (Fig. 3-7A) while cohesion between sister chromatids were dissolved (Fig. 3-7B-E). The trilaminar structures were retained, and the inner plates were slightly more electron dense than the chromatin.

3.3.4-2 Mid anaphase

Kinetochores of separated sister chromatids were leading the way to the opposite poles (Fig. 3-8 A). Layered structure of the kinetochores was retained (Fig. 3-8B), although many of them were less distinct and showed the fuzzy ball structure at the same time (Fig. 3-8C, D). Robust microtubule interactions were detected.

3.3.4-3 Late anaphase

Sister chromatids gather at the poles (Fig. 3-9A), microtubules gathered as a stem body at spindle equator (Fig. 3-9B). The layered structure of the kinetochores was visible, although they were fuzzy as in mid anaphase (Fig. 3-9C, D). Microtubule interactions were detected.

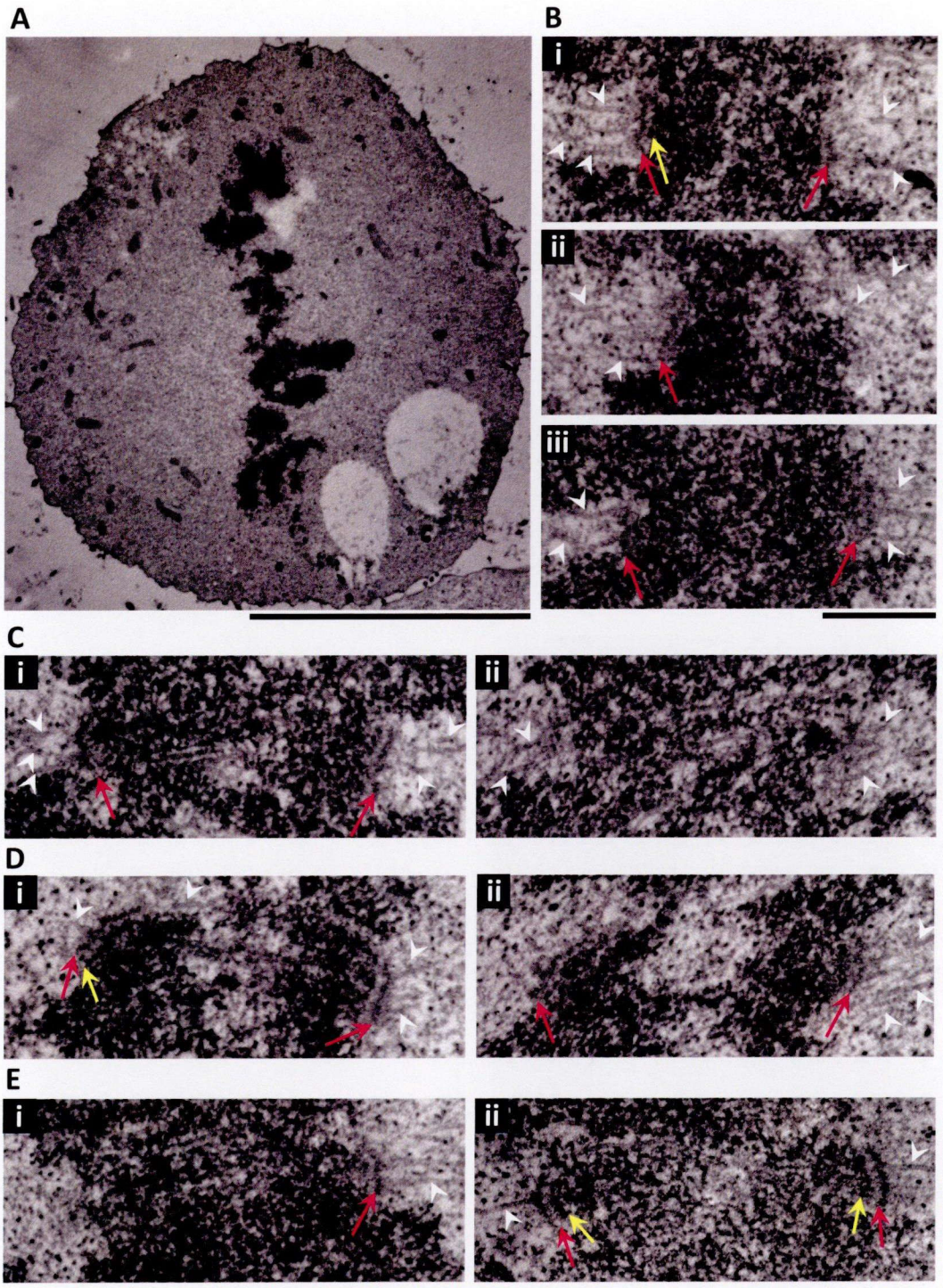

Fig. 3-7 Very early anaphase. Red and yellow arrows showed the outer and inner plates, respectively. Microtubules are indicated by white arrowheads. (**A**) Bi-oriented chromosomes aligned at the metaphase plate. Scale bar is 10 µm. (**B-E**) Unambiguous trilaminar kinetochores with robust microtubules interaction. Sister chromatids began to separate. All micrographs are shown in the same magnification. Scale bar is 500 nm

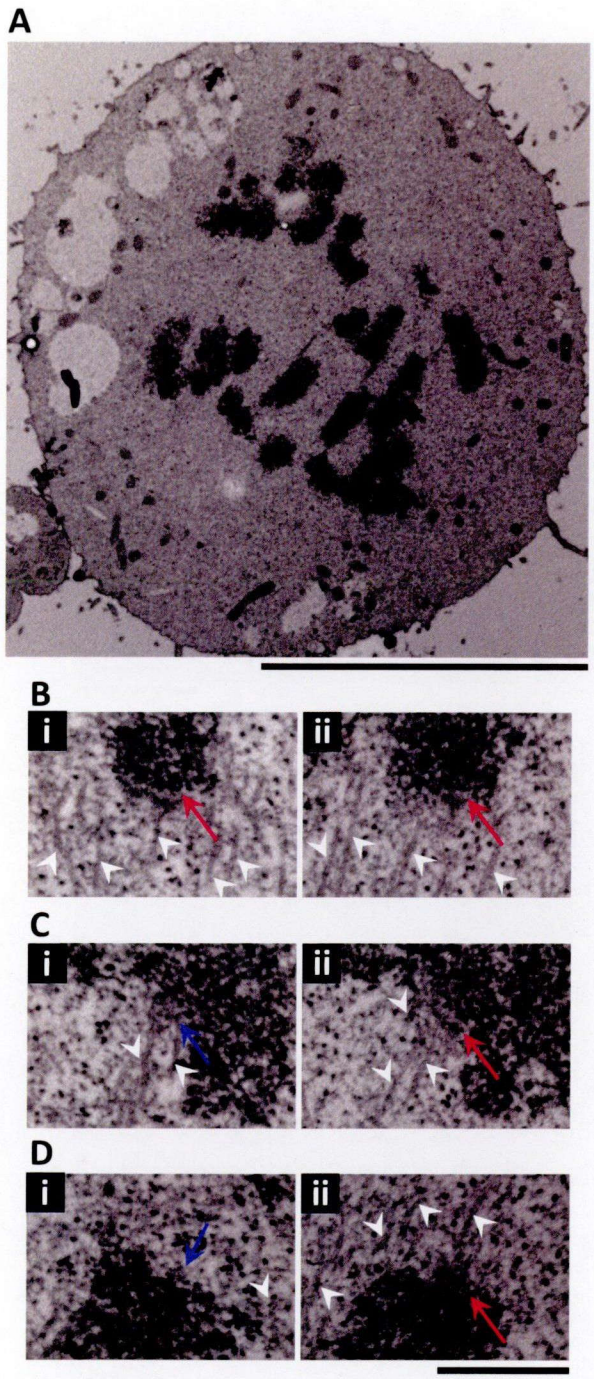

Fig. 3-8 Mid anaphase. Red arrows showed the outer plates and blue arrows revealed the fuzzy ball appearance. Microtubules are indicated by white arrowheads. (**A**) Sister chromatids were moving to the opposite poles. Scale bar is 10 µm. (**B**) Distinct layered structure with robust microtubules interaction. (**C**, **D**) Outer plates were visible although kinetochores were slightly fuzzy. (**B**-**D**) All micrographs are shown in the same magnification. Scale bar is 500 nm

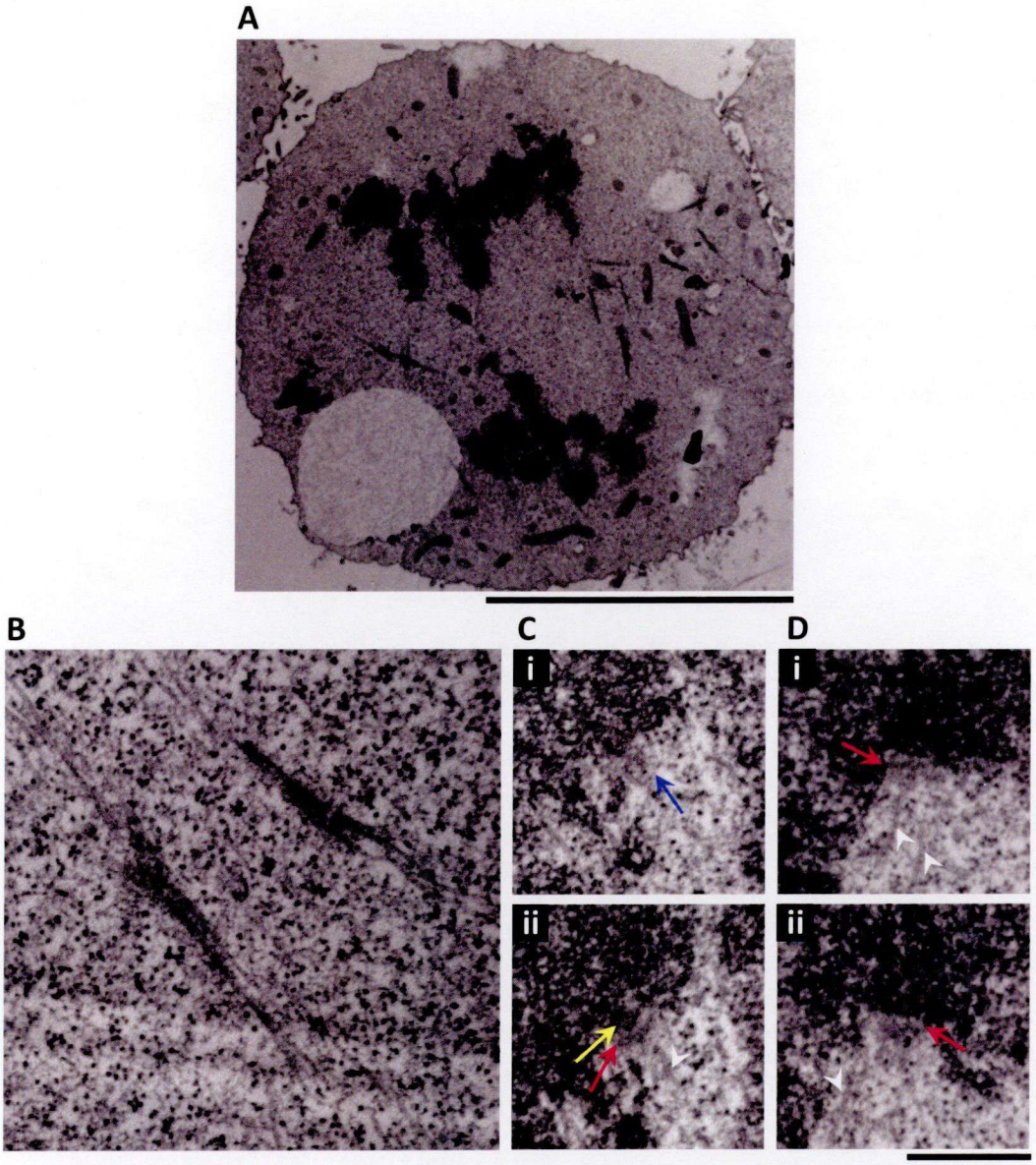

Fig. 3-9 Late anaphase. Red and yellow arrows indicated the outer and inner plates, respectively. Blue arrows revealed the fuzzy ball appearance. Microtubules are indicated by white arrowheads. (**A**) Sister chromatids reached the opposite poles. Scale bar is 10 µm. (**B**) Stem body observed at the spindle equator. (**C**) Kinetochore is trilaminar but slightly fuzzy. (**D**) Outer plate is visible but less distinct. (**B-D**) All micrographs are shown in the same magnification. Scale bar is 500 nm

3.3.5 Telophase

Nuclear envelope reconstructed (Fig. 3-10B) and chromosomes were no longer distinguishable but fused into a continuous mass while an equatorial constriction is initiated (Fig. 3-10A). Two types of kinetochores were visible at the polar faces of daughter nuclei. 1. Less distinct but layered kinetochores interacting with microtubules (Fig. 3-10C). 2. Kinetochore dissolved into fuzzy patches (Fig. 3-10D). However, they were not covered by the nuclear envelope yet (Fig. 3-10C, D).

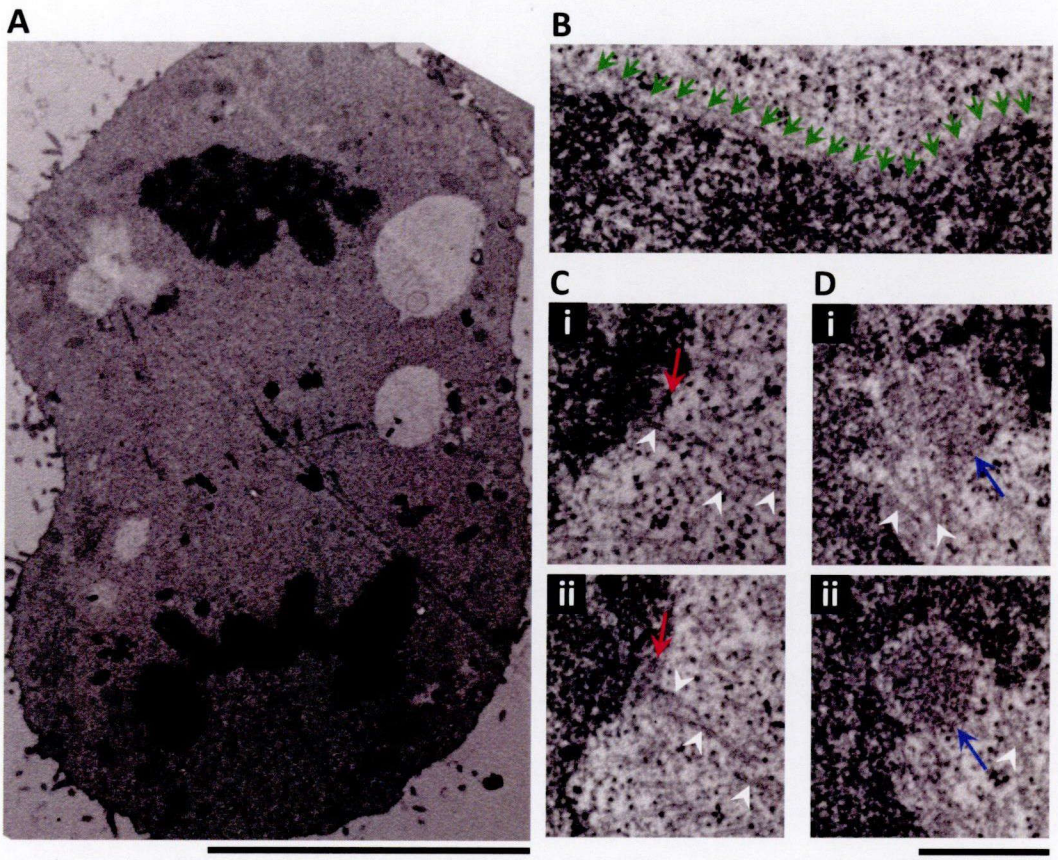

Fig. 3-10 Telophase. Red arrows showed the outer plates and blue arrows revealed the fuzzy ball appearance. Microtubules are indicated by white arrowheads. (**A**) Sister chromatids at the poles fused into a chromatin mass. Scale bar is 10 µm. (**B**) Nuclear envelope is denoted by green arrows. (**C**) Kinetochore with less distinct outer plate. (**D**) Fuzzy ball. (**B-D**) All micrographs are shown in the same magnification. Scale bar is 500 nm

3.4 Discussion

There are generally three types of kinetochore structures (Table 1). 1. The fuzzy ball structure which is often observed in prophase until early prometaphase and after mid anaphase. 2. Fuzzy ball with faint outer plate which usually observed from prophase to mid prometaphase and after mid anaphase. 3. Trilaminar structure which is observed from early prometaphase to late anaphase, and formed the majority from late prometaphase until early anaphase. Therefore, in HeLa cells, trilaminar kinetochore assembled from prophase to metaphase and disassembled from mid anaphase until the end of mitosis.

	Fuzzy ball	Fuzzy ball with faint outer plate	Trilaminar structure
prophase	+	+	-
early prometaphase	+	+	+
mid prometaphase	-	+	+
late prometaphase	-	-	+
metaphase	-	-	+
early anaphase	-	-	+
mid anaphase	+	+	+
late anaphase	+	+	+
telophase	+	+	-

Table 1 Kinetochore structure in each mitotic phase. + indicated structures that are usually visible. – indicated structures that are visible in less than 15% of total kinetochores examined at the corresponding mitotic phase

3.5 Summary

A classification scheme for kinetochore maturation in human cells is presented (Fig. 3-11) based on the ultrastructural analysis; microtubules are omitted to avoid complexity. Kinetochores are classified into 3 groups, Class 1, Class 2 and Class 3.

Class 1 represents kinetochore with amorphous fibrillar mass without internal structure (also refer to as fibrillar/fuzzy ball or prekinetochore) (orange shades in Fig. 3-11). Class 1 kinetochore is mainly visible during prophase and early prometaphase, and also after mid anaphase. Virtually, this is the initial stage of the kinetochore assembly and also the final stage of kinetochore disassembly in mitosis. Once the outer plate (pink layer in Fig. 3-11) is developed, kinetochore appeared as fibrillar ball with a faint outer plate is referred to as Class 2. Class 2 kinetochores are mainly visible from prophase to mid prometaphase and after mid anaphase. As cell cycle progress toward metaphase, the outer plate became more and more electron dense and the fuzzy appearance gradually disappeared (yellow shades in Fig. 3-11). Once the electron dense outer plate and distinct electron-lucent middle zone became apparent, kinetochores are classified as trilaminar kinetochore (also known as the matured kinetochore) or Class 3. In most cases, inner plates (red layer in Fig. 3-11) were visible. Class 3 kinetochore is visible mainly from late prometaphase until early anaphase. Differences between Class 2 and Class 3 kinetochores are the electron density of the outer plate and the middle zone. It is notable that in many individual cells, all three types of kinetochores are visible, particularly in prometaphase. This observation indicate that for an individual cell, proteins from the mitotic pool assemble randomly to the kinetochores, until the full complement of kinetochore proteins is achieved, usually by late prometaphase.

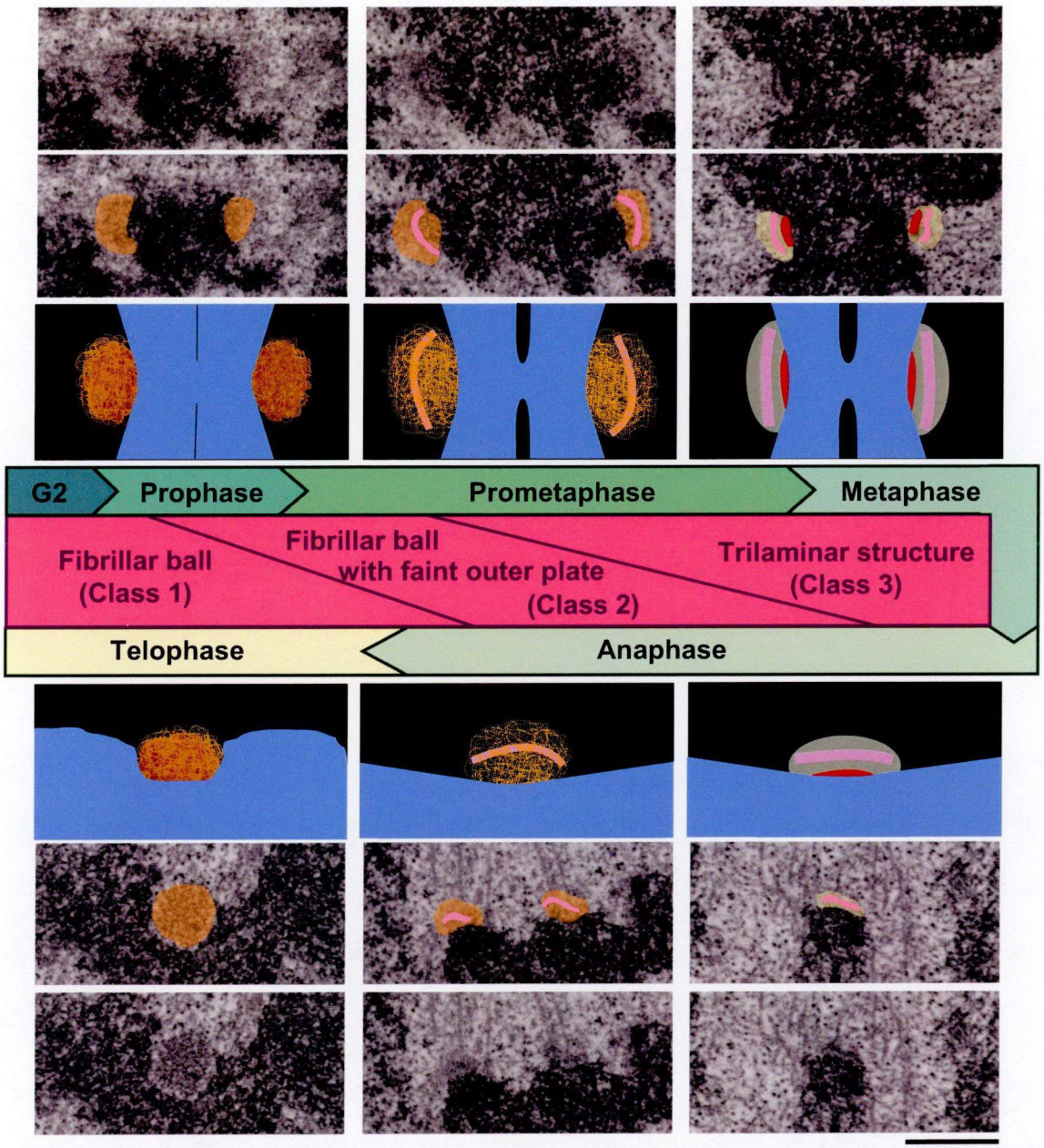

Fig. 3-11 A schematic model of kinetochore development. Kinetochore maturation (i.e. transformation of fibrillar ball to a trilaminar kinetochore) is classified as 3 groups, Class 1, 2, and 3. Note that kinetochores are grouped based on their structures, and therefore kinetochores in an individual group are not necessarily containing the same protein composition (See Fig. 2-1A for kinetochore composition). The maturation process occurs in parallel with chromosome condensation from prophase until the onset of anaphase, however does not depend on NEB or on the degree of chromosome condensation (Ghosh and Paweletz 1987). After anaphase, sister chromatid separated, and kinetochore gradually degraded into the fuzzy ball structure. Microtubules were eliminated from the figure to avoid complexity. Scale bar is 500 nm

Chapter 4

ASURA and RBMX are required for kinetochore assembly

4.1 Introduction: Kinetochore assembly pathways

Kinetochore proteins assemble to the kinetochore by a stepwise self-assembly manner. Inner kinetochore proteins, CCAN localize to the centromere throughout the cell cycle, and the rest of the kinetochore proteins localizes gradually to the kinetochore outer plate and/or fibrous corona. This is known as the kinetochore assembly. Several early studies provided good profiles of the effect of over thirty kinetochore proteins to the kinetochore structure, and Liu et al. (2006) carefully classified the assembly pathways into three, the CENP-I, CENP-C and Aurora B pathways (Fig. 4-1).

CENP-I pathway is thought to be the main stream of the trilaminar structure formation. CENP-I was later found to be downstream of CENP-T/W complex (Fig. 2-7; Hori et al. 2008). Knockout or knockdown of components in this pathway always resulted in a majority of kinetochores with fibrous mass without internal structure, resembling the prekinetochores (Fig. 4-1B, Liu et al. 2006). These suggested that kinetochore proteins in this pathway are required for plate formation or differentiation itself. A recent study showed that CENP-T/W complex interacts directly with Ndc80 complex (Gascoigne et al. 2011). When Hec1 and/or Nuf2 are disrupted, more than 50% of the kinetochores observed failed to construct the plate structure, suggesting that this complex play an important role in kinetochore maturation and differentiation

(DeLuca et al. 2005), where similar phenotype observed in CENP-I depletion (Liu et al. 2006) may be due partially to the mislocalization of Hec1-Nuf2. CENP-F is another outer kinetochore and fibrous corona component placed downstream of CENP-I (Liu et al. 2006). CENP-F displays weak microtubule-binding activity (Feng et al. 2006). CENP-F repression resulted in unstable kinetochore-microtubule interaction, while Ndc80 complex is unaltered. Therefore, Ndc80 complex and CENP-F are thought to be constructing two independent branches downstream of CENP-I.

CENP-C pathway is essential to maintain the size, shape and structural integrity of kinetochore plates. Mis12 complex associated directly with CENP-C, while Mis14 provided the attachment site of Spc24-Spc25 (Ndc80 complex) and KNL1 (Petrovic et al. 2010). In either of the CENP-C or Mis12 knockout and/or knockdown analyses, trilaminar kinetochores were observed in more than 70% of the kinetochores, although the majority of them were either forming the thin and/or punctate plates, partial and/or pulled out plates or small kinetochore plates (Fig. 4-1C, Liu et al. 2006). Even though this pathway is also affecting kinetochore association of Hec1-Nuf2 and CENP-F, the effects were less severe than those of CENP-I.

Aurora B pathway affects the shape and structural integrity of kinetochore plates. When Aurora B is depleted from the cells, more than 90% of the kinetochores were trilaminar with C-shaped outer plates (Fig. 4-1D, Liu et al. 2006), while the others sometimes showed inner and outer plates seemingly fused at one end (Fig. 4-1E, Liu et al. 2006). As the biochemical analyses failed to provide important clues about ASURA and RBMX localization and/or interaction partners at kinetochore, I turned to EM analysis to examine the defects in kinetochore formation after the RNAi treatments.

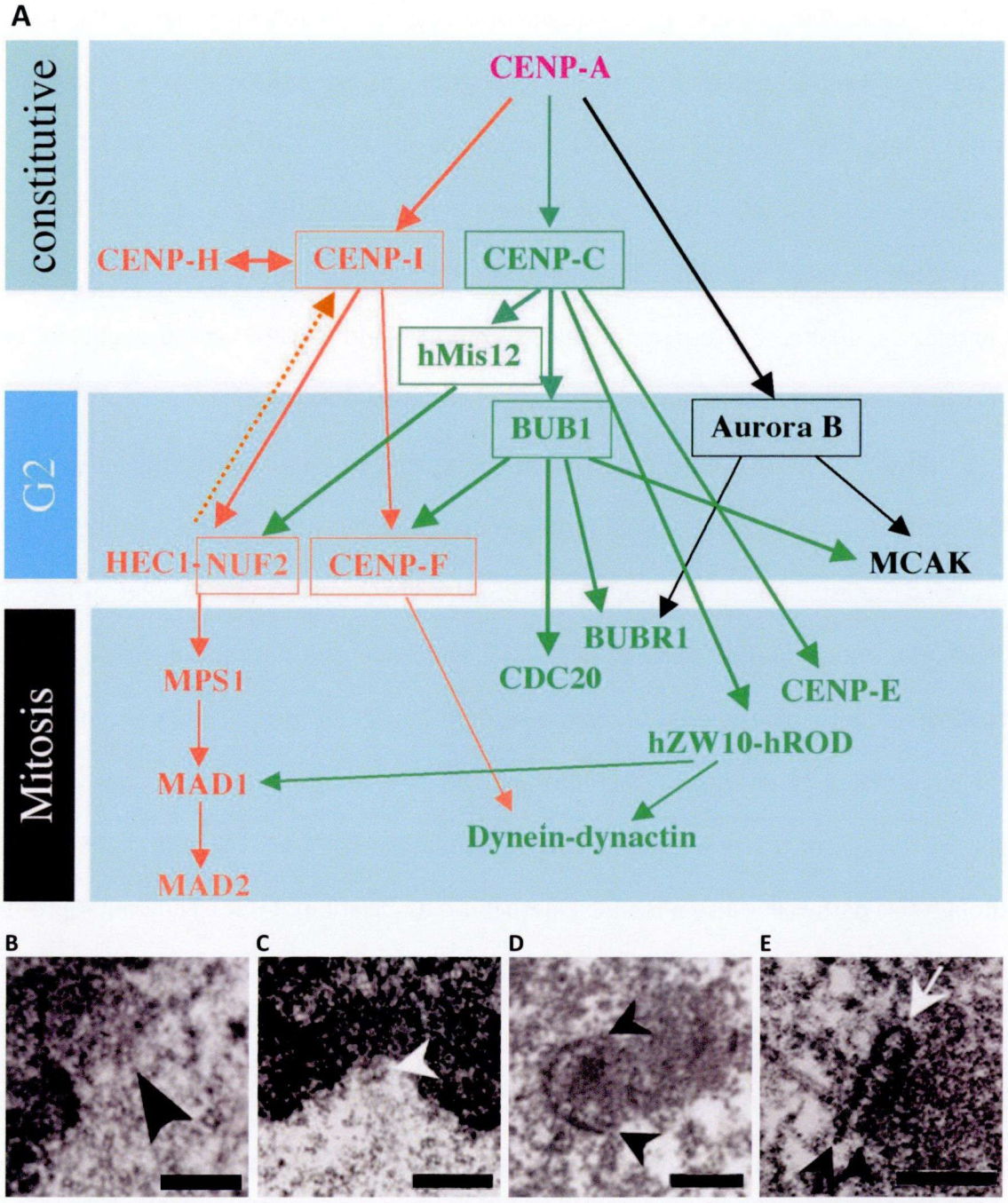

Fig. 4-1 Kinetochore assembly pathways in human based on molecular and EM analyses and typical phenotypes of kinetochores when each pathway is disrupted (**A**) A network of intersecting pathways that specify kinetochore formation (Liu et al. 2006). Inner kinetochore proteins are the constitutive components. CENP-A is at the top of a hierarchy that directs three major pathways, which are specified by CENP-I (orange), CENP-C (green) and Aurora B (black). Proteins are arranged in a top down model with respect to their relative temporal order of appearance at kinetochores. Thick solid arrows show connections examined by Liu et al. (2006). The dashed arrow denotes a

potential feedback mechanism between CENP-I and the Hec1-Nuf2 complex. Boxes denote proteins whose roles in kinetochore assembly were examined by EM. (**B**) Kinetochore in CENP-I depleted cells. Black arrowhead indicates the fuzzy ball appearance. Scale bar is 400 nm. (**C**) Kinetochore with smaller plates in CENP-C RNAi cells. Trilaminar structure (white arrowhead) is remained. Scale bar is 400 nm. (**D, E**) Kinetochores in cells lacking Aurora B. (**D**) Kinetochores maintain the plate structures, but extend significantly to a C-shape without microtubule binding. (**E**) Outer and inner plates (black arrowheads) seemingly fused at one end displaying hairpin-like structure (white arrow). (**B-E**) Cited from Liu et al. (2006)

4.2 Materials and methods

Cell culture

HeLa cells were grown in DMEM (GIBCO BRL) supplemented with 10% FBS; (Equitech-Bio) at 37°C and 5% CO_2 as described in Chapter 2.

siRNA methods

HeLa cells were transfected at a final concentration of 100 nM with ASURA-siRNA (5'-GAAUCGUAUCUAUCUCACATT-3' PHB2 siRNA-1 in Takata et al. 2007b), RBMX-siRNA (5'-UCAAGAGGAUAUAGCGAUATT-3') or Hec1 siRNA (5'-AAGTTCAAAAGCTGGATGATC-3', Martin-Lluesma et al. 2002) using Lipofectamine 2000 according to the manufacturer's instructions. Cells transfected with Lipofectamine alone were used as a mock control. 48 hours after transfection, cells in each treatment were collected for EM analysis.

Electron microscopy

HeLa cells grown on plastic coverslips (mono-layer) were transfected as in Chapter 2. 48 hours post transfection, cells were fixed in 3% glutaraldehyde containing 0.2% tannic acid diluted in PBS buffer for 1 hour at room temperature. Post-fixation was in 2% OsO_4 for 20 minutes. The cells were dehydrated through an increasing ethanol series and

infiltrated with epoxy resin (Quetol 812). The resin was polymerized at 37°C for 12 hours, 45°C for 12 hours and 60°C for 48 hours. Cells of interest embedded in the resin were chosen under an optical microscope and trimmed to ~1.0 mm^2. Samples were cut into 70-80 nm thick serial sections with an ultramicrotome equipped with a diamond knife (ULTRACUT E; Reichart-Jung). The sections were stained with uranyl acetate and lead citrate for examination with a transmission electron microscope (JEM-1200EX; JOEL).

The EM analyses were based on those of DeLuca et al. (2005) with some alterations. For control, cells that apparently aligned at metaphase were chosen for analysis (Fig 4-2A). ASURA, RBMX and Hec1 RNAi cells were chosen based on their phenotypes, poor chromosome alignment as shown in Fig. 4-3A, 4-4A, B and 4-5A. All kinetochores observed were included in the analyses regardless of their appearance. For individual cells, only a few sections, containing chromosome-rich regions, which were often close to the center of the cells, were examined. To obtain an overall view of the RNAi effects, kinetochores from several cells were chosen rather than examining all the kinetochores in a single cell. As the boundary between individual chromosomes is not obvious, and sister kinetochore appearances can sometimes show differences depended on kinetochore fiber attachment, kinetochores were analyzed individually rather than as a kinetochore pair of a chromosome. Several adjacent serial sections were observed to elucidate the structural and developmental stages of the kinetochores.

4.3 Results

4.3.1 Immature kinetochore development in ASURA and RBMX depletion

To test the possible pathway(s) ASURA and RBMX may be involved in, kinetochores in mock control (Fig. 4-2) and RNAi treated cells (Fig. 4-3, 4-4 and 4-5) were analyzed. Kinetochores were classified by referring to their maturation process (Fig. 3-11). Several adjacent serial sections (indicated by serial numbers of i, ii, iii in Fig. 4-2 to 4-5) were analyzed to classify individual kinetochores. A kinetochore structure is classified as trilaminar (Class 3) once the canonical layered structure is visible in any of the adjacent serial sections for an individual kinetochore (Fig. 4-2Ei), even the structure was rather fuzzy in the next section (Fig. 4-2Eii).

The quantitative data are shown in Fig. 4-6. The control cells (Fig. 4-2) are identical to the metaphase and very early anaphase cells in Chapter 3. Normally, Class 3 kinetochores (Fig. 4-2D, E) form the majority, more than 75% of the population. This is rarely the case in the Hec1, ASURA and RBMX RNAi cultures, where less than 20% were Class 3. Consistent with previous reports for Nuf2 RNAi (DeLuca et al. 2005; Liu et al. 2006), typical fuzzy ball structures (Class 1, Fig. 4-3B, C) were increased in Hec1 RNAi cells (Fig. 4-3). Class 2 (Fig. 4-3D, E) kinetochores were also increased significantly. As expected, kinetochores were either fuzzy ball (Class 1, blue arrows in Fig. 4-4C-G, N, 4-5B-E) or poorly-formed (Class 2, Fig. 4-4C, H-J, L-P, 4-5E) with ASURA (Fig. 4-4) and RBMX (Fig. 4-5) depletion. Kinetochore structure were severely perturbed in RBMX RNAi, similar or even greater than that of the Hec1 RNAi cultures, consistent with the immunofluorescence results showing low population of Hec1 and many other kinetochore proteins in RBMX depleted cells. Plate development seemed to be proceeded further in ASURA RNAi cells, but is nevertheless compromised. Even when a layered structure was constructed, the outer plates, and sometimes even the inner

plates, were often pulled out or stretched (Fig. 4-4L-P), indicating that without ASURA the kinetochore lacks physical rigidity against the microtubule pulling forces, although microtubule attachment were less frequent compared to the control (Fig. 4-2D, E).

Increased Class 1 and Class 2 kinetochores after the RNAi treatments indicated that kinetochore assembly is prolonged or terminated at early mitotic stages, due to the declined accumulation of certain important components of the outer kinetochore, as indicated by immunofluorescence studies (Fig. 2-4, 2-7). It is notably that these structures are not totally identical to those in the early mitotic stages in their protein components. Considering that the amount of kinetochore proteins in the mitotic pool is unaltered, the importance of ASURA and RBMX as the targeting factors of kinetochore components in early mitotic stages is evident.

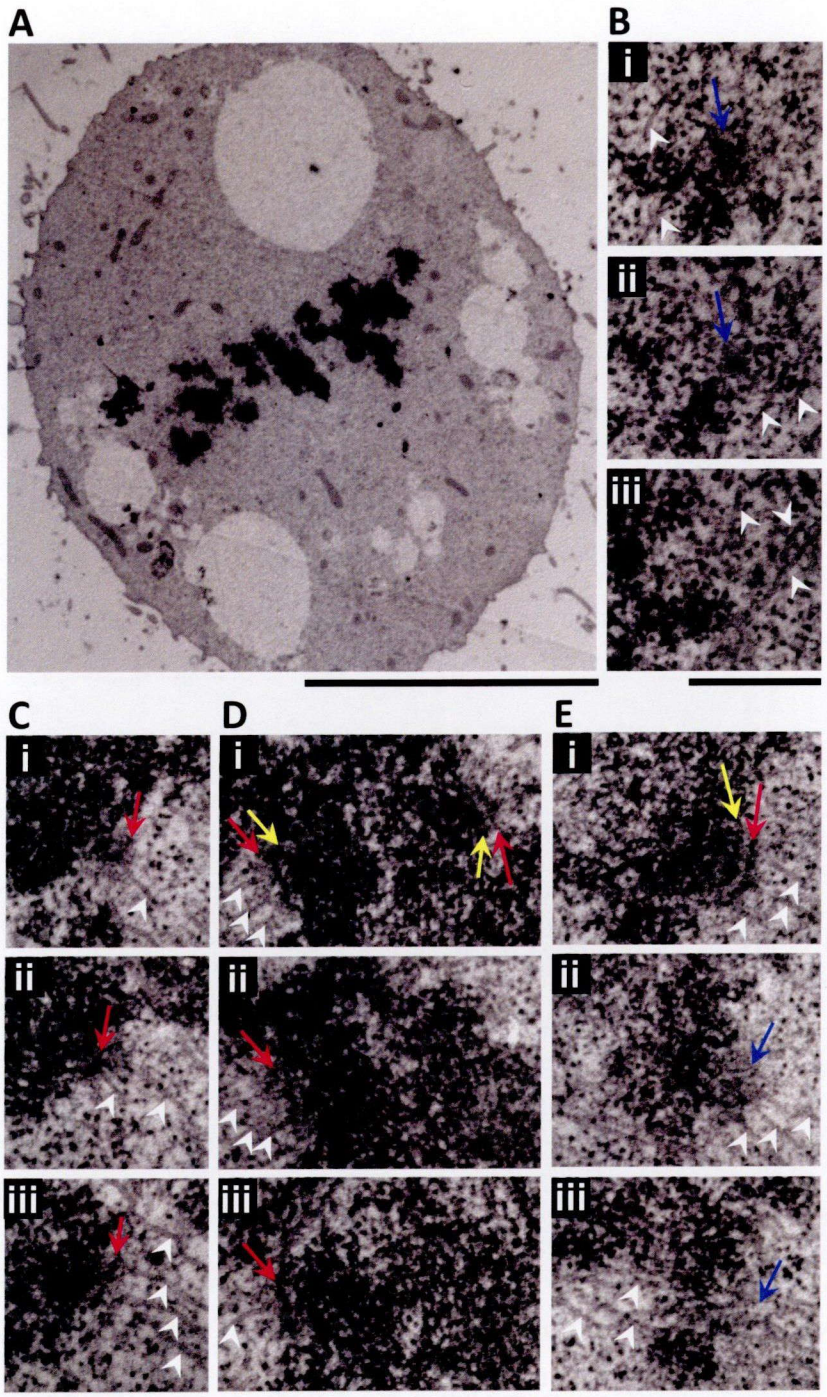

Fig. 4-2 Control cells. Red and yellow arrows show the outer and the inner plates, respectively. Blue arrows show the kinetochore with fuzzy appearance. White arrowheads indicate microtubules. (**A**) An overview of a control cell, forming the metaphase plate. Scale bar is 10 µm. (**B**) Kinetochore with fibrillar ball appearance (Class 1). (**C**) An immature kinetochore with a faint outer plate (Class 2). (**D**, **E**) Trilaminar kinetochores with microtubule attachment, classified as Class 3 kinetochores. (**B**-**E**) All micrographs are shown in the same magnification. Scale bar is 500 nm

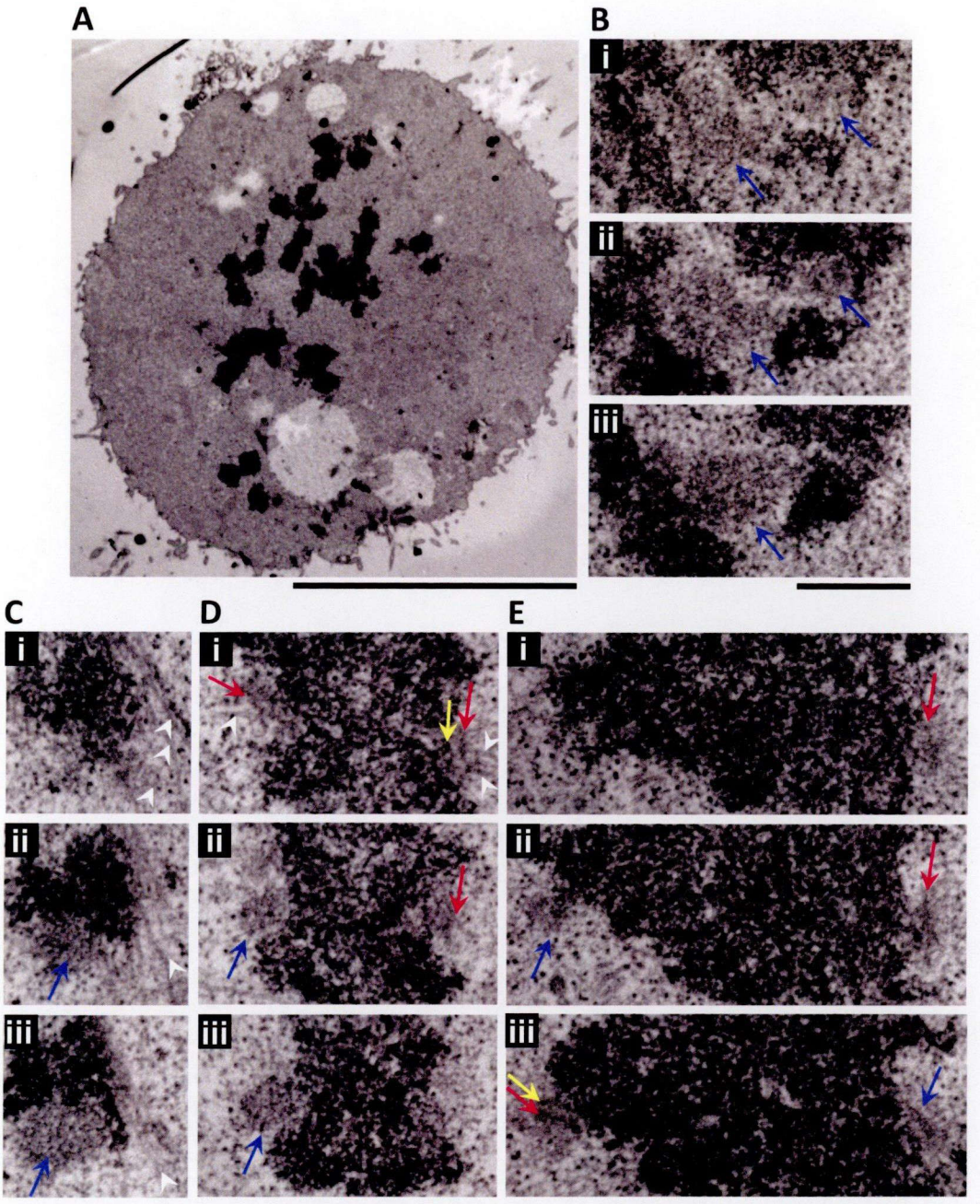

Fig. 4-3 Kinetochore disorganization in Hec1 RNAi cells. (**A**) Nonalignment phenotypes were significant in Hec1 RNAi. Scale bar is 10 μm. (**B**, **C**) Kinetochores showing fibrillar structure (Class 1), the typical phenotype in Hec1 RNAi. (**D**, **E**) Partially formed outer plates are visible (Class 2). (**E**) Both inner and outer plates of the left kinetochore are pull-away from the centromere. (**B**-**E**) All micrographs are shown in the same magnification. Scale bar represent 500 nm

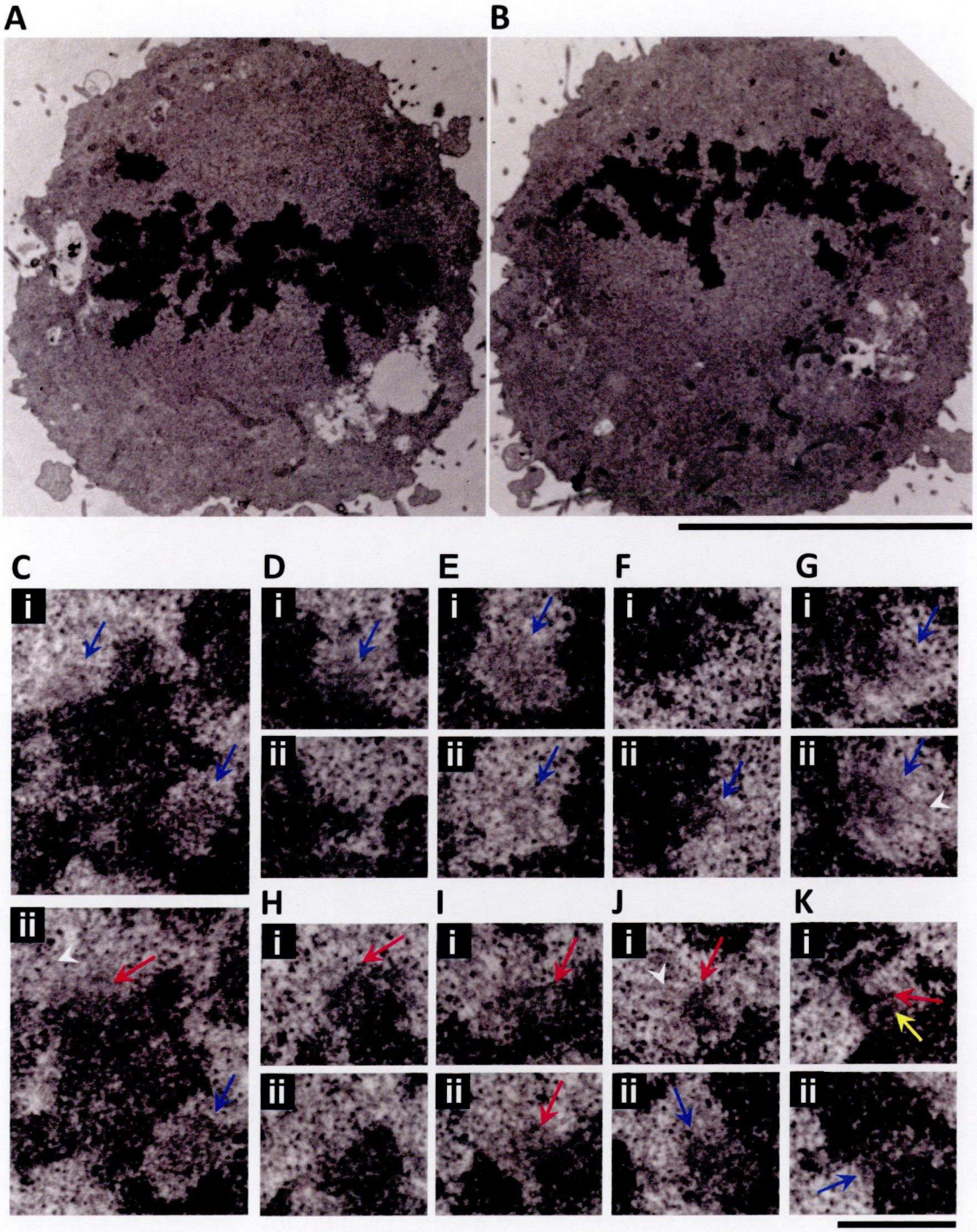
A
B
C
D
E
F
G
H
I
J
K
i
ii

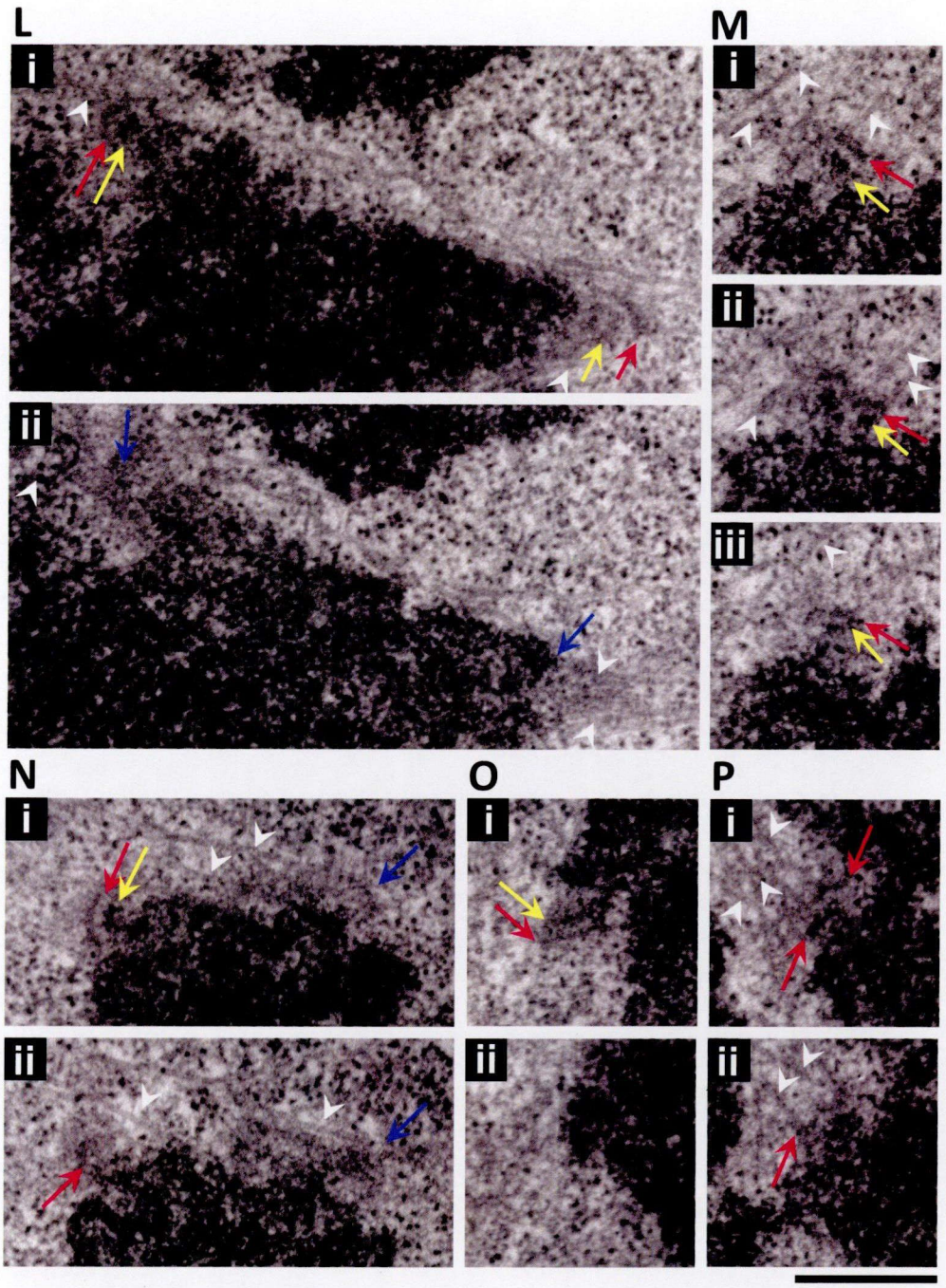

Fig. 4-4 ASURA depletion resulted in kinetochore assembly disorder. (**A**, **B**) Low magnification electron micrographs showing an ASURA depleted cell with nonalignment. Serial sections are not adjacent. Scale bar represent 10 μm. (**C-P**) Inner plates (yellow arrows), outer plates (red arrows) and fuzzy ball appearance (blue arrows) are indicated. Microtubules are denoted as white arrowheads. (**C**) Sister kinetochores showed faint outer plate (left, Class 2) and fuzzy ball structure (right, Class 1). (**D-G**) Kinetochores showing fibrillar structure (Class 1). (**H-J**) Partially formed outer plates (Class 2) are visible. (**K**) Trilaminar kinetochore (Class 3). (**L-P**) Class 2

kinetochores, most are stretched and some inner plates were even pulled-away from the centromeres. Right kinetochore in (**N**) is a fuzzy ball (Class 1). (**C**-**P**) All micrographs are shown in the same magnification. Scale bars represent 500 nm

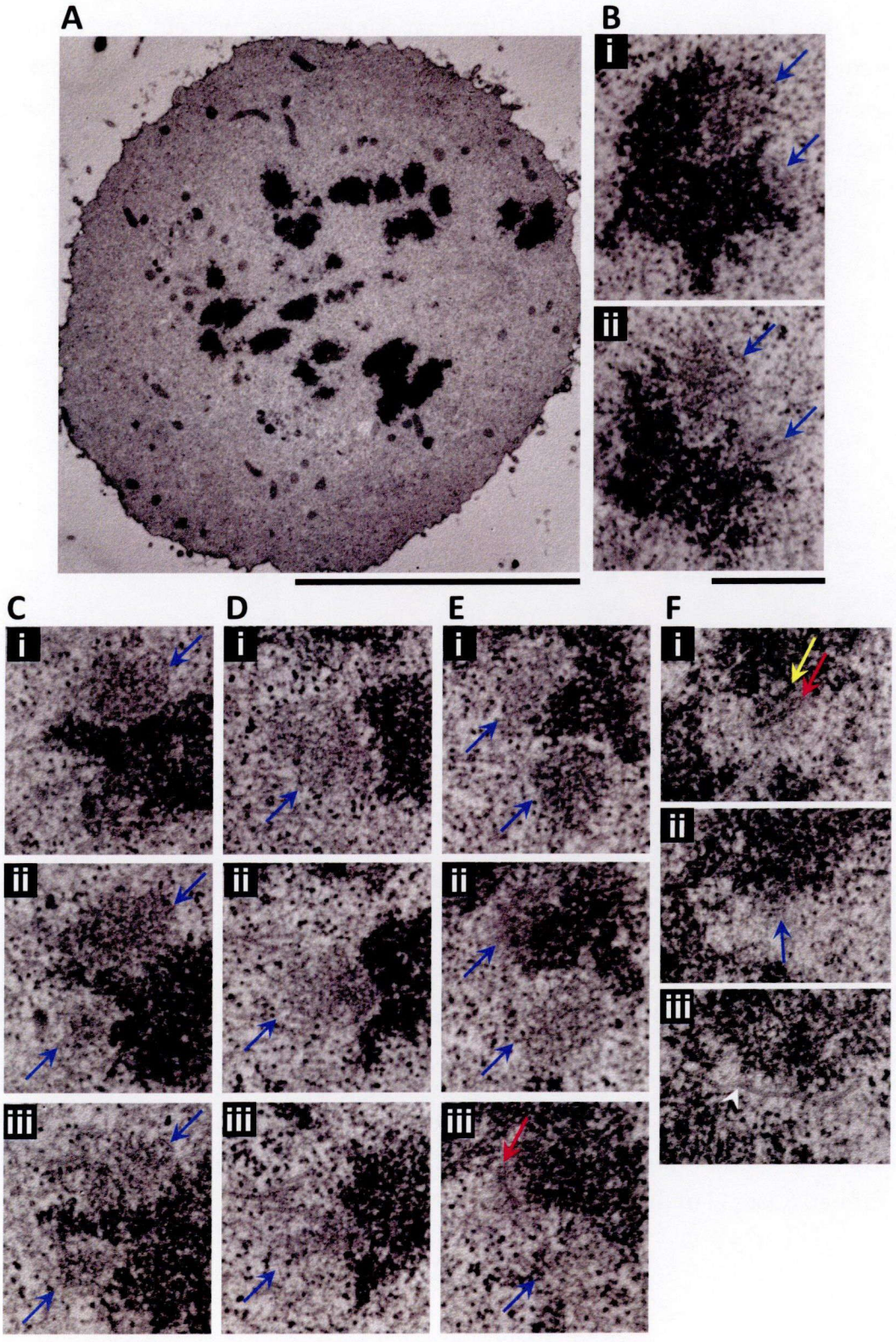

Fig. 4-5 Kinetochores in RBMX disrupted cells. (**A**) An overview of RBMX RNAi cell. Chromosomes distributed in the cell with various degrees. Scale bar is 10 μm. (**B-D**) Kinetochores with fibrillar appearance (Class 1), the major phenotype of RBMX depletion. (**E**) Sister kinetochores showed poorly-formed outer plate (upper, Class 2) and fuzzy ball (lower, Class 1). (**F**) Trilaminar kinetochore without microtubule attachment (Class 3). (**B-F**) Red and yellow arrows show the outer and the inner plates, respectively. Blue arrows show the kinetochore with fuzzy appearance. Microtubules are denoted as white arrowheads. All micrographs are shown in the same magnification. Scale bar is 500 nm

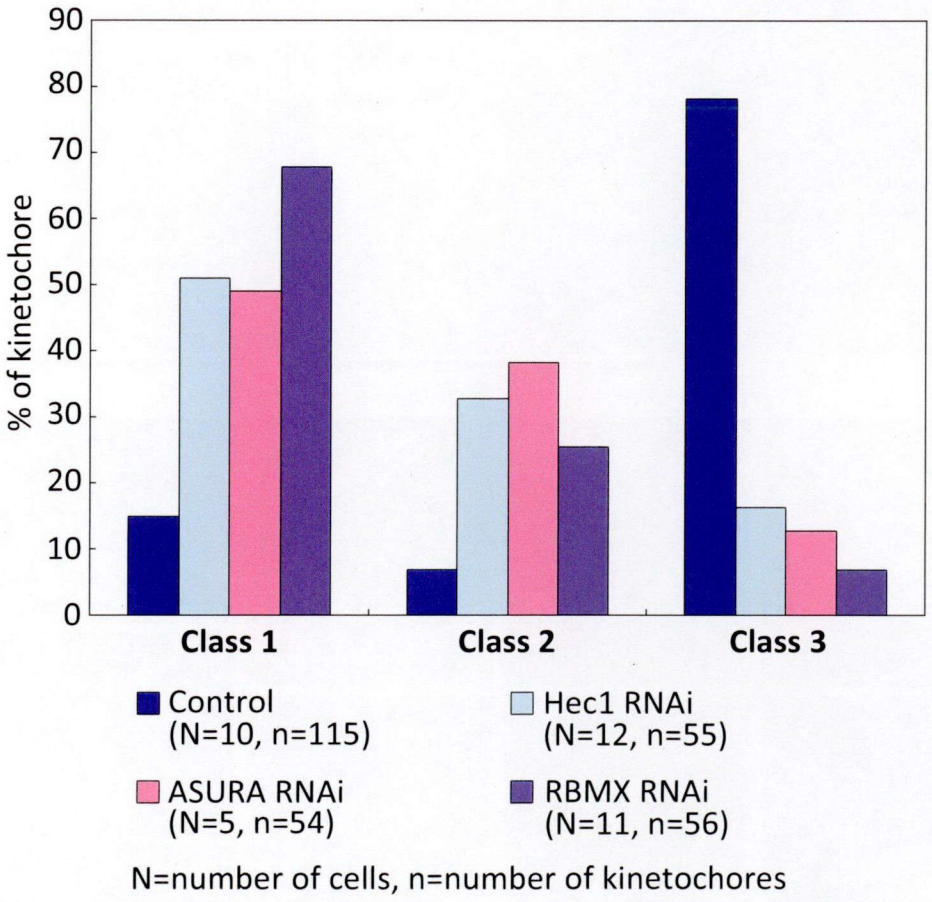

Fig. 4-6 Quantitative analysis of kinetochores in each treatment. Kinetochores were classified as Class 1, 2, and 3, according to the maturation stages (Chapter 3, Fig 3-11). In ASURA and RBMX RNAi, the majority of the kinetochore plates were either poorly-formed (Class 2) or unrecognized (Class 1), similar to that of the Hec1 RNAi cells

4.3.2 Microtubule attachment was decreased in ASURA and RBMX RNAi

Mammalian outer kinetochore is a fibrous network, providing the physical attachment site for microtubules (Dong et al. 2007). Over 90% of the kinetochore microtubule plus ends terminate in the outer plate of the trilaminar kinetochore (VandenBeldt et al. 2006). Each human kinetochore can interact with 15-25 microtubules (Cheeseman and Desai 2008; Raaijmakers et al. 2009). Although microtubules do not attach evenly throughout the kinetochore plate, normally, in 70-80 nm thick serial sections, approximately 3-6 microtubules attached end-on to the kinetochores. When I examined the number of microtubule attachment, I found that usually more than 50% of the kinetochores in the control cultures were capable to bind more than 3 microtubules, even in the early prometaphase (EP), mid prometaphase (MP) and late prometaphase (LP). Kinetochores in the RNAi treated cultures were overall associated with fewer microtubules. Microtubule capturing occurred in a random manner, largely depending on the spatial location of the kinetochores. In addition, it is also reflecting the ability of kinetochores in stabilizing microtubule binding, which is largely affected by the protein composition at a given time point. Although the latter may not always be the case in normal cells except for those kinetochores before achieving full complement of their constituents, shortly after NEB such as the EP cells, it is especially true in the RNAi treated cells lacking a subset of important components for microtubule capturing and stabilization. Therefore, it is obvious that the number of stable microtubule attachment was decreased after ASURA and RBMX RNAi, particularly in Class 1 and Class 2 kinetochores.

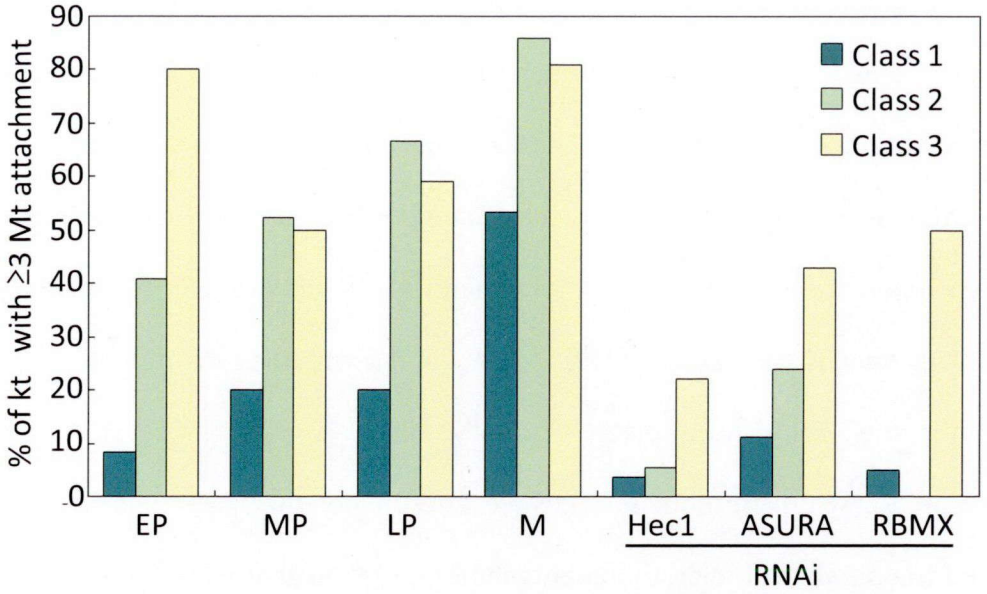

Fig. 4-7 Percentage of kinetochores with ≥3 microtubules association. EP, MP and LP are the normal prometaphase cells described in Chapter 3. Metaphase cells (M) refer to the mock control cells. Microtubule interactions are not necessarily detected in every serial section. Therefore, for individual kinetochore, only serial section with the highest number of microtubule interaction was analyzed

4.3.3 Defects in kinetochore formation after ASURA or RBMX depletion were similar to that of Hec1 disruption

The morphological defects observed in ASURA- and RBMX-depleted cultures were similar to those of Hec1 disruption. In addition, the level of plate disorganization tends to reflect kinetochore proteins population at the kinetochore after RNAi treatment. This suggests that the abnormalities observed in kinetochore formation derived from the degree of mislocalization of Hec1 and perhaps many other kinetochore proteins, either upstream or downstream.

Immunofluorescence results (Fig. 2-4) suggested the possible involvement of ASURA and RBMX in CENP-I and/or CENP-C pathways (Fig. 2-7). From the structural analysis, the majority of the kinetochores were fibrillar balls, while the rest failed to form the rigid trilaminar structure. Although the latter is similar to that of CENP-C depletion, these features were also observed in Hec1-Nuf2 RNAi cells. Together with high percentage of kinetochores showing fuzzy ball appearance, which is a representative defect in CENP-I pathway (Liu et al. 2006), particularly when the Hec1 localization is highly disrupted, these data suggested the involvement of both ASURA and RBMX in the CENP-I pathway.

4.4 Discussion

In both ASURA and RBMX RNAi, kinetochore maturation, in particular, outer plate development was severely perturbed. Defects in kinetochore maturation observed were similar to that of Hec1 depletion. As kinetochore localization of Hec1 were disrupted after both ASURA and RBMX RNAi, the phenotypes observed may recapitulate partially, if not all, those of Hec1 depletion due to its mislocalization. In addition, end-on microtubule attachment was decreased in both ASURA and RBMX RNAi, reflecting the lost of the important microtubule capturing protein(s), most probably Hec1. This suggested that kinetochore aberration observed in ASURA and RBMX RNAi were mainly caused by mislocalization of Hec1 or other components in the CENP-I pathway. Importantly, the kinetochore structures were highly disorganized in RBMX depletion, even more severe than that of Hec1 RNAi alone. This can be explained by loss of Mis13 (and Mis12 complex) and perhaps other components from the CENP-C pathway, although CENP-C localization itself is not affected in RBMX depletion (Matsunaga et al. unpublished data). Although kinetochore association of Hec1 decreased in Mis12 RNAi, Mis12 depletion alone only affected the size of the outer plate (Liu et al. 2006). Interestingly, synergy in phenotypic defects has been reported for double depletion of CENP-K (an inner kinetochore protein downstream of CENP-I) and KNL1 (a member of the KMN network, showing dependency on Mis12) (Cheeseman et al. 2008). CENP-K and KNL1 depletion alone give little effect to each other and also the localization of Hec1, while double knockdown of these proteins nearly diminished Hec1 localization totally. Hec1 is supported by CENP-T/W, Mis12 and perhaps also by KNL1. Therefore, the degree of kinetochore disorganization may also reflect the remaining population of proteins working together to support the outer plate.

4.5 Summary

In this study, we found that cells lacking either ASURA or RBMX showed particularly aberrant chromosome congression, suggesting that they are defective with respect to microtubule capture. EM studies support this conclusion. Authentic trilaminar kinetochores are notably rarer in both ASURA and RBMX RNAi cultures. In addition, significant increase in fuzzy ball structures, resembling the prekinetochores often observed in early mitotic stages, suggest that kinetochore maturation was highly disrupted. Normally, most of the kinetochores interact with microtubules after NEB, even when the trilaminar structure has not been fully constructed. Only a few kinetochores in RBMX RNAi cells associate with microtubules; those with a particularly low population appeared as fuzzy balls.

Notably, similar observation was made for Hec1 depleted cultures, consistent with previous reports. The EM study significantly showed that kinetochores in ASURA and RBMX RNAi cells mainly recapitulated the defects observed in Hec1 depletion. This result reinforced the possible involvement of both proteins mainly in the CENP-I assembly pathway. Although both ASURA and RBMX RNAi showed similar mitotic defects, and is feasible to be involved in the CENP-I pathway, their contributions to kinetochore assembly seem different. RBMX is likely to recruit the upstream component(s) of Hec1, in CENP-I and/or CENP-C pathways, whereas ASURA is likely to be the Hec1 targeting factor. Altogether, this clearly shows that ASURA and RBMX play critical roles in kinetochore plate development and stable microtubule attachment, which are the prerequisites for accurate chromosome congression and segregation.

Chapter 5

General conclusion

In this study, I found that two relatively abundant chromosomal proteins, ASURA and RBMX play critical roles in kinetochore formation, in addition to our initial finding on their functions in protecting sister chromatid cohesion. By analyzing RNAi cells using electron microscope, I demonstrated how ASURA and RBMX are required for kinetochore assembly.

In Chapter 2, I investigated the localization pattern of ASURA and RBMX. Both ASURA and RBMX localize to the nucleus during interphase and associated with chromosomes during prophase until late prometaphase. However, no specific localization of both proteins was detected either at the centromere or kinetochore, and therefore they are not the kinetochore component proteins. To assess the roles of ASURA and RBMX in chromosome segregation, both proteins were depleted from HeLa cells using RNAi and were examined for the localization of a subset of kinetochore proteins. Depletion of ASURA and RBMX decreased the localization of Hec1, CENP-E and CENP-F, while RBMX was also required for Mis13 targeting. Therefore, the possible pathway involved in is Mis13 → Hec1 → CENP-F → CENP-E. RBMX is likely to recruit Mis13 or Mis12 complex, while ASURA is targeting Hec1 or Ndc80 complex. Given that interactions between ASURA and RBMX with the kinetochore proteins were not detected, this prompted me to test the consequences of ASURA and RBMX in kinetochore formation by electron microscopic study.

In Chapter 3, I examined kinetochore structures in each mitotic phase to obtain a

better insight into kinetochore assembly and disassembly in HeLa cells. Prophase kinetochores appear as roughly circular patches of finely fibrillar material at the primary constriction of chromosomes. This structure was classified as Class 1. Occasionally, a faint layer representing outer kinetochore was observed within the fibrillar material. This structure was classified as Class 2. The outer kinetochore was gradually distinct and finally the trilaminar kinetochore, conspicuous outer plate and the inner plate separated by the unambiguous electron-lucent middle layer, is established in almost all chromosomes by late prometaphase. This structure was classified as Class 3. After NEB, all three types of kinetochores were able to interact with microtubules, although robust end-on attachment was mainly observed in Class 3 kinetochore. After sister chromatid separation in anaphase, as the chromosomes moved to the opposite poles, Class 3 kinetochores gradually dedifferentiated into Class 2 and finally Class 1 at the end of mitosis. A classification scheme featuring the stepwise ultrastructural changes of human kinetochore assembly and disassembly with corresponding mitotic stage was develop.

In Chapter 4, I analyzed the kinetochore structures in each siRNA transfected cultures based on the classification scheme developed in Chapter 3. Metaphase and early anaphase cells were used as control. Hec1 RNAi cells showed a significant increase of Class 1 kinetochores. Similarly, both in ASURA and RBMX RNAi, most of the kinetochores examined lacked trilaminar plates, and displayed the Class 1 phenotype. This is followed by a significant increase in the Class 2 kinetochores. Although these structures resembled those of the early mitotic stages, the ability to form stable microtubule interaction was significantly decreased, comparing to the prometaphase and metaphase kinetochores. ASURA and RBMX RNAi exhibited very similar phenotypes associated with Hec1 depletion, although they were varied in the degree

of disorganization.

In conclusion, despite not being integrated into the kinetochore, ASURA and RBMX play critical roles in recruiting several kinetochore components of to the CENP-C and/or CENP-I assembly pathways. This conclusion is reinforced by ultrastructural analysis of kinetochores in ASURA- and RBMX-depleted cells. Kinetochore defects were mainly due to the lost of Hec1, suggesting that both ASURA and RBMX are involved in the CENP-I pathway (the assembly pathway to which Hec1 and CENP-F belong). ASURA is likely to recruit Hec1, whereas RBMX may either contribute to the loading of other CENP-I pathway component upstream or both proteins from CENP-C and CENP-I pathways (Fig. 5-1A).

This finding revealed for the first time that non-kinetochore component proteins (i.e., proteins required for kinetochore functions but not being integrated into the kinetochore) are involved in targeting of kinetochore proteins to facilitate kinetochore assembly (Fig. 5-1B). Despite a nearly complete list of more than 120 proteins are found to localize at the kinetochore (kinetochore component proteins), the underlying mechanism of kinetochore assembly remain murky, partly because all studies are focusing on the kinetochore itself. This finding suggested the contribution of non-kinetochore component proteins, and thus provided an important future direction for kinetochore research.

In-depth insight the molecular mechanisms of kinetochore assembly and functions will provide the foundation for cancer therapy as well as cellular and chromosome engineering. Uncontrolled proliferation is the most distinctive characteristic of cancer cells, and therefore many anticancer drugs directly inhibit cell growth. Currently available anti-proliferative anticancer drugs are the microtubule poisons (e.g., pactitaxel, vinblastine, etc.), although very efficient, drug resistance is a

serious problem. Since microtubules involved in both mitosis and other cellular functions outside the mitosis, total inhibition of the microtubule functions produces dose-limiting toxicities such as peripheral neuropathy. Kinetochore plays essential roles in mitotic segregation and mitotic checkpoint signaling, and therefore is attractive as a potential target for developing mitosis-specific anticancer drugs (Liu and Yen 2009). In addition, understanding the process of kinetochore formation in details may be able to stimulate kinetochore assembly in a process that could lead to new genetic research tools, such as efficient creation of artificial human chromosomes.

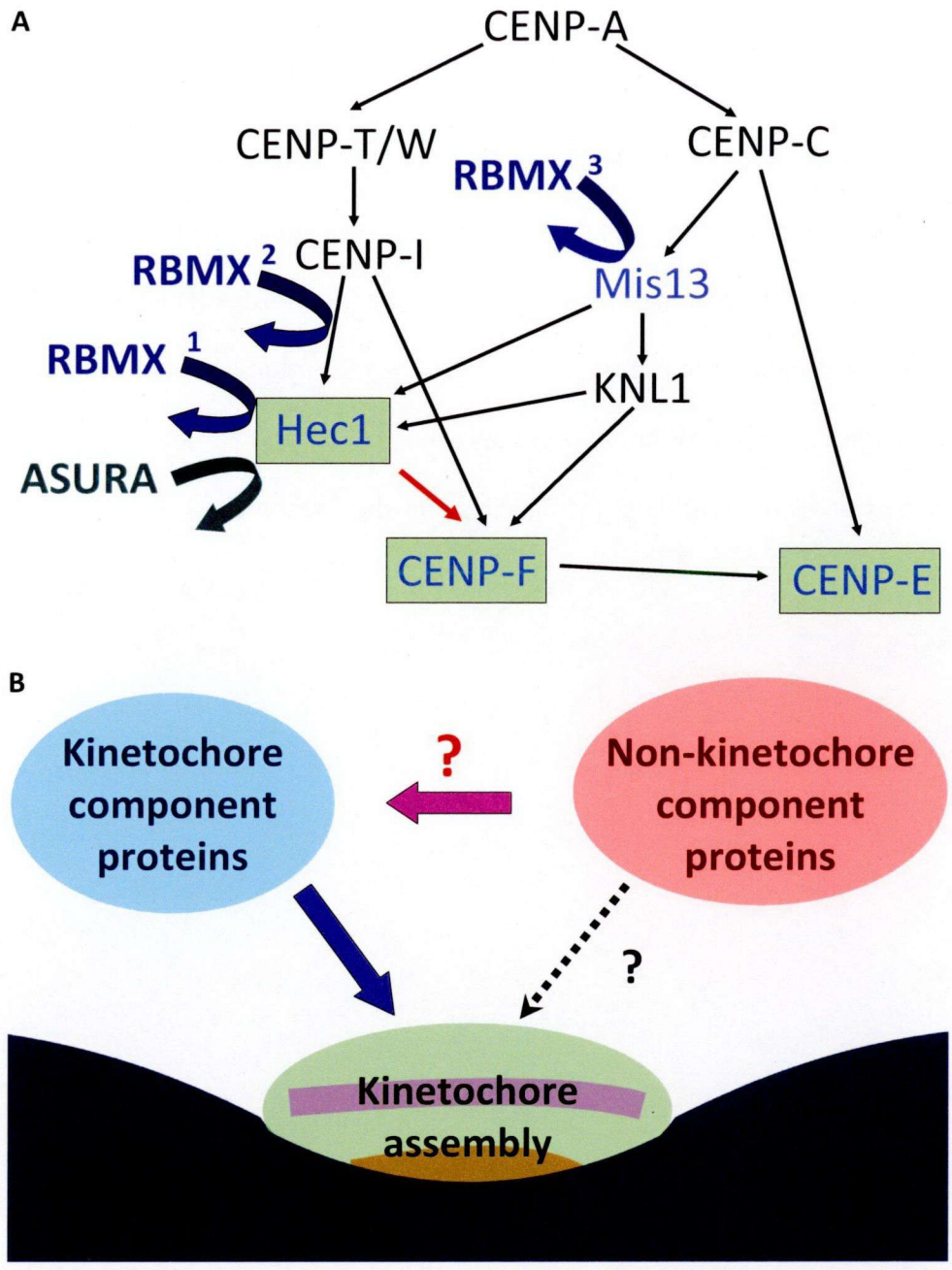

Fig. 5-1 Possible involvements of ASURA and RBMX in targeting kinetochore protein(s) and the importance of non-kinetochore component proteins in kinetochore assembly. (**A**) Proteins mislocalized after ASURA and RBMX depletion were indicated as green boxes and in blue font, respectively. Red arrow indicates dependency of CENP-F on Hec1 as defined in this study. Round arrows show the possible involvement of loading factor. ASURA is likely to recruit Hec1, whereas RBMX may involve in CENP-I and/or CENP-C pathways as indicated by 1, or 1+3, or 2+3. 1 represents Hec1 targeting factor. 2 represents the loading of protein upstream of Hec1 in the CENP-I pathway. 3 represents recruitment of Mis13 or other component in the

CENP-C pathway, upstream of Hec1 but downstream of CENP-C. + represents possible synergistic effect. (**B**) Possible contributions of non-kinetochore component proteins in kinetochore assembly. Non-kinetochore component proteins, including ASURA and RBMX, facilitate kinetochore assembly most probably by targeting kinetochore components. Whether non-kinetochore component proteins involve directly in kinetochore assembly (dotted arrow) is under determination

References

Alushin GM, Ramey VH, Pasqualato S, Ball DA, Grigorieff N, Musacchio A, Nogales E (2010) The Ndc80 kinetochore complex forms oligomeric arrays along microtubules. Nature 467:805-810.

Amano M, Suzuki A, Hori T, Backer C, Okawa K, Cheeseman IM, Fukagawa T (2009) The CENP-S complex is essential for the stable assembly of outer kinetochore structure. J Cell Biol 186:173-182.

Artal-Sanz M, Tavernarakis N (2009) Prohibitin and mitochondrial biology. Trends Endocrinol Metab 20:394-401.

Brinkley BR, Stubblefield E (1966) The fine structure of the kinetochore of a mammalian cell *in vitro*. Chromosoma 19:28-43.

Brinkley BR, Valdivia MM, Tousson A, Balczon RD (1989) The kinetochore: structure and molecular organization. In Mitosis: Molecules and Mechanisms. Hyams JS and Brinkley BR, editors. Academic Press, New York. 77-118.

Cai S, O'Connell CB, Khodjakov A, Walczak CE (2009) Chromosome congression in the absence of kinetochore fibres. Nat Cell Biol 11:832-838.

Chan GK, Liu ST, Yen TJ (2005) Kinetochore structure and function. Trends Cell Biol 15:589-598.

Cheeseman IM, Chappie JS, Wilson-Kubalek EM, Desai A (2006) The conserved KMN network constitutes the core microtubule-binding site of the kinetochore. Cell 127:983-997.

Cheeseman IM, Desai A (2008) Molecular architecture of the kinetochore-microtubule interface. Nat Rev Mol Cell Biol 9:33-46.

Cheeseman IM, Hori T, Fukagawa T, Desai A (2008) KNL1 and the CENP-H/I/K complex coordinately direct kinetochore assembly in vertebrates. Mol Biol Cell 19:587-594.

Choy JS, Acuña R, Au WC, Basrai MA (2011) A role for histone H4K16 hypoacetylation in *Saccharomyces cerevisiae* kinetochore function. Genetics 189:11-21.

Ciferri C, Pasqualato S, Screpanti E, Varetti G, Santaguida S, Dos Reis G, Maiolica A, Polka J, De Luca JG, De Wulf P, Salek M, Rappsilber J, Moores CA, Salmon ED, Musacchio A (2008) Implications for kinetochore-microtubule attachment from

the structure of an engineered Ndc80 complex. Cell 133:427-439.

Cleveland DW, Mao Y, Sullivan KF (2003) Centromeres and kinetochores: from epigenetics to mitotic checkpoint signaling. Cell 112:407-421.

Comings DE, Okada TA (1971) Fine structure of kinetochore in Indian muntjac. Exp Cell Res 67:97-110.

Compton DA (2007) Chromosome orientation. J Cell Biol 179:179-181.

Darlington CD (1937) Recent advances in cytology. Philadelphia, Blakiston.

Daum JR, Potapova TA, Sivakumar S, Daniel JJ, Flynn JN, Rankin S, Gorbsky GJ (2011) Cohesion fatigue induces chromatid separation in cells delayed at metaphase. Curr Biol 21:1018-1024.

DeLuca JG, Dong Y, Hergert P, Strauss J, Hickey JM, Salmon ED, McEwen BF (2005) Hec1 and Nuf2 are core components of the kinetochore outer plate essential for organizing microtubule attachment sites. Mol Biol Cell 16:519-531.

DeLuca JG, Gall WE, Ciferri C, Cimini D, Musacchio A, Salmon ED (2006) Kinetochore microtubule dynamics and attachment stability are regulated by Hec1. Cell 127:969-982.

Dichmann DS, Fletcher RB, Harland RM (2008) Expression cloning in Xenopus identifies RNA-binding proteins as regulators of embryogenesis and Rbmx as necessary for neural and muscle development. Dev Dyn 237:1755-1766.

Dong Y, Vanden Beldt KJ, Meng X, Khodjakov A, McEwen BF (2007) The outer plate in vertebrate kinetochores is a flexible network with multiple microtubule interactions. Nat Cell Biol 9:516-522.

Du Y, Topp CN, Dawe RK (2010) DNA binding of centromere protein C (CENPC) is stabilized by single-stranded RNA. PLoS Genet 6:e1000835.

Dunleavy EM, Roche D, Tagami H, Lacoste N, Ray-Gallet D, Nakamura Y, Daigo Y, Nakatani Y, Almouzni-Pettinotti G (2009) HJURP is a cell-cycle-dependent maintenance and deposition factor of CENP-A at centromeres. Cell 137:485-497.

Earnshaw WC, Rothfield N (1985) Identification of a family of human centromere proteins using autoimmune sera from patients with scleroderma. Chromosoma 91:313-321.

Ewing RM, Chu P, Elisma F, Li H, Taylor P, Climie S, McBroom-Cerajewski L, Robinson MD, O'Connor L, Li M, Taylor R, Dharsee M, Ho Y, Heilbut A, Moore L, Zhang S,

Ornatsky O, Bukhman YV, Ethier M, Sheng Y, Vasilescu J, Abu-Farha M, Lambert JP, Duewel HS, Stewart II, Kuehl B, Hogue K, Colwill K, Gladwish K, Muskat B, Kinach R, Adams SL, Moran MF, Morin GB, Topaloglou T, Figeys D (2007) Large-scale mapping of human protein-protein interactions by mass spectrometry. Mol Syst Biol 3:89.

Feng J, Huang H, Yen TJ (2006) CENP-F is a novel microtubule-binding protein that is essential for kinetochore attachments and affects the duration of the mitotic checkpoint delay. Chromosoma 115:320-329.

Foltz DR, Jansen LE, Bailey AO, Yates JR 3rd, Bassett EA, Wood S, Black BE, Cleveland DW (2009) Centromere-specific assembly of CENP-A nucleosomes is mediated by HJURP. Cell 137:472-484.

Fukui K, Uchiyama S (2007) Chromosome protein framework from proteome analysis of isolated human metaphase chromosomes. Chem Rec 7:230-237.

Fusaro G, Dasgupta P, Rastogi S, Joshi B, Chellappan S (2003) Prohibitin induces the transcriptional activity of p53 and is exported from the nucleus upon apoptotic signaling. J Biol Chem 278:47853-47861.

Gandhi R, Gillespie PJ, Hirano T (2006) Human Wapl is a cohesin-binding protein that promotes sister-chromatid resolution in mitotic prophase. Curr Biol 16:2406-2417.

Gascoigne KE, Takeuchi K, Suzuki A, Hori T, Fukagawa T, Cheeseman IM (2011) Induced ectopic kinetochore assembly bypasses the requirement for CENP-A nucleosomes. Cell 145:410-422.

Ghosh S, Paweletz N (1987) Centrosome-kinetochore interaction in multinucleate cells. Chromosoma 95:136-143.

Gimenez-Abian JF, Sumara I, Hirota T, Hauf S, Gerlich D, de la Torre C, Ellenberg J, Peters JM (2004) Regulation of sister chromatid cohesion between chromosome arms. Curr Biol 14: 1187-1193.

Glisovic T, Bachorik JL, Yong J, Dreyfuss G (2008) RNA-binding proteins and post-transcriptional gene regulation. FEBS Lett 582:1977-1986.

Gorbsky GJ, Sammak PJ, Borisy GG (1987) Chromosomes move poleward in anaphase along stationary microtubules that coordinately disassemble from their kinetochore ends. J Cell Biol 104:9-18.

Goshima G, Kiyomitsu T, Yoda K, Yanagida M (2003) Human centromere chromatin protein hMis12, essential for equal segregation, is independent of CENP-A loading pathway. J Cell Biol 160:25-39.

Hauf S, Watanabe Y (2004) Kinetochore orientation in mitosis and meiosis. Cell 119:317-327.

Hauf S, Roitinger E, Koch B, Dittrich CM, Mechtler K, Peters JM (2005) Dissociation of cohesin from chromosome arms and loss of arm cohesion during early mitosis depends on phosphorylation of SA2. PLoS Biol 3:419-432.

He D, Brinkley BR (1996) Structure and dynamic organization of centromeres/ prekinetochores in the nucleus of mammalian cells. J Cell Sci 109:2693-2704.

Hirota T, Gerlich D, Koch B, Ellenberg J, Peters JM (2004) Distinct functions of condensin I and II in mitotic chromosome assembly. J Cell Sci 117:6435-6445.

Hofmann Y, Wirth B (2002) hnRNP-G promotes exon 7 inclusion of survival motor neuron (SMN) via direct interaction with Htra2-beta1. Hum Mol Genet 11:2037-2049.

Holt SV, Vergnolle MA, Hussein D, Wozniak MJ, Allan VJ, Taylor SS (2005) Silencing Cenp-F weakens centromeric cohesion, prevents chromosome alignment and activates the spindle checkpoint. J Cell Sci 118:4889-4900.

Hori T, Haraguchi T, Hiraoka Y, Kimura H, Fukagawa T (2003) Dynamic behavior of Nuf2-Hec1 complex that localizes to the centrosome and centromere and is essential for mitotic progression in vertebrate cells. J Cell Sci 116:3347-3362.

Hori T, Amano M, Suzuki A, Backer CB, Welburn JP, Dong Y, McEwen BF, Shang W-H, Suzuki E, Okawa K, Cheeseman IM, Fukagawa T (2008) The CCAN makes multiple contacts with centromeric DNA to provide distinct pathways to the outer kinetochore. Cell 135:1039-1052.

Inoue T, Hiratsuka M, Osaki M, Yamada H, Kishimoto I, Yamaguchi S, Nakano S, Katoh M, Ito H, Oshimura M (2007) SIRT2, a tubulin deacetylase, acts to block the entry to chromosome condensation in response to mitotic stress. Oncogene 26:945-957.

Janke C, Ortiz J, Lechner J, Shevchenko A, Magiera MM, Schramm C, Schiebel E (2001) The budding yeast proteins Spc24p and Spc25p interact with Ndc80p and Nuf2p at the kinetochore and are important for kinetochore clustering and checkpoint control. EMBO J 20:777-791.

Jokelainen PT (1967) The ultrastructure and spatial organization of the metaphase kinetochore in mitotic rat cells. J Ultrastruct Res 19:19-44.

Kanhoush R, Beenders B, Perrin C, Moreau J, Bellini M, Penrad-Mobayed M (2010) Novel domains in the hnRNP G/RBMX protein with distinct roles in RNA binding and targeting nascent transcripts. Nucleus 1:109-122.

Kapoor TM, Lampson MA, Hergert P, Cameron L, Cimini D, Salmon ED, McEwen BF, Khodjakov A (2006) Chromosomes can congress to the metaphase plate before biorientation. Science 311:388-391.

Kasashima K, Ohta E, Kagawa Y, Endo H (2006) Mitochondrial functions and estrogen receptor-dependent nuclear translocation of pleiotropic human prohibitin 2. J Biol Chem 281:36401-36410.

Kingsbury MA, Yung YC, Peterson SE, Westra JW, Chun J (2006) Aneuploidy in the normal and diseased brain. Cell Mol Life Sci 63:2626-2641.

Kitajima TS, Sakuno T, Ishiguro K, Iemura S, Natsume T, Kawashima SA, Watanabe Y (2006) Shugoshin collaborates with protein phosphatase 2A to protect cohesin. Nature 441:46-52.

Kline SL, Cheeseman IM, Hori T, Fukagawa T, Desai A (2006) The human Mis12 complex is required for kinetochore assembly and proper chromosome segregation. J Cell Biol 173:9-17.

Kops GJ, Weaver BA, Cleveland DW (2005) On the road to cancer: aneuploidy and the mitotic checkpoint. Nat Rev Cancer 5:773-785.

Kops GJ, Saurin AT, Meraldi P (2010) Finding the middle ground: how kinetochores power chromosome congression. Cell Mol Life Sci 67:2145-2161.

Kueng S, Hegemann B, Peters BH, Lipp JJ, Schleiffer A, Mechtler K, Peters JM (2006) Wapl controls the dynamic association of cohesin with chromatin. Cell 127:955-967.

Kurtev V, Margueron R, Kroboth K, Ogris E, Cavailles V, Seiser C (2004) Transcriptional regulation by the repressor of estrogen receptor activity via recruitment of histone deacetylases. J Biol Chem 279:24834-24843.

Lamers MC, Bacher S (1997) Prohibitin and prohibitone, ubiquitous and abundant proteins that are reluctant to reveal their real identity. Int Arch Allergy Immunol 113:146-149.

Liao H, Winkfein RJ, Mack G, Rattner JB, Yen TJ (1995) CENP-F is a protein of the nuclear matrix that assembles onto kinetochores at late G2 and is rapidly degraded after mitosis. J Cell Biol 130:507-518.

Lingenfelter PA, Delbridge ML, Thomas S, Hoekstra HE, Mitchell MJ, Graves JA, Disteche CM (2001) Expression and conservation of processed copies of the RBMX gene Mamm Genome 12:538-545.

Liu D, Ding X, Du J, Cai X, Huang Y, Ward T, Shaw A, Yang Y, Hu R, Jin C, Yao X (2007) Human NUF2 interacts with centromere-associated protein E and is essential for a stable spindle microtubule-kinetochore attachment. J Biol Chem 282:21415-21424.

Liu ST, Rattner JB, Jablonski SA, Yen TJ (2006) Mapping the assembly pathways that specify formation of the trilaminar kinetochore plates in human cells. J Cell Biol 175:41-53.

Liu ST, Yen TJ (2009) The kinetochore: from molecular discoveries to cancer therapy. The Kinetochore as Target for Cancer Drug Development. De Wulf P and Earnshaw WC, editors. Springer, New York. 455.

Losada A, Hirano M, Hirano T (1998) Identification of *Xenopus* SMC protein complexes required for sister chromatid cohesion. Genes Dev 12:1986-1997.

Losada A, Yokochi T, Kobayashi R, Hirano T (2000) Identification and characterization of SA/Scc3p subunits in the *Xenopus* and human cohesin complexes. J Cell Biol 150:405-416.

Losada A, Hirano M, Hirano T (2002) Cohesin release is required for sister chromatid resolution, but not for condensin-mediated compaction, at the onset of mitosis. Genes Dev 16:3004-3016.

Ma N, Matsunaga S, Takata H, Ono-Maniwa R, Uchiyama S, Fukui K (2007) Nucleolin functions in nucleolus formation and chromosome congression. J Cell Sci 120: 2091-2105.

Maddox PS, Portier N, Desai A, Oegema K (2006) Molecular analysis of mitotic chromosome condensation using a quantitative time-resolved fluorescence microscopy assay. Proc Natl Acad Sci U S A 103:15097-15102.

Maiato H, DeLuca J, Salmon ED, Earnshaw WC (2004) The dynamic kinetochore-microtubule interface. J Cell Sci 117:5461-5477.

Maresca TJ (2011) Chromosome segregation: a kinetochore missing link is found. Curr Biol 21:261-263.

Marshall OW, Choo KHA (2008) Three-dimensional localization of CENP-A suggests a complex higher order structure of centromeric chromatin. J Cell Biol 183:1193-1202.

Martin-Lluesma S, Stucke VM, Nigg EA (2002) Role of Hec1 in spindle checkpoint signaling and kinetochore recruitment of Mad1/Mad2. Science 297:2267-2270.

Martinez-Contreras R, Cloutier P, Shkreta L, Fisette JF, Revil T, Chabot B (2007) hnRNP proteins and splicing control. Adv Exp Med Biol 623:123-147.

McClung JK, Danner DB, Stewart DA, Smith JR, Schneider EL, Lumpkin CK, Dell'Orco RT, Nuell MJ (1989) Isolation of a cDNA that hybrid selects antiproliferative mRNA from rat liver. Biochem Biophys Res Commun 164:1316-1322.

McEwen BF, Dong Y (2010) Contrasting models for kinetochore microtubule attachment in mammalian cells. Cell Mol Life Sci 67:2163-2172.

Meraldi P, Draviam VM, Sorger PK (2004) Timing and checkpoints in the regulation of mitotic progression. Dev Cell 7:45-60.

Merkwirth C, Langer T (2009) Prohibitin function within mitochondria: essential roles for cell proliferation and cristae morphogenesis. Biochim Biophys Acta 1793:27-32.

Miller SA, Johnson ML, Stukenberg PT (2008) Kinetochore attachments require an interaction between unstructured tails on microtubules and Ndc80 (Hec1). Curr Biol 18:1785-1791.

Mitchison T, Evans L, Schulze E, Kirschner M (1986) Sites of microtubule assembly and disassembly in the mitotic spindle. Cell 45:515-527.

Mitchison TJ (1988) Microtubule dynamics and kinetochore function in mitosis. Annu Rev Cell Biol 4:527-549.

Montano MM, Ekena K, Delage-Mourroux R, Chang W, Martini P, Katzenellenbogen BS (1999) An estrogen receptor-selective coregulator that potentiates the effectiveness of antiestrogens and represses the activity of estrogens. Proc Natl Acad Sci U S A 96:6947-6952.

Nasim MT, Chernova TK, Chowdhury HM, Yue BG, Eperon IC (2003) HnRNP G and Tra2beta: opposite effects on splicing matched by antagonism in RNA binding. Hum Mol Genet 12:1337-1348.

Neumann B, Walter T, Hériché JK, Bulkescher J, Erfle H, Conrad C, Rogers P, Poser I, Held M, Liebel U, Cetin C, Sieckmann F, Pau G, Kabbe R, Wünsche A, Satagopam V, Schmitz MH, Chapuis C, Gerlich DW, Schneider R, Eils R, Huber W, Peters JM, Hyman AA, Durbin R, Pepperkok R, Ellenberg J (2010) Phenotypic profiling of the human genome by time-lapse microscopy reveals cell division genes. Nature 464:721-727.

Nicklas RB (1989) The motor for poleward chromosome movement in anaphase is in or near the kinetochore. J Cell Biol 109:2245-2255.

Ohta S, Bukowski-Wills JC, Sanchez-Pulido L, Alves Fde L, Wood L, Chen ZA, Platani M, Fischer L, Hudson DF, Ponting CP, Fukagawa T, Earnshaw WC, Rappsilber J (2010) The protein composition of mitotic chromosomes determined using multiclassifier combinatorial proteomics. Cell 142:810-821.

Okada M, Okawa K, Isobe T, Fukagawa T (2009) CENP-H containing complex facilitates centromere deposition of CENP-A with FACT and CHD1. Mol Biol Cell 20:3986-3995.

Peters JM, Tedeschi A, Schmitz J (2008) The cohesin complex and its roles in chromosome biology. Genes Dev 22:3089-3114.

Petrovic A, Pasqualato S, Dube P, Krenn V, Santaguida S, Cittaro D, Monzani S, Massimiliano L, Keller J, Tarricone A, Maiolica A, Stark H, Musacchio A (2010) The MIS12 complex is a protein interaction hub for outer kinetochore assembly. J Cell Biol 190:835-852.

Przewloka MR, Venkei Z, Bolanos-Garcia VM, Debski J, Dadlez M, Glover DM (2011) CENP-C is a structural platform for kinetochore assembly. Curr Biol 21:399-405.

Raaijmakers JA, Tanenbaum ME, Maia AF, Medema RH (2009) RAMA1 is a novel kinetochore protein involved in kinetochore-microtubule attachment. J Cell Sci 122:2436-2445.

Rattner JB, Rao A, Fritzler MJ, Valencia DW, Yen TJ (1993) CENP-F is a .ca 400 kDa kinetochore protein that exhibits a cell-cycle dependent localization. Cell Motil Cytoskeleton 26:214-226.

Ribeiro SA, Vagnarelli P, Dong Y, Hori T, McEwen BF, Fukagawa T, Flors C, Earnshaw WC (2010) A super-resolution map of the vertebrate kinetochore. Proc Natl Acad Sci U S A 107:10484-10489.

Rieder CL (1982) The formation, structure, and composition of the mammalian kinetochore and kinetochore fiber. Int Rev Cytol 79:1-58.

Rieder CL, Alexander SP (1990) Kinetochores are transported poleward along a single astral microtubule during chromosome attachment to the spindle in newt lung cells. J Cell Biol 110:81-95.

Rieder CL, Salmon ED (1998) The vertebrate cell kinetochore and its roles during mitosis. Trends Cell Biol 8:310-318.

Roos UP (1973) Light and electron microscopy of rat kangaroo cells in mitosis. II. Kinetochore structure and function. Chromosoma 41:195-220.

Salic A, Waters JC, Mitchison TJ (2004) Vertebrate shugoshin links sister centromere cohesion and kinetochore microtubule stability in mitosis. Cell 118:567-578.

Santaguida S, Musacchio A (2009) The life and miracles of kinetochores. EMBO J 28:2511-2531.

Saurin AT, van der Waal MS, Medema RH, Lens SM, Kops GJ (2011) Aurora B potentiates Mps1 activation to ensure rapid checkpoint establishment at the onset of mitosis. Nat Commun 2:316.

Screpanti E, De Antoni A, Alushin GM, Petrovic A, Melis T, Nogales E, Musacchio A (2011) Direct binding of Cenp-C to the Mis12 complex joins the inner and outer kinetochore. Curr Biol 21:391-398.

Schrader F (1953) Mitosis, the Movements of Chromosomes in Cell Division. Dunn LC, editor. Columbia University Press, New York. 170.

Schvartzman JM, Sotillo R, Benezra R (2010) Mitotic chromosomal instability and cancer: mouse modelling of the human disease. Nat Rev Cancer 10:102-115.

Sharp LW (1934) Introduction to cytology. McGraw-Hill, New York.

Shin KH, Kim RH, Kang MK, Kim RH, Kim SG, Lim PK, Yochim JM, Baluda MA, Park NH (2007) p53 promotes the fidelity of DNA end-joining activity by, in part, enhancing the expression of heterogeneous nuclear ribonucleoprotein G. DNA Repair (Amst) 6:830-840.

Shin KH, Kim RH, Kim RH, Kang MK, Park NH (2008) hnRNP G elicits tumor-suppressive activity in part by upregulating the expression of Txnip. Biochem Biophys Res Commun 372:880-885.

Soulard M, Barque JP, Della Valle V, Hernandez-Verdun D, Masson C, Danon F, Larsen CJ (1991) A novel 43-kDa glycoprotein is detected in the nucleus of mammalian cells by autoantibodies from dogs with autoimmune disorders. Exp Cell Res 193: 59-71.

Soulard M, Della Valle V, Siomi MC, Piñol-Roma S, Codogno P, Bauvy C, Bellini M, Lacroix JC, Monod G, Dreyfuss G, et al. (1993) hnRNP G sequence and characterization of a glycosylated RNA-binding protein. Nucleic Acids Res 21:4210-4217.

Sumara I, Vorlaufer E, Gieffers C, Peters BH, Peters JM (2000) Characterization of vertebrate cohesin complexes and their regulation in prophase. J Cell Biol 151: 749-761.

Sundin LJ, Guimaraes GJ, Deluca JG (2011) The NDC80 complex proteins Nuf2 and Hec1 make distinct contributions to kinetochore-microtubule attachment in mitosis. Mol Biol Cell 22:759-768.

Takata H, Uchiyama S, Nakamura N, Nakashima S, Kobayashi S, Sone T, Kimura S, Lahmers S, Granzier H, Labeit S, Matsunaga S, Fukui K (2007a) A comparative proteome analysis of human metaphase chromosomes isolated from two different cell lines reveals a set of conserved chromosome-associated proteins. Genes Cells 12:269-284.

Takata H, Matsunaga S, Morimoto A, Ma N, Kurihara D, Ono-Maniwa R, Nakagawa M, Azuma T, Uchiyama S, Fukui K (2007b) PHB2 protects sister-chromatid cohesion in mitosis. Curr Biol 17:1356-1361.

Tanaka TU (2005) Chromosome bi-orientation on the mitotic spindle. Philos Trans R Soc Lond B Biol Sci 360:581-589.

Tanaka TU, Stark MJ, Tanaka K (2005) Kinetochore capture and bi-orientation on the mitotic spindle. Nat Rev Mol Cell Biol 6:929-942.

Tatsuta T, Model K, Langer T (2005) Formation of membrane-bound ring complexes by prohibitins in mitochondria. Mol Biol Cell 16:248-259.

Terashima M, Kim KM, Adachi T, Nielsen PJ, Reth M, Köhler G, Lamers MC (1994) The IgM antigen receptor of B lymphocytes is associated with prohibitin and a prohibitin-related protein. EMBO J 13:3782-3792.

Tsend-Ayush E, O'Sullivan LA, Grützner FS, Onnebo SM, Lewis RS, Delbridge ML, Marshall Graves JA, Ward AC (2005) RBMX gene is essential for brain development in zebrafish. Dev Dyn 234:682-688.

Uchiyama S, Kobayashi S, Takata H, Ishihara T, Hori N, Higashi T, Hayashihara K, Sone T, Higo D, Nirasawa T, Takao T, Matsunaga S, Fukui K (2005) Proteome analysis of human metaphase chromosomes. J Biol Chem 280:16994-17004.

Vagnarelli P, Morrison C, Dodson H, Sonoda E, Takeda S, Earnshaw WC (2004) Analysis of Scc1-deficient cells defines a key metaphase role of vertebrate cohesin in linking sister kinetochores. EMBO Rep 5:167-171.

VandenBeldt KJ, Barnard RM, Hergert PJ, Meng X, Maiato H, McEwen BF (2006) Kinetochores use a novel mechanism for coordinating the dynamics of individual microtubules. Curr Biol 16:1217-1223.

Wan X, O'Quinn RP, Pierce HL, Joglekar AP, Gall WE, DeLuca JG, Carroll CW, Liu ST, Yen TJ, McEwen BF, Stukenberg PT, Desai A, Salmon ED (2009) Protein architecture of

the human kinetochore microtubule attachment site. Cell 137:672-684.

Wendell KL, Wilson L, Jordan MA (1993) Mitotic block in HeLa cells by vinblastine: ultrastructural changes in kinetochore-microtubule attachment and in centrosomes. J Cell Sci 104:261-274.

Wigge PA, Kilmartin JV (2001) The Ndc80p complex from *Saccharomyces cerevisiae* contains conserved centromere components and has a function in chromosome segregation. J Cell Biol 152:349-360.

Winter A, Kämäräinen O, Hofmann A (2007) Molecular modeling of prohibitin domains. Proteins 68:353-362.

Wise D, Cassimeris L, Rieder CL, Wadsworth P, Salmon ED (1991) Chromosome fiber dynamics and congression oscillations in metaphase PtK2 cells at 23 degrees C. Cell Motil Cytoskel 18:1313-1342.

Wu CS, Chen YF, Gartenberg MR (2011) Targeted sister chromatid cohesion by Sir2. PLoS Genet 7:e1002000.

Zinkowski RP, Meyne J, Brinkley BR (1991) The centromere-kinetochore complex: a repeat subunit model. J Cell Biol 113:1091-1110.

List of publications

Lee MH, Lin L, Ilma Equilibrina, Uchiyama S, Matsunaga S and Fukui K: ASURA (PHB2) is required for kinetochore assembly and subsequent chromosome congression. *Acta Histochem Cytochem*. (In press)

Lee MH, Lin L, Takata H, Morimoto A, Uchiyama S, Matsunaga S and Fukui K: An X-chromosome RNA-binding motif protein (RBMX) is required for proper kinetochore formation. *Chrom Sci*. (In press)

Acknowledgements

This current thesis summarized my studies from October, 2008 to September, 2011. I would like to express my gratitude to all those who gave me the possibility to complete this thesis.

In the first instance, I am deeply indebted to my dedicated supervisor Professor Dr. Kiichi Fukui, for kindly giving me permission to commence this thesis in the Laboratory of Dynamic Cell Biology, Department of Biotechnology, Graduate School of Engineering, Osaka University, and offered me stimulating suggestions which always helped me in deciding future directions during the course of this study. I have furthermore to convey my appreciation to my former group leader, Assistant Professor Dr. Susumu Uchiyama for his helpful discussions and encouragement all the time of research for and writing of this thesis.

I am deeply grateful to Professor Dr. Satoshi Harashima and Professor Dr. Hajime Watanabe, Department of Biotechnology, Graduate School of Engineering, Osaka University, for their valuable suggestions.

I would like to express my cordial thanks to Associate Professor Dr. Sachihiro Matsunaga (Tokyo University of Science), Professor Dr. Shinichiro Kajiyama (School of Biology-Oriented Science and technology, Kinki University) and Professor Dr. Nobuko Ohmido (Faculty of human Development, Kobe University) for interest and valuable hints.

Especially I am obliged to Professor Dr. Hirotaro Mori and Professor Dr. Akio Takaoka from Research Center for Ultra-High Voltage Electron Microscopy, Osaka University, for generously providing reagents for electron microscopic experiments and permission for using the facilities. Besides, the patience and kindness of Associate Professor Dr. Ryuji Nishi are greatly appreciated. I want to thank all the staffs in the research center for all sorts of technical supports. I also want to thank Dr. Tomoki Nishida and Dr. Linyen Lin for all their assistance in recording and computing electron micrographs as well as suggestions, which are indispensable to the completion of this study. I am extremely grateful to Mr. Toshiaki Hasegawa, for the meticulous guidance, and invaluable ideas with his profound knowledge in electron microscopy.

I owe special thanks to Associate Professor Dr. Sumire Inaga and Dr. Tetsuo Katsumoto from Faculty of Medicine, Tottori University for their helpful advices and for sharing the protocols of electron microscopy.

I also would like to thank Dr. Satoru Fujimoto (Okayama University), Dr. Hideaki

Takata (National institute of Genetics), Dr. Joyce A. Cartagena (Nagoya University), Dr. Daisuke Kurihara (Nagoya University), Dr. Arni E. Gambe (Republic of the Philippines), Dr. Kayoko Hayashihara (Osaka University), Dr. Akihiro Morimoto (University of Tokyo) and Ms. Naruemon Khemkladngoen (Okayama University) for their priceless comments and critique of my initial research works and results.

My appreciation is extended to all the members of Fukui laboratory. I wish to thank Mr. Tomoyuki Doi, Ms. Reiko Isobe, Ms. Sachiko Kurihara, Ms. Keiko Ueda-Sarson and Ms. Junko Tanaka, for their administrative supports. Special thanks are also extended to Dr. Masanori Noda and Ms. Masami Yokoyama for their encouragement and advices. The members of Chromosome Comprehensive Group, Ms. Astari Dwiranti, Mr. Ken Goto, Mr. Kiichi Morii, Mr. Tohru Hamano, Ms. Rawin Poonperm and Ms. Chiaki Egawa are always supportive. I want to thank them for all their helps and useful discussion. I am grateful to Ms. Elena Krayukhina, Ms. Ilma Equilibrina, Ms. Atefeh Alipour and Mr. Yusuke Koga for their invaluable suggestions when I failed coming up with ideas. I also want to thank all the Master course students and undergraduates for helping me during difficult times.

I am honored to express my gratitude to the Japanese Government, Ministry of Education, Culture, Sports, Science and Technology (MEXT), for the financial support of my stay in Japan, enable me to concentrate in the necessary research works to complete this thesis.